

MESHFREE TECHNIQUE WITH ADAPTIVE REFINEMENT STRATEGY FOR CRACK PROPAGATION ANALYSIS

Thesis

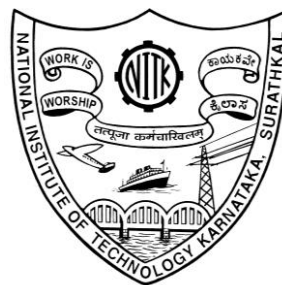
Submitted in partial fulfilment of the requirements for the
degree of

DOCTOR OF PHILOSOPHY

by

BHAVANA PATEL S.S.

(Reg. No. 121171CV12F05)



**DEPARTMENT OF CIVIL ENGINEERING
NATIONAL INSTITUTE OF TECHNOLOGY
KARNATAKA, SURATHKAL, MANGALORE – 575 025**

May, 2016

DECLARATION

I hereby declare that the Research Thesis entitled “**Meshfree Technique with Adaptive Refinement Strategy for Crack Propagation Analysis**” which is being submitted to the **National Institute of Technology Karnataka, Surathkal** in partial fulfilment of the requirements for the award of the Degree of **Doctor of Philosophy in Civil Engineering** is *a bonafide report of the research work carried out by me.* The material contained in this Research Thesis has not been submitted to any University or Institution for the award of any degree

Place: NITK Surathkal

Date: 06/05/2016

BHAVANA PATEL S.S.

Register No. 121171CV12F05

Dept. of Civil Engg., NITK Surathkal

C E R T I F I C A T E

This is to *certify* that the Research Thesis entitled “**Meshfree Technique With Adaptive Refinement Strategy For Crack Propagation Analysis**” submitted by **Bhavana Patel S.S.** (Register Number: **121171CV12F05**) as the record of the research work carried out by her, is *accepted as the Research Thesis submission* in partial fulfilment of the requirements for the award of degree of **Doctor of Philosophy**.

Prof. K. S. Babu Narayan

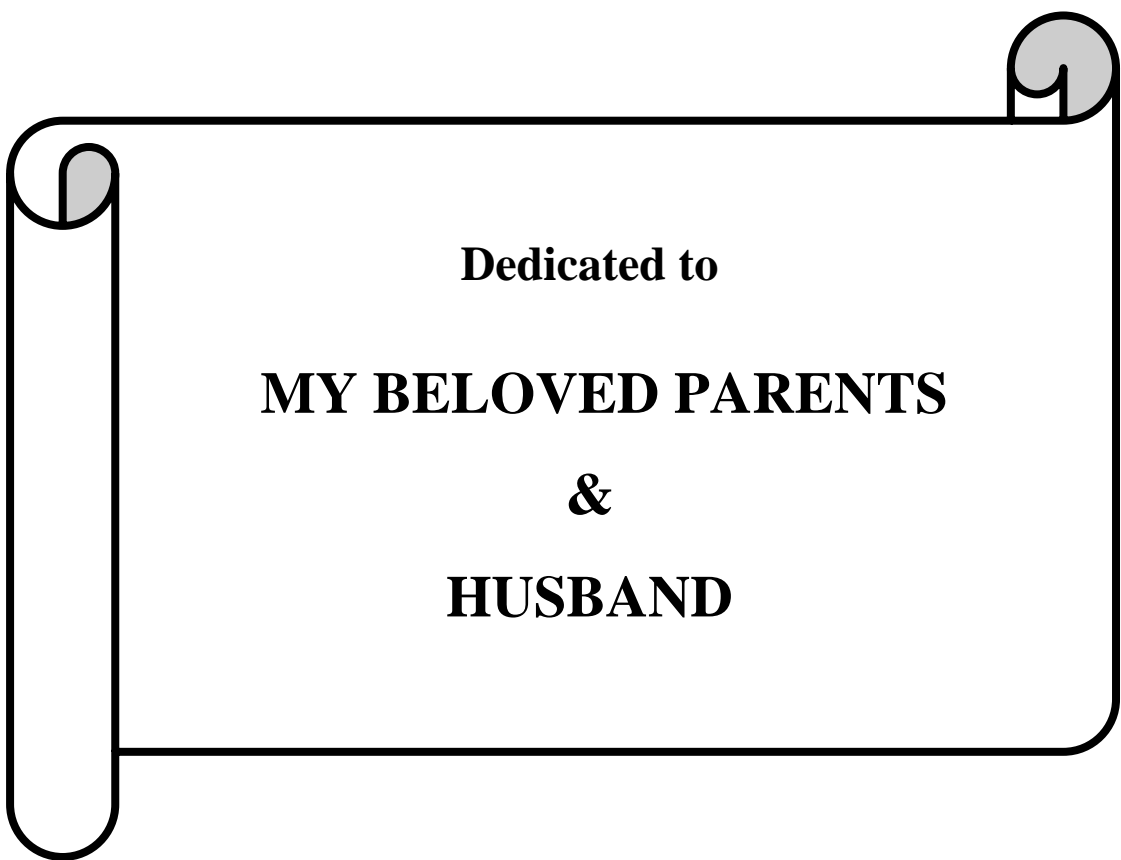
Department of Civil Engineering
(Research Supervisor)

Prof. KattaVenkataramana

Department of Civil Engineering
(Research Supervisor)

Prof. K.N. Lokesh

Chairman – DRPC & Head
Department of Civil Engineering



Dedicated to

MY BELOVED PARENTS

&

HUSBAND

ACKNOWLEDGEMENT

I owe a debt of gratitude to my research supervisors **Prof. K. S. Babu Narayan** and **Prof. Katta Venkataramana** for their invaluable inputs and their continuous support in guiding me in this research work. I sincerely thank them with all due respect for the successful completion of the research work.

I express my gratitude to RPAC members, Associate Prof. B.R. Jayalekshmi (Dept. of Civil Engg.) and Prof. Prasad Krishna (TEQIP Coordinator & Dept. of Mechanical Engg.) for their very useful suggestions during the progress of the work.

I am thankful to Prof. K.N. Lokesh (Head, Dept. of Civil Engg. & Chairman DRPC), Prof. Sitaram Nayak (Secretary DRPC) and Prof. A. U. Ravi Shankar (Fr. Head, Dept. of Civil Engg.) for their continuous support during my research period.

I gratefully acknowledge the financial support received from the Technical Education Quality Improvement Programme (TEQIP) Phase II. I am thankful to Prof. T. Laxminidhi (Nodal officer, TEQIP), Ravikiran Kadoli (Nodal officer, TEQIP) and U. Sripathi (Co-Coordinator, TEQIP) for their kind support. I extend my heartfelt thanks to all the TEQIP staff members for their continuous cooperation.

I also thank each of the teaching faculty, supporting staff and fellow research scholars of the Civil Engineering Department for their direct and indirect support.

I am indebted to my parents', sister and extended family for their continuous love, care, support, encouragement and efforts to make me what I am today. I thank my husband from the bottom of my heart who stood beside me in every step and constantly educated and motivated me during my thesis work.

Finally I thank my almighty for his grace which has protected me till today.

Place: NITK Surathkal

Bhavana Patel S. S.

Date: 06/05/2016

ABSTRACT

“MeshFree Technique with Adaptive Refinement Strategy for Crack Propagation Analysis” is an investigation that has aimed to develop an adaptive refinement scheme for EFG based MeshFree method for modeling and simulating high stress gradients in plate structures.

Modelling high stress gradients like crack propagation are still a challenge to numerical methods and this has been addressed to a certain extent using MeshFree. Crack path follows the edge of the element in case of Finite Element Method (FEM) and getting the true path even with remeshing is complicated. Use of special functions to model discontinuity within the element (Extended Finite Element Method) has made modelling much simpler by reducing remeshing to a certain extent, but fails to arrive at smoother stress distribution. MeshFree method can offer solutions to the problems discussed and many researchers have thrown light in this direction.

This work has focused on development of a MeshFree method that can be of help in crack propagation studies. On the Element-Free Galerkin (EFG) platform with Moving Least Square (MLS) technique for shape function construction, Lagrangian multipliers for imposition of constraints and satisfaction of Kronecker delta property has been attempted successfully. With strain energy release rate as basis, crack formation-propagation analysis formulation has been done and strategies for adaptive refinement have been suggested. The mathematical formulations have been verified and validated. Comparison with traditional FEM to highlight the superiority of MeshFree methods in handling high stress gradient problem have been detailed with illustrations.

Key words: Element-Free Galerkin Method, MeshFree Method, Crack Propagation, Stress Intensity Factor, Stress Concentration Factor

TABLE OF CONTENTS

| | |
|---|-----------------|
| LIST OF FIGURES | i-iii |
| LIST OF TABLES | v |
| NOTATIONS..... | vii-viii |
| ABBREVIATIONS | ix |
| | |
| CHAPTER 1 INTRODUCTION | 1-13 |
| 1.1 CHAPTER PROLOGUE | 1 |
| 1.2 MATHEMATICAL MODELLING AND SIMULATION..... | 1 |
| 1.2.1 Strong and Weak Form | 1 |
| 1.2.2 Finite Element Method | 2 |
| 1.2.3 Extended Finite Element Method | 3 |
| 1.2.4 MeshFree Method | 4 |
| 1.3 DIFFERENT METHODS IN MESHFREE TECHNIQUE..... | 4 |
| 1.3.1 Classification Based on Shape Function Construction | 4 |
| 1.3.2 Classification Based on Formulation | 5 |
| 1.3.3 Classification Based on Integration | 5 |
| 1.4 ELEMENT-FREE GALERKIN METHOD | 5 |
| 1.4.1 Discretization of Problem Space..... | 5 |
| 1.4.2 Support and Influence Domain | 7 |
| 1.4.3 Formulation of System Equations..... | 8 |
| 1.5 CRACK PROPAGATION..... | 8 |
| 1.6 ADAPTIVE REFINEMENT | 10 |
| 1.6.1 Refinement Strategy..... | 10 |
| 1.7 OBJECTIVES | 11 |
| 1.7.1 Motivation for the Work | 11 |
| 1.7.2 Objective of the Research Work | 12 |
| 1.8 ORGANISATION OF THE THESIS | 11 |
| | |
| CHAPTER 2 OVERVIEW OF LITERATURE | 15-31 |
| 2.1 CHAPTER PROLOGUE | 15 |
| 2.2 FINITE ELEMENT METHOD | 15 |
| 2.3 EXTENDED FINITE ELEMENT METHOD (XFEM) | 16 |

| | | |
|---|---|--------------|
| 2.4 | MESHFREE METHOD..... | 18 |
| 2.4.1 | Element-Free Galerkin (EFG) method..... | 19 |
| 2.4.2 | Point Interpolation and Other Methods..... | 22 |
| 2.4.3 | Coupling MeshFree Methods..... | 24 |
| 2.5 | HYBRID NUMERICAL METHODS | 25 |
| 2.5.1 | Hybrid of FEM and XFEM..... | 25 |
| 2.5.2 | Hybrid of FEM and MeshFree Method | 26 |
| 2.6 | ADAPTIVE REFINEMENT | 28 |
| CHAPTER 3 FORMULATION OF EFG METHOD | | 33-48 |
| 3.1 | CHAPTER PROLOGUE | 33 |
| 3.2 | SHAPE FUNCTION BY MOVING LEAST SQUARE METHOD | 33 |
| 3.3 | WEIGHTING FUNCTIONS | 35 |
| 3.4 | 2D PLATE FORMULATION | 39 |
| 3.5 | 1D BEAM FORMULATION | 43 |
| 3.6 | APPLICATION OF BOUNDARY CONDITION AND TRACTION FORCE..... | 45 |
| 3.6.1 | Application of Boundary Condition by Lagrange Multipliers..... | 45 |
| 3.6.2 | Application of Traction Force along a Line in Problem Space | 46 |
| 3.7 | DISPLACEMENTS, STRAINS AND STRESSES..... | 47 |
| CHAPTER 4 EFG CODE FOR BEAMS AND PLATES – TESTING AND VERIFICATION | | 49-61 |
| 4.1 | CHAPTER PROLOGUE | 49 |
| 4.2 | VERIFICATION USING 1D BEAM STRUCTURES | 49 |
| 4.3 | VERIFICATION USING 2D PLATE STRUCTURES | 54 |
| 4.3.1 | A Simple 2D Beam | 54 |
| 4.3.2 | Rectangular Plates with Geometrically Induced Stress Concentrations | 55 |
| CHAPTER 5 EFG IN CRACK PROPAGATION ANALYSIS | | 63-81 |
| 5.1 | CHAPTER PROLOGUE | 63 |
| 5.2 | FORMULATION FOR MODELLING CRACK PROPAGATION..... | 63 |
| 5.2.1 | SIF from Strain Energy Release Rate | 63 |
| 5.2.2 | Stresses and Displacements in Arbitrarily Orientated Crack | 64 |

| | | |
|--|---|--------------|
| 5.2.3 | SIF Condition for Crack Growth | 65 |
| 5.2.4 | Crack Propagation Angle under Combined Mode I, Mode II Loading | 65 |
| 5.3 | NUMERICAL DEMONSTRATION OF CRACK PROPAGATION ANALYSIS..... | 66 |
| 5.3.1 | Verification of SIF Computation | 66 |
| 5.3.2 | Crack Propagation in a Plate with Inclined Edge Crack..... | 68 |
| 5.3.3 | Crack Propagation in a Punctured Plate with Edge Crack..... | 70 |
| 5.4 | DEVELOPED METHODOLOGY FOR ADAPTIVE REFINEMENT | 73 |
| 5.4.1 | Strain Energy Density in Integration Cell..... | 73 |
| 5.4.2 | Cell Refinement Based on Strain Energy | 73 |
| 5.4.3 | Strain Energy Density in Triangular Cell | 73 |
| 5.4.4 | Node Refinement Based on Strain Energy | 74 |
| 5.5 | ILLUSTRATION OF ADAPTIVE REFINEMENT | 75 |
| 5.5.1 | Adaptive Refinement on Rectangular Plate with Semi-Circular Notches | 75 |
| 5.5.2 | Adaptive Refinement on Rectangular Plate with Angled Edge Crack | 79 |
| CHAPTER 6 CONCLUSIONS..... | | 83-85 |
| 6.1 | BRIEF SUMMARY OF THE WORK | 83 |
| 6.2 | CONCLUSIONS..... | 83 |
| 6.3 | SCOPE FOR FUTURE WORK | 85 |
| APPENDIX I | | 87-89 |
| I.1 | CLOSED-FORM SOLUTION FOR BEAM UNDER TRANSVERSE LOADING | 87 |
| I.2 | ANALYTICALLY COMPUTED SCF FOR PLATES..... | 88 |
| I.3 | ANALYTICALLY COMPUTED SIF FOR PLATES | 89 |
| REFERENCES..... | | 91-96 |
| PUBLICATIONS FROM THE PRESENT WORK..... | | 97-98 |
| CURRICULUM VITAE..... | | 99 |

LIST OF FIGURES

| Fig. No. | Figure Title | Pg. No. |
|----------|--|---------|
| 1.1 | Different types of linear finite elements used for domain discretization | 3 |
| 1.2 | Flow chart for Finite Element Method | 3 |
| 1.3 | Problem space with triangular cells and integration cells | 6 |
| 1.4 | Problem space with integration cells (background cells) | 6 |
| 1.5 | Problem space in MeshFree method with nodes, point-of-interest, domain and integration cells | 7 |
| 1.6 | Methodology in MeshFree | 9 |
| 1.7 | Modes of crack propagation | 10 |
| 1.8 | Voronoi cell for nodal refinement | 11 |
| 3.1 | Shape function at point-of-interest in a plate with circular cut-out | 34 |
| 3.2 | First-order differential of the shape function w.r.t ξ on the plate | 34 |
| 3.3 | First-order differential of the shape function w.r.t η on the plate | 34 |
| 3.4 | Distribution of weights in the weight function for $\xi = -1$ to 1 | 36 |
| 3.5 | First-order differential of the weighting functions for $\xi = -1$ to 1 | 37 |
| 3.6 | Second-order differential of the weighting functions for $\xi = -1$ to 1 | 37 |
| 3.7 | Exponential weight function in 2D space for $\xi, \eta = -1$ to 1 | 38 |
| 3.8 | First-order differential of the 2D exponential weight function w.r.t. ξ | 39 |
| 3.9 | First-order differential of the 2D exponential weight function w.r.t. η | 39 |
| 3.10 | Stress orientation in a unit cell | 40 |
| 3.11 | Displacements and rotations about the mid-surface in plate formulation | 41 |
| 3.12 | Stress resultants on 1D beam | 43 |

LIST OF FIGURES

| | | |
|------|---|----|
| 3.13 | Displacements and rotation on 1D beam | 44 |
| 4.1 | Cantilever beam with vertical tip load | 49 |
| 4.2 | Simply-supported beam with vertical centre load | 50 |
| 4.3 | Displacement convergence in cantilever beam | 51 |
| 4.4 | Displacement convergence in simply-supported beam | 51 |
| 4.5 | Displacement distribution along the length of cantilever beam | 52 |
| 4.6 | Displacement distribution along the length of simply-supported beam | 52 |
| 4.7 | Stress distribution along the length of cantilever beam | 53 |
| 4.8 | Stress distribution along the length of simply-supported beam | 53 |
| 4.9 | A simple 2D beam structure | 54 |
| 4.10 | Displacement convergence in 2D beam structure | 54 |
| 4.11 | Displacement plot for coarse and fine nodal density in 2D beam | 55 |
| 4.12 | Von Mises stress plot for coarse and fine nodal density in 2D beam | 55 |
| 4.13 | Geometry of plate with centre circular cut-out (Plate 1) | 56 |
| 4.14 | Geometry of plate with two semi-circular notches (Plate 2) | 56 |
| 4.15 | Geometry of plate with two V-notches (Plate 3) | 57 |
| 4.16 | Displacement plot for fine and coarse nodal density in Plate 1 | 58 |
| 4.17 | Displacement plot for fine and coarse nodal density in Plate 2 | 59 |
| 4.18 | Displacement plot for coarse and fine nodal density in Plate 3 | 59 |
| 4.19 | Von Mises stress plot for coarse and fine nodal density in Plate 1 | 60 |
| 4.20 | Von Mises stress plot for coarse and fine nodal density in Plate 2 | 60 |
| 4.21 | Von Mises stress plot for coarse and fine nodal density in Plate 3 | 61 |
| 5.1 | Crack Tip | 64 |

| | | |
|------|---|----|
| 5.2 | Iterative process involved in crack propagation | 66 |
| 5.3 | Geometry of the plate with centre vertical crack | 67 |
| 5.4 | Node and displacement distribution in plate with centre vertical crack | 67 |
| 5.5 | Von Mises stress distribution in plate with centre vertical crack | 67 |
| 5.6 | Geometry of the plate with inclined edge crack | 68 |
| 5.7 | Displacement and node distribution for plate with inclined edge crack | 69 |
| 5.8 | Von Mises stress distribuion for plate with inclined edge crack | 69 |
| 5.9 | Crack path as shown in literature for plate with inclined crack | 70 |
| 5.10 | Geometry of the punctured plate with edge crack | 71 |
| 5.11 | Displacement and nodal distribution in punctured plate with edge crack | 72 |
| 5.12 | Von Mises stress distribution for punctured plate with edge crack | 72 |
| 5.13 | Refinement of integration cells by sub-dividing each cell into four cells | 73 |
| 5.14 | Refinement of nodes by sub-dividing each triangular cell into four cells | 74 |
| 5.15 | Adaptive refinement of integration cells and nodal density | 75 |
| 5.16 | Strain energy in integration cells of plate with semi-circular notches | 77 |
| 5.17 | Strain energy in triangular cells of plate with semi-circular notches | 77 |
| 5.18 | Displacement plot of adaptively refined plate with semi-circular notches | 78 |
| 5.19 | Von Mises stress of adaptively refined plate with semi-circular notches | 78 |
| 5.20 | Strain energy in integration cells for plate with inclined edge crack | 80 |
| 5.21 | Strain energy in triangular cells for plate with inclined edge crack | 80 |
| 5.22 | Displacement plot of adaptively refined plate with inclined edge crack | 81 |
| 5.23 | Von Mises stress of adaptively refined plate with inclined edge crack | 81 |

LIST OF TABLES

| Fig. No. | Table Title | Pg. No. |
|-----------------|--|----------------|
| 4.1 | Material properties of mild steel used in the thesis | 50 |
| 4.2 | Displacement and stress in the considered 1D beams | 50 |
| 4.3 | SCF values from different methods | 57 |
| 4.4 | Computed displacements and stresses | 61 |
| 5.1 | Computed results for plate with centre crack | 68 |
| 5.2 | Displacement, stress and SIF for plate with inclined edge crack | 70 |
| 5.3 | Displacement, stress and SIF for punctured plate with edge crack | 71 |
| 5.4 | Adaptive refinement iterations in plate with semi-circular notches | 76 |
| 5.5 | Adaptive refinement iterations in plate with inclined edge crack | 79 |

NOTATIONS

| | |
|--------------------------------|---|
| α | Constant in exponential weighting function |
| $\overline{A}, \overline{B}_l$ | Constants in MLS Shape function construction |
| A_C | Cross-sectional area |
| $[A],[D],[Y]$ | Material matrices relating elemental forces and strains |
| \overline{A}_{TC} | Area common to integration and triangular cells |
| a | Crack length |
| B | Strain-displacement matrix |
| b | Width of beam/plate |
| C | Material constants |
| \overline{C} | Material constant under plane stress condition ($\sigma_{zz} = 0$) |
| d | Normalized distance with respect to smoothing length |
| d_w | Smoothing length of the domain in the directions ξ, η |
| δ | Crack opening upon application of load |
| E | Young's modulus |
| ε | Normal strain vector |
| F | Applied force |
| G | Modulus of rigidity |
| \overline{G} | Lagrange multiplier matrix |
| G_I/G_{II} | Energy release rate in mode I/II |
| h | Thickness of beam/plate |
| I | Area moment of inertia |
| J | Jacobian matrix |
| K | Stiffness matrix relating the degrees of freedom in the problem space |
| KI/KII | Stress intensity factor in mode I/II |
| K_{IC} | Critical stress intensity factor |
| κ | Curvature strain vector |
| L | Reference length in a domain |
| l | Length of the plate/beam |

NOTATIONS

| | |
|--------------------------------|---|
| λ | Lagrange multiplier |
| \overline{M} | Elemental moment vector |
| N | Shape function |
| \overline{N} | Elemental Force vector |
| n | Number of Gauss points in the problem space |
| θ | Crack propagation angle |
| $\theta_x, \theta_y, \theta_z$ | Rotations about x, y, z axis |
| P | Applied pressure |
| p | Polynomial defined using Pascal's triangle |
| Q | Shear force vector |
| r | Variable defining the crack length |
| γ | Shear strain vector |
| \overline{S} | Threshold strain energy |
| S_{IC} | Strain energy of the integration cell |
| S_{TC} | Strain energy of the triangular cell |
| σ | Normal stress vector |
| σ_v | Von Mises stress |
| Γ_λ | 1D domain along which the boundary constraints to be imposed |
| τ | Shear stress vector |
| u, v, w | Field variable defining the translations in x, y, z directions respectively |
| W | MLS Weighting function |
| x, y, z | Cartesian co-ordinate system |
| ξ_l, η_l | Nodal coordinates in ξ, η space |
| ξ, η | Natural Co-ordinates system |

ABBREVIATIONS

| | |
|---------|--|
| CDLS | Collocated Discrete Least Squares |
| DLS | Discrete Least Squares |
| EFG | Element Free Galerkin |
| ES-FEM | Edge-based Smoothed Finite Element Method |
| ES-PIM | Edge-based Smoothed Point Interpolation Method |
| EXFEM | Extended Finite Element Method |
| FDM | Finite Difference Method |
| FEM | Finite Element Method |
| FETI | Finite Element Tearing and Interconnect |
| IEFG | Improved Element Free Galerkin |
| MDLS | Mixed Discrete Least Squares |
| MLPG | Meshless Local Petrov-Galerkin |
| MLS | Moving Least Square |
| MLS-SLS | Moving Least Square Stationary Least Square |
| MPM | Material Point Method |
| NE | Natural Element |
| NS-PIM | Node-based Smoothed Point Interpolation Method |
| PIM | Point Interpolation Method |
| RKPM | Reproducing Kernel Particle Method |
| SCF | Stress Concentration Factor |
| SIF | Stress Intensity Factor |
| SOCP | Second-Order Cone Programming |
| SPH | Smoothed Particle Hydrodynamics |

CHAPTER 1

INTRODUCTION

1.1 CHAPTER PROLOGUE

Satisfaction of stability, strength, safety, serviceability and sustainability at affordable costs is the hallmark of good design. Accomplishment of these objectives relies on thorough understanding of geometry and material modelling. An overview of Finite Element Method (FEM), Extended FEM (XFEM) and MeshFree method in modelling structures with high stress gradients, their strengths and weakness have been highlighted. Element-Free Galerkin formulations which are the most popular in MeshFree methods have been discussed and motivation for “Meshfree Technique with Adaptive Refinement Strategy for Crack Propagation Analysis” research, objectives and organisation of thesis are presented.

1.2 MATHEMATICAL MODELLING AND SIMULATION

Tremendous progress and advancements in FEM has greatly helped modelling and simulation of high stress gradients and crack propagation analysis. XFEM and MeshFree methods have evolved from FEM, further enhancing modelling and simulation in crack formation- propagation studies and the following section presents the development.

1.2.1 Strong and Weak-Form

Satisfying equilibrium of the structure is essential boundary condition and compatibility criterion is non-essential boundary condition. Strong-form solutions satisfy both essential and non-essential boundary conditions, at every point with the partial differential representation. When it is difficult to arrive at strong-form solutions, weak-form approach is adopted, where the differential equations are converted to an integral form, which requires lower order of polynomial function as solution to the problem. Weak-form satisfies essential boundary conditions and non-essentials are satisfied on an average sense over the entire problem space. Galerkin’s

INTRODUCTION

weighted residual method or Rayleigh-Ritz's stationary energy principle are the popular solution techniques. Wherein polynomial / trigonometric functions, Fourier / Taylor series etc. that satisfy the essential boundary conditions are assumed as approximate solution to the partial differential equation. The constants involved in these assumed approximation functions are determined by making the weighted residual or potential energy minimum.

Complex geometries and satisfaction of essential boundary conditions when are difficult, piece-wise polynomial that satisfy partial differential equations within a smaller domain is assumed. This is accomplished by discretizing the problem space. Discretization is named as finite elements in FEM, grids in finite difference method, finite volumes in finite volume method and domains in MeshFree method.

1.2.2 Finite Element Method

FEM is one of the very well developed numerical techniques used for solving most of the engineering problems. FEM gained its popularity as it is generic and can be applied to any kind of problems related to structural mechanics, heat transfer, fluid flow or electromagnetic field. In FEM (Robert et al., 2001, Zienkiwicz et al., 2005), the whole structure is discretized into finite elements. These elements have regular shapes, such as a line in case of 1D, triangle or quadrilateral in case of 2D, tetrahedron, pentagon or hexagon shape in case of 3D modelling approaches. These elements are interpolated using linear, quadratic or cubic polynomials. Figure 1.1 shows the different types of linear interpolation finite elements that are popularly used to discretize the problem space in structural mechanics. The computed stiffness matrices of the elements are assembled to form the global stiffness matrix. The loading and boundary conditions are then applied to solve for nodal displacements. The strains and stresses are computed from the displacements using strain-displacement and material matrices. The flow chart of FEM is given in Figure 1.2. The method is simple and very effective in solving most of the engineering problems.

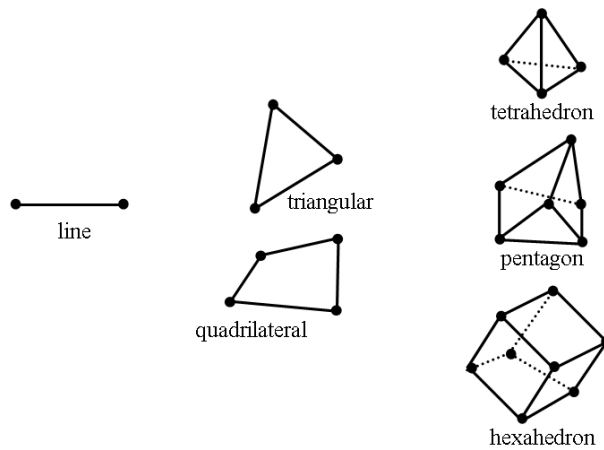


Figure 1.1 – Different types of linear finite elements used for domain discretization

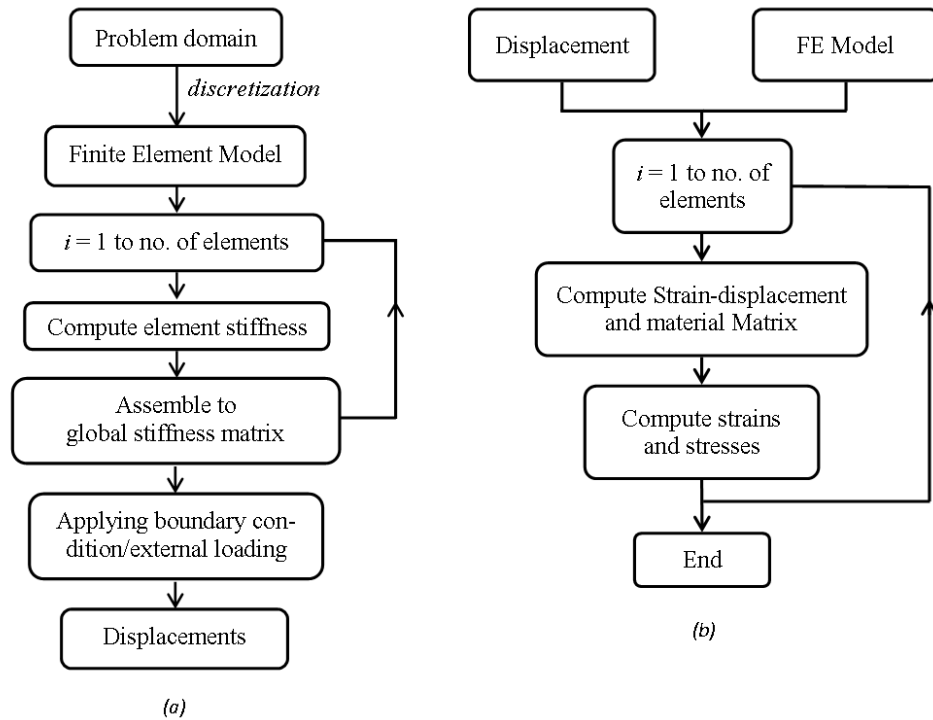


Figure 1.2 – Flow chart for Finite Element Method

1.2.3 Extended Finite Element Method

When discontinuities within the elements like crack propagation have to be modelled, the problem space needs to be remeshed at each stage of propagation and reliance on an automated remeshing algorithm is inevitable. Automated remeshing in FEM is very complex to achieve a pre-defined mesh quality as human intervention is necessary. This difficulty has been overcome in XFEM by enriching with

INTRODUCTION

discontinuous functions to model cracks. XFEM coupled with FEM helps in modelling propagation of crack tip.

1.2.4 MeshFree Method

It is well known and understood that analysis results of FEM are heavily influenced by the discretization i.e. meshing. MeshFree methods do away with requirement of a predefined mesh. In MeshFree techniques shape functions are constructed at points of interest using neighbouring nodes during the analysis stage. The MeshFree method offers additional advantages and capabilities to enhance compliance, convergence and completeness. Computed stresses using neighbouring nodes in MeshFree formulations will be much smoother across problem space, which is not accomplished in FEM at element boundaries. Further, the method is amenable for automating the nodal distribution by triangulation of the problem space. Nodes may be added or deleted as and when required to study more comprehensively the stress concentration and crack propagation problems. The node based approach of MeshFree methods permit employment of polynomials of any order as warranted by the smoothness of the stress distribution desired.

1.3 DIFFERENT METHODS IN MESHFREE TECHNIQUE

Some of the commonly adopted MeshFree methods are Smoothed Particle Hydrodynamics (SPH), Element-Free Galerkin (EFG) method, Meshless Local Petrov-Galerkin (MLPG) method, Reproducing Kernel Particle Method (RKPM), Point Interpolation Method (PIM), Finite Difference Method (FDM), Natural Element (NE). Further, they are also classified on the following basis

1.3.1 Classification Based on Shape Function Construction

MeshFree methods get classified to three groups based on shape function representation in terms of field variables as integral (SPH, RKPM), series (MLS, PIM) and differential (FDM) representations. A good comparison of these methods and their application with effect on computation and accuracy are discussed by Belytschko et al. (1996).

1.3.2 Classification Based on Formulation

Formulations by both strong and weak-form are available (Liu and Gu 2005). Collocation methods are strong-form that do not need background cells and hence are truly MeshFree. Notwithstanding their truly MeshFree characteristics, these methods pose numerical instabilities and convergence problems. PIM which is a weak-form formulation helps reduce numerical instability and permits usage of higher order polynomials for better convergence. Weak-strong-form that are combinations of strong and weak-forms like SPH, offer combined advantage of both the formulations and suppress the disadvantages. An extension of weak-form formulations called global or local are adopted that help in smoothing of response. EFG, RKPM, MLPG method, *hp*-cloud and partition of unity FEM fall into this form.

1.3.3 Classification Based on Integration

Integration required for computation of sub-domain stiffness necessitates employment of background cells. In addition to utility in integration to determine stiffness, it influences convergence and accuracy. Direct usage of background cells as in EFG, node/edge based smoothing techniques as in PIM ranging from very simple to sophisticated suggestions for implementation of integration are available.

1.4 ELEMENT-FREE GALERKIN METHOD

EFG is the most popular MeshFree method used to address problems related to structural mechanics. Belytschko et al. (1994) proposed the development of EFG method from diffuse element method which uses MLS for shape function construction. The important steps in implementation of EFG method are discussed in the sections that follow.

1.4.1 Discretization of Problem Space

Discretization includes the distribution of nodes and the arrangement of square integration cells in the problem space. The nodes are distributed by triangulation scheme, for 2D problem with finite number of triangular cells such that the geometry of the problem space is effectively captured. In case of 3D space, tetrahedral cells

INTRODUCTION

may be used for the purpose. The vertices of the triangular or tetrahedral space also aids in identifying the neighbouring nodes, geometrical free edges and application of forces, boundary conditions. There are various algorithms available for triangulation schemes such as the Delaunay algorithm and advanced front-end algorithms which are commonly adopted in MeshFree methods for nodal distribution.

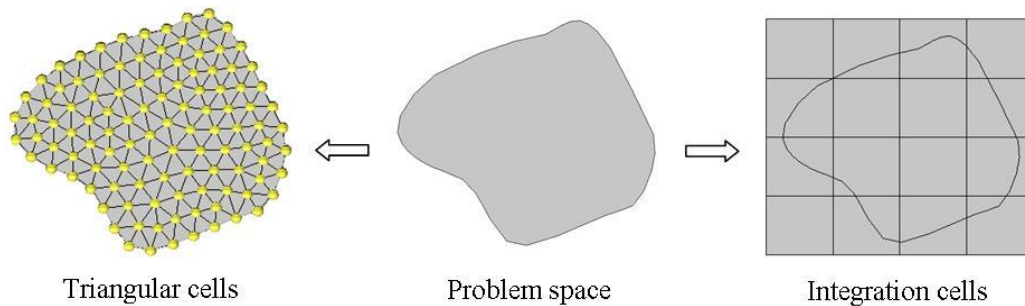


Figure 1.3 – Problem space with triangular cells and integration cells

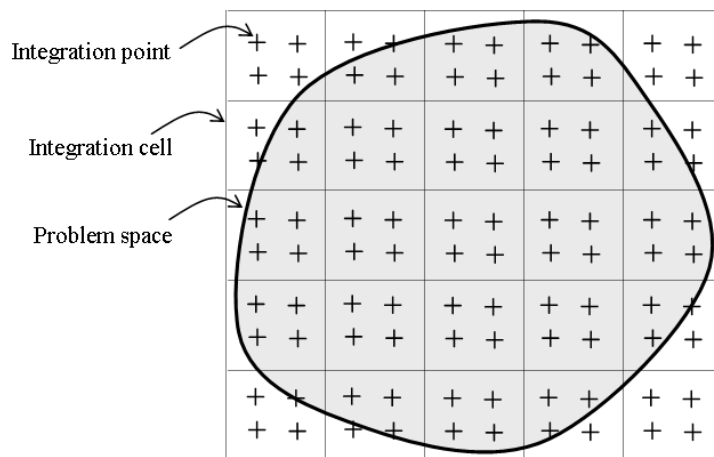


Figure 1.4 – Problem space with integration cells (background cells)

Further, to carry out numerical integration, square cells are identified using horizontal and vertical lines, so as to cover the entire problem space (Figure 1.3). The Gauss points (Figure 1.4) lying within the problem space is taken for integration. The number of Gauss points considered plays a major role in the accuracy of the solution. Liu (2009) gives suitable recommendations for Gauss and node point allocation in problem space.

1.4.2 Support and Influence Domain

Some important terms in MeshFree method like node, influence domain, support domain, integration point and integration cell are shown in Figure 1.5.

Node - is a point in the problem space where response characteristics are required.

Influence domain – is the region of the problem space around a node inquisition where response characteristics are interpolated locally.

Integration point – point in the background cell at which stiffness is determined.

Support domain – region around an integration point that identifies nodes supporting the point for formulation of shape functions.

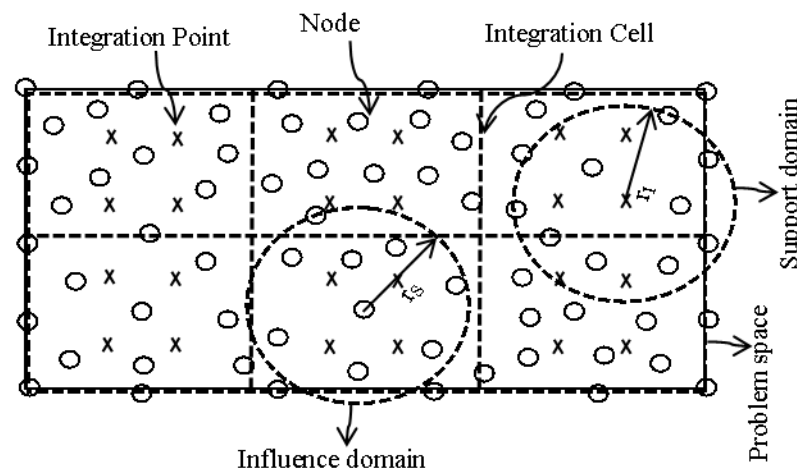


Figure 1.5 – Problem space in MeshFree method with nodes, point-of-interest, domain and integration cells

The support or influence domain determines the number of nodes to be used for approximation of the unit cell's interpolation function. These can have different shapes such as circle, ellipse, square or rectangular. The radius of the domain is constructed by taking the average distance to the neighbouring nodes and these nodes are chosen by T6 or T2L schemes as discussed by Liu (2009). Further the nodes in the domain are assigned with weights, which vanish as they tend to boundary.

The support domain is centric to the point-of-interest and it works well when the nodes are uniformly distributed and the nodes chosen are balanced about the point-of-interest. When the nodes are non-uniformly distributed the influence domain is

INTRODUCTION

advantageous as it is centric to node. Each node in the problem space has a domain of influence and the nodes exerting the influence over the point-of-interest are chosen for the construction of shape function. Figure 1.5 shows the influence region of support and influence domains.

1.4.3 Formulation of System Equations

The shape function in EFG method is formulated using MLS technique and the integration cells are used to carry out integration of the problem space. The integration cell has distributed Gauss points (Figure 1.4) and at each Gauss point (point-of-interest/ integration point) the shape function and subsequently the stiffness matrix is computed. The shape functions computed using MLS technique generally does not satisfy the Kronecker delta property. Therefore, the boundary conditions are imposed through Lagrange multipliers. The sequential steps in implementation of EFG using MLS are shown in flow chart (Figure 1.6).

1.5 CRACK PROPAGATION

A crack is a structural damage in the form of propagating fracture characterized by sharp tip and high ratio of length to width. High stresses during fabrication or service are causes for crack formation and propagation. It is one type of damage which many times cannot be seen through naked eyes. Cracking can lead to catastrophic failure of the structure. Crack formation-propagation studies are being extensively made to understand the phenomenon better and to render structures more safe and reliable.

Primary modes of crack propagations are identified as Mode I (opening mode), where tensile load normal to the crack surface is applied, Mode II and Mode III are sliding modes which occur when shear force parallel to the crack surface and perpendicular to crack front (Mode II) and parallel to crack front (Mode III). Pictorial representations of the modes are shown in Figure 1.7. Crack formation and propagation patterns usually observed may be of the above type and many a times are due to a combination of the types making classification to any one mode impossible.

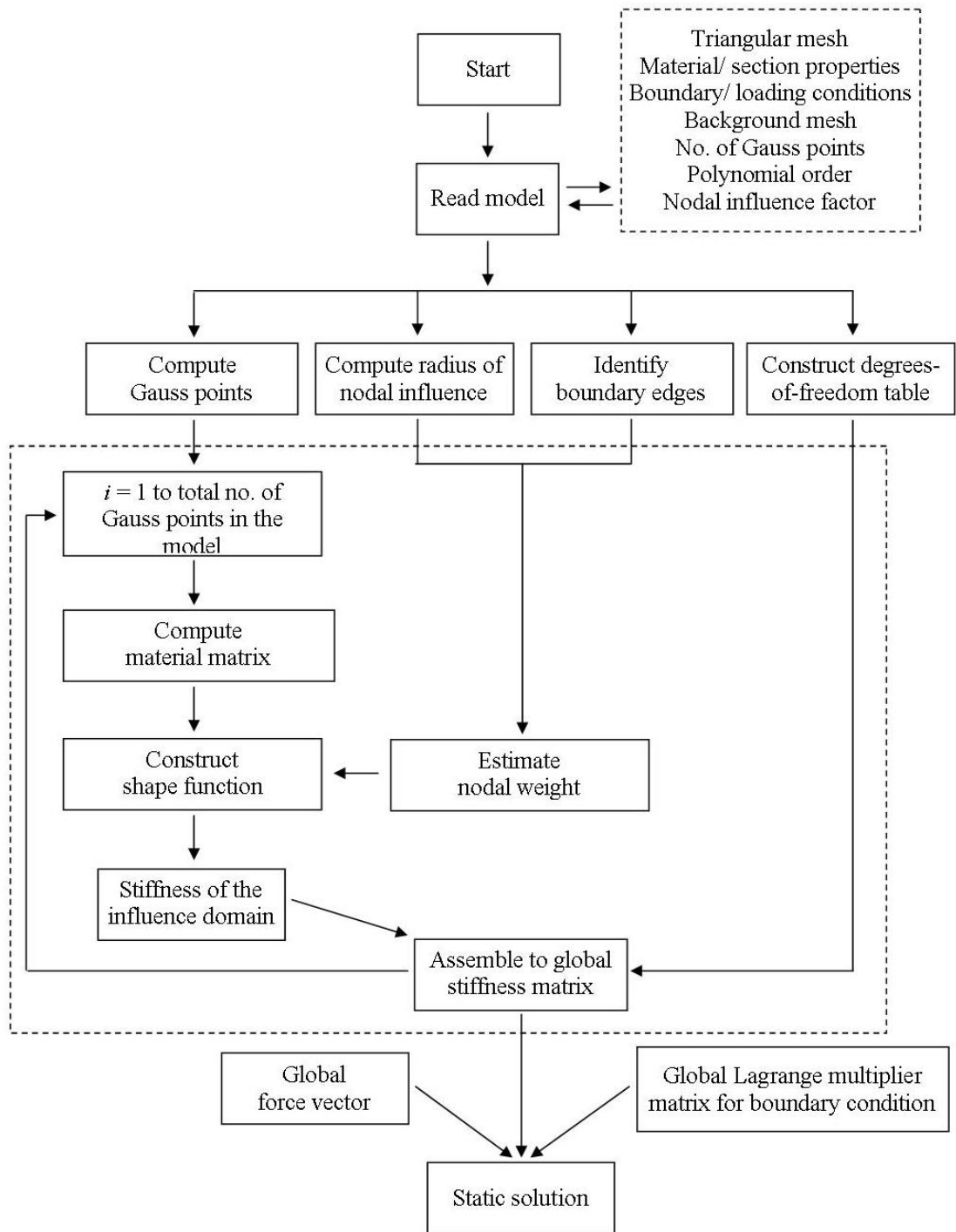


Figure 1.6 - Methodology in MeshFree

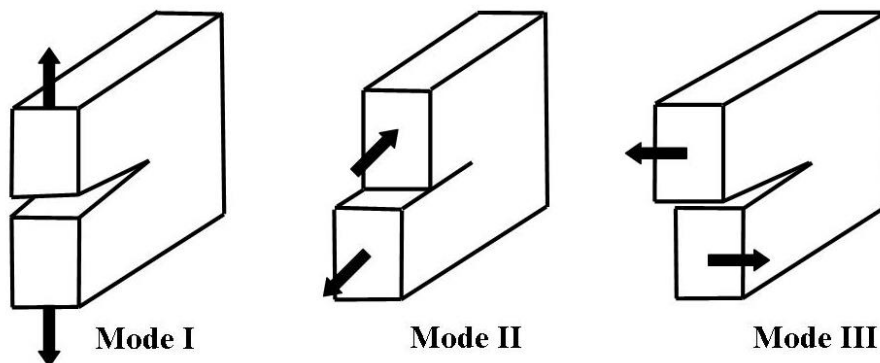


Figure 1.7– Modes of crack propagation

1.6 ADAPTIVE REFINEMENT

In numerical modelling and analysis of any structural system, arriving at the right number of nodes and their distribution is not an easy task. Intuitive judgments, past experience are of help sometimes. Usually one starts with coarse nodal density in the first attempt that gets refined in subsequent attempts by way of increase or decrease of nodes and their relocation. This approach though is interactive is a time consuming feed forward, feedback technique. Availability of an adaptive refinement algorithm greatly enhances understanding of crack formation and propagation studies. This approach is gaining popularity.

1.6.1 Refinement Strategy

MeshFree method has the advantage of using adaptive techniques in a much simpler way because of its ease to introduce, discard or move the nodes within the problem space as there is no predefined connectivity between them. There are mainly two types of errors that are associated with some numerical methods, namely interpolation and integration errors. Interpolation error can be reduced by increasing the order of a polynomial or number of nodes in the domain; whereas an integration error is minimized by increasing the Gauss points (Liu and Tu, 2002) or integration cells. The two important aspects to be considered while using adaptive refinement are error estimation and identification of refinement region.

The popular methods of error estimation are residual method, posterior method and smoothing based methods. Further refinements are carried out by p -refinement and h -

refinement. In p -refinement the order of the polynomial is increased and in h -refinement more nodes are added to the problem space. Mesh refinement has three types, namely, type one called mesh movement where the number of nodes are fixed and based on the errors, the nodes are relocated to minimize errors. Type two is known as mesh enrichment, which keeps the original nodes fixed and additional nodes are added when and where required. Remeshing is type three refinements which generates the new mesh from the previous data.

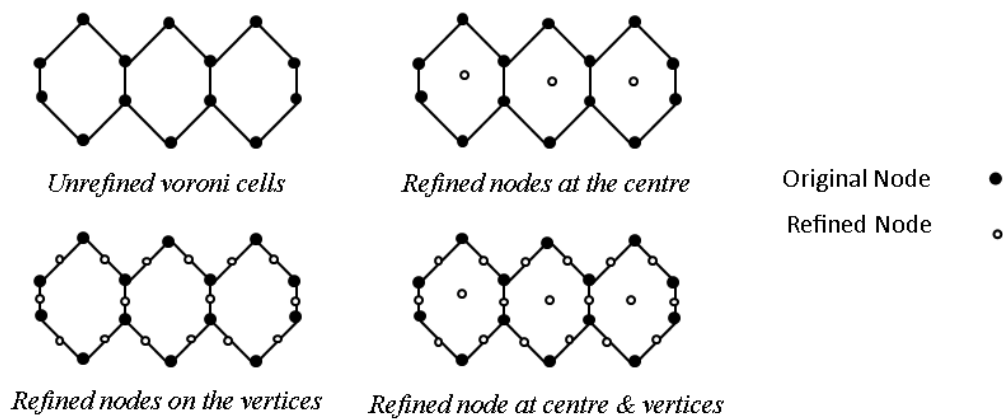


Figure 1.8 – Voronoi cell for nodal refinement

Generally remeshing is avoided as this is cumbersome and more of human intervention is required that makes coding difficult. Mesh movement can be well adapted to MeshFree methods. The mesh enrichment method is more convenient for automation. Usually triangular elements are used for the nodal distribution and during refinement nodes are placed at the centre of the cell and on the vertices. The same strategy can be used in case of quadrilateral elements or Voronoi cells (Figure 1.8) for nodal distribution.

1.7 OBJECTIVES

1.7.1 Motivation for the Work

FEM has the advantage of being computationally very efficient, but has unresolved issues in capturing the high stress gradients. This difficulty is overcome by MeshFree methods which can handle high stress gradients very efficiently. The high

INTRODUCTION

computational time demands of MeshFree methods offer tremendous scope for refinement and enhancement of capabilities of the technique in crack formation-propagation studies. Wherein adaptive refinement schemes are a necessity, deserving attention and exploitation.

1.7.2 Objective of the Research Work

The primary objective of the thesis work is to develop an *Adaptive refinement scheme for EFG based MeshFree method for modelling and simulating high stress gradients in plate structures*. The proposed objective has been accomplished by the phases as detailed.

- ✓ Mathematical formulation of EFG based MeshFree method for 1D beam analysis and its programming in MATLAB[®] and its verification and validation using benchmark problems of beam bending.
- ✓ Algorithm development for analysis of stress concentration effects and its extension to crack formation-propagation studies.
- ✓ Development of strain energy based adaptive refinement scheme to improve the computational efficacy of the 2D MeshFree analysis code considering refinements to node distribution and integration cells and demonstration of efficacy of scheme proposed.

1.8 ORGANISATION OF THE THESIS

A general introduction to mathematical modelling and simulation in the emerging area of MeshFree, FEM and its utility in crack formation-propagation studies has been highlighted in Chapter 1. Motivation for the present work, scope and objectives has also been outlined.

Chapter 2 provides an overview of the state-of-art of MeshFree for modelling crack propagation and the utility of adaptive refinement techniques in improvement of computational efficiency. Comparison of FEM, XFEM and MeshFree methods in modelling crack and its propagation has been detailed. Advancements in PIM, EFG and other MeshFree methods techniques have been discussed and adaptive refinement strategies have been reviewed, highlighting the need for the present work.

The formulation of EFG method based on MLS technique has been presented. Construction of MLS shape functions using nodal weighting functions has been explained. The modelling of 1D and 2D MeshFree formulation, strategies for addressing boundary conditions by Lagrange multipliers are elaborated in Chapter 3.

The verification of the developed code based on the EFG method for both 1D and 2D problems are discussed in Chapter 4 with convergence studies that have been carried out for 1D beam and 2D beam using EFG method and FEM, and have been verified with the closed-form solutions. Comparison of Stress Concentration Factor (SCF) for plates having high stress gradients regions by EFG method, FEM and closed-form equations has been done to demonstrate the efficacy of the EFG method.

Chapter 5 explains utility of MeshFree method in crack propagation analysis. The superiority of the method in computing the stresses around the crack tip has been illustrated. Crack propagation pattern prediction capabilities have been checked and verified for mixed mode (mode I and II) loading with results reported in literature (Patricio and Mattheij, 2007). Refinement strategy developed based on strain energy computed in the integration and triangular cells has been tested and validated.

Highlights of the current investigation on utility of EFG method in crack formation-propagation studies has been presented with details of accomplishments of the objectives, contribution to advancement of the current analytical investigation to the area of research interest has been elaborated. Suggestions have been made on scope for future work in the concluding Chapter 6.

CHAPTER 2

OVERVIEW OF LITERATURE

2.1 CHAPTER PROLOGUE

MeshFree methods for modelling crack propagation are becoming popular, with adaptive refinement technique. Limitations of FEM in crack propagation studies and extension of FEM to XFEM and recognition of potentials of MeshFree methods in crack analysis, tremendous need and scope for research in this area discussing the state of the art has been presented in the sections that follows.

2.2 FINITE ELEMENT METHOD

Tremendous efforts have gone into modelling cracks and simulate its propagation through the structure. A crack cannot be numerically initiated. A pre-initiated crack is first modelled and then the propagation is simulated. Crack propagation involves topological changes and necessitates continuous remeshing in its analysis. Crack growth and its direction are derived using the many criteria based on stress. One such approach is by using asymptotic FEM (Andrzej, 2002), where analytical constraints of asymptotic crack tip field are applied to conform the solution. Here, the quadrilateral element having linear or constant stress distribution is converted into triangular elements with hyperbolic singularity. With this method, highly discontinuous and local phenomenon has been observed. Modelling of cracks involving mixed modes has been attempted (Bouchard et al., 2003), where different crack growth and path criteria such as maximum energy release and circumferential stress/strain energy densities have been considered. This method involves remeshing based on attaining the criteria at the end of each iteration step. Further, a scheme based on unfitted FEM (Anita and Peter, 2004), where the region of crack interface is separated by modelling it as a spring type constraint and has been used to model perfectly and imperfectly debond conditions. Penalty parameters are used to define the bonding at the interfaces and has been arrived at its value based on the interface and mesh conditions. The modelling of crack as discontinuity by introducing additional degrees-of-freedom at

existing nodes (Mergheim et al. 2005) though similar to XFEM, but cannot be applied to explicit problem. The element here is represented by two sets of basis functions, one which will be zero on one side of the discontinuity and will take the usual values on the other side and vice versa for the other basis function. To further address the modelling of stress gradients, Moving Least Square (MLS) technique for shape function construction in FEM to solve non-matching mesh has been attempted (Liu et al., 2009). This approach becomes very useful when one needs to have a very refined model in the place of high stress gradients. Therefore the model will now have regions with fine and coarse mesh, which have non-matching boundaries. The challenging work of simulating dynamic crack growth using time-integration scheme has been reported (Rethore et al., 2004), where the major concern of stabilization of scheme and energy from the crack has been highlighted. Various numerical problems with different meshing were considered in the study to arrive at the required condition for stability and accuracy. Based on this study a theoretical scheme using an energy approach had been proposed, which lists the conditions required to guarantee the stability and accuracy of time integration step. Further the paper concludes that even using a coarse mesh and a large time step, if projections are balanced and time integration for the given crack length is stable, then accurate results from the energy standpoint can still be obtained.

As one may understand from the above discussion that in FEM, the shape functions are pre-defined for a set of nodes and the stiffness matrices are defined for the regular standard shapes. Therefore, in FEM for any given shape of element the stiffness matrices are derived by mapping. This mapping procedure is the one that introduces the major interpolation errors in FEM and is very severe when the elements are distorted. Therefore, in FEM, one follows predefined mesh quality criteria during meshing and this requires human intervention. These make FEM computationally very expensive for adaptive refinement and modelling crack propagation.

2.3 EXTENDED FINITE ELEMENT METHOD (XFEM)

FEM follows the crack edge for the propagation of crack in spite of all the efforts made to address crack related problems. In XFEM, the crack tip is enriched using

additional degrees-of-freedom and the interpolation is defined using enrichment functions. The basic idea of XFEM is that of using discontinuous fields in the required region and continuous fields where it is not required. The addition of these two gives the actual displacement interpolation in the domain.

Cracks which are arbitrarily aligned within the mesh are dealt with using the enrichment functions which consists of discontinuous displacement fields. Enrichment or smoothing is done using some of the special functions such as Haar function (Equation 1), Heaveside function (Equation 2) and partition of unity.

$$f(x) = \begin{cases} 1, & 0 \leq x < \frac{1}{2} \\ -1, & \frac{1}{2} < x \leq 1 \\ 0, & \text{otherwise} \end{cases} \quad \dots 2.1$$

$$f(x) = \begin{cases} 0, & x < 0 \\ \frac{1}{2}, & x = 0 \\ 1, & x > 0 \end{cases} \quad \dots 2.2$$

The enrichment and smoothing functions used to model the crack path and tip has been discussed in detail by Belytschko and Black (1999). Studies on enriching the displacement approximations by the discontinuous fields to model the crack and asymptotic field near crack tip using a partition of unity has been reported by Nicolas et al. (1999) and John et al. (2000). Further the use of partition of unity to the displacement fields can solve branching and intersecting cracks (Sukumar et al. 2000) and demonstration of the procedure by computing Stress Intensity Factor (SIF) using different benchmark problems have been addressed in the work. The modelling of 2D and 3D cracks in discontinuous displacement field using the partition of unity (Sukumar et al., 2003) proved to be efficient without remeshing.

In literature, the level set Method has been used to track the interface motion. If the interface which has to be captured is set to zero, then the order of the space is taken 1D more than the interface, i.e. if the crack is 2D, then space should be 3D. Level set theory with FEM has been used to update discontinuities on the surfaces by Belytschko et al. (2001) and signed distance functions have been used to represent the discontinuous functions. In XFEM with level set method, where the mesh remains

same with the growth of the crack has been attempted (Stolarska et al. 2001). Signed distance functions are used to model the enrichments and these satisfy partition of unity property in the entire problem space and have been used by Goangseup and Belytschko (2003). One type of enrichment function is sufficient and it is applied on three and six noded triangular elements. The Newton - Raphson method has been adopted to solve the equilibrium equation to obtain field variables. Curved cracks with higher order enrichments applied to static cohesive cracks has been demonstrated by the authors. A detailed review on various problems dealing with modelling individual crack, representing crack in level set method and also various enrichment techniques have been reported by Karihaloo and Xiao (2003). The stress fields similar to that of the analytical solution are combined with the FE shape function; to arrive at the partition of unity around the crack tip has been attempted by Fan et al. (2004). Further, Goangseup et al. (2004) attempted to capture multiple cracks using step and tip enrichment functions. Improved techniques in crack tip enrichment and use of asymptotic function has been addressed by Yazid and Abdelmadjid (2008). The authors have also discussed on methods to deal with calculation of stresses, SIF and various convergence techniques. Adaptation of this method using ABAQUS[®] software has been discussed by Giner et al. (2009), where the software uses Heaviside function for the enrichment of the region around the crack. Some of the problems dealing with jumps, kink cracks, singularities are solved using XFEM and has been reviewed by Thomas and Belytschko (2010). They have discussed on various methodologies in XFEM, which deals with the application of boundary condition, blending of elements with different shape function, use of higher order polynomials, time integration and integration errors. In spite of incorporation of above mentioned advancements, XFEM has limitations in computing smoother stresses in the high stress gradient regions and this has led to the need for development of MeshFree methods.

2.4 MESHFREE METHOD

FEM is an element based method, whereas MeshFree (Antonio et al., 2004) is a node based technique. In MeshFree method, the stiffness matrix is derived for a given point-of-interest by constructing shape function using neighbouring nodes. This

approach of shape function construction ensures smoother interpolation of field variables and its derivatives throughout the problem space. The stress distribution, thus computed will be smoother and will not have a stress/strain jump at the same node as seen in FEM. The following are some of the methods that are adopted for construction of shape function in MeshFree methods, namely Kernel approximation, radial basis function and Moving Least Square (MLS) (Lancaster and Salkauskas, 1981) method. A good comparison of these methods (VinhPhu et al. 2008) and its application with its effect on computation and accuracy has been discussed by Belytschko et al. (1996).

2.4.1 Element-Free Galerkin (EFG) Method

In the EFG method, arriving at an appropriate size of the domain is very critical as this plays the role of coupling the neighbouring nodes. Krysl and Belytschko (1999) have studied the influence of choosing the domain size, where they have arrived at a size of 3.9 times the nodal spacing. Small domain of influence improves local resolution and increases sparsity of the stiffness matrix. EFG based modelling schemes for 1D beam and 2D plate structures have been discussed by Dolbow and Belytschko (1998). Even the EFG method undergoes volumetric locking when the size of the domain is small. In case of large domains, more nodes contribute to the approximation resulting in no volumetric locking. Linear approximations will not satisfy the incompressibility constraint and do not match the deformation field resulting in the deterioration of accuracy and rate of convergence. Reduced integration has been adopted to overcome locking by John and Belytschko (1999a). Further, John and Belytschko (1999b) have discussed on the alignment of the support domain with background cells in order to reduce integration error. A bounding box technique for numerical integration that is the use of the intersected area for the integration has improved the rate of convergence. Modal analyses have been carried out to study the locking effect (Antonio and Sonia, 2001).

Studies on the initiation and propagation of cracks have been carried out based on the different stress criteria; some of them are strain gradients, SIF, Rankine criterion (principal tensile stress reaches the uniaxial tensile strength at a node) and Loss of

hyperbolicity criterion. The arbitrary crack growth in static problems without much remeshing has been attempted by Belytschko et al. (1995a). EFG has proved to be effective without any enrichment of the displacement field near a crack tip and crack growth has been modelled without remeshing. In this work (Belytschko et al. 1995a) penalty method has been adopted to impose boundary conditions, which has advantages of arriving at banded positive definite stiffness matrix. The authors (Belytschko et al. 1995a) have validated EFG method using some of the numerical problems such as hole and edge crack in an infinite plate to obtain the SIF and it has been proved to be near to the exact solution. Crack propagation has been studied by considering different patterns of node distribution in the domain, of which radial pattern is proven to be effective. They have also thrown light on the studies of dynamic crack propagation. Modelling of growing cracks has been carried out without remeshing, just by extending its surfaces. Moving mesh technique in which nodes are fixed and have been moved till equilibrium is maintained. But the method has the difficulty in propagating cracks in arbitrary directions. Belytschko and Tabbara (1996) have addressed the problems related to arbitrary crack growth in anisotropic materials and also nonlinear problems.

In linear elastic problems, EFG method has been adopted by Mark (1997) using enrichment techniques. The two methods of enriching the field approximation in EFG method, namely intrinsic and extrinsic enrichments have been discussed. The crack contact analysis algorithm has been presented that simulate cracks in sliding contact. Problems involving fatigue and quasi-static crack propagation have been solved to demonstrate the efficiency of EFG. Fleming et al. (1997) have extended the same work on curved cracks. Modelling of crack in 2D and 3D modelshave been discussed by Petrand Belytschko (1999). As the crack propagates, shape functions are approximated without remeshing the region. Star shaped nodal arrangement around the tip and regular nodal distribution elsewhere to simulate arbitrary dynamic cracks in the elastic model has been suggested by Belytschko et al. (2000).

The use of the level set method for the studies on crack propagation has been carried out using nodal data by Ventura (2002). Crack approximation using a jump function that accounts for displacement continuity and Westergard's solution for enrichment at

crack tip has been presented. Further studies on stationary crack in 2D functionally graded materials of arbitrary geometry have been carried out by Rao and Rahman (2003). Problems dealing with first mode and mixed mode for calculating SIF and validating with other numerical techniques have been illustrated. Further, the authors have suggested on the study of multiple cracks as a scope for future work. Rabczuk and Belytschko (2003) presented a scheme to model cracks, where the discontinuity introduced due to crack has been brought in through the discrete crack model. The plasticity in the model is applied till the region (where crack is to be introduced) reaches the threshold stress value, after which the discrete crack has been introduced; numerical results were verified with experimental data. Further Rabczuk and Belytschko (2004) modelled arbitrarily oriented cracks by use of local enrichment sign functions. MLS method for the construction of shape function by Huerta et al. (2004) has shown increased accuracy and convergence without the problem of locking.

The jump in the displacement field has been used to represent the crack, which is defined by discontinuous function and the closing of the crack tip by crack front function. Extended MeshFree method based on local partition of unity for cohesive crack has been presented by Timon et al. (2007), Goangseup et al. (2007) and Timon and Goangseup (2007). In the second paper instead of crack front function, Lagrangian multiplier has been used to achieve the same. In the last paper 3D MeshFree methods with non-linear material models for crack (with crack tip in influence domain) initiation and propagation have been discussed. Numerical results have been presented for several quasi static and dynamic crack propagation problems. Further comparisons have been made with the available analytical and experimental results.

Extended EFG method for modelling crack initiation, propagation and branching have been discussed by Bordas et al. (2008). The intrinsic and extrinsic approaches of modelling crack have been discussed; where the intrinsic approach can model only straight crack. The former uses discontinuous enrichment along with a Lagrange multiplier to close the crack front. Non-linearity has been introduced in crack propagation by Arun et al. (2010); this problem was tackled using EFG and Newton-

Raphson algorithm. The aspects such as the effect of initial crack, its growth and its effect on structural responses have been discussed. The concept of Bordas et al. (2008) has been extended by Pant et al. (2013) by introducing modifications to the intrinsic approach for modelling kinked cracks and discussions about the successful implementation of simulating quasi-static crack growth have been presented.

EFG method for modelling crack without surface creation has been attempted by Wang and Wang (2010). In this work, local enrichment of the trial function (sine function) for modelling and the effect of discontinuity on the influence domain of the node have been studied. Application of partition of unity in EFG method improved the rate of convergence and also accuracy as shown by Eigel et al. (2010). Pinkang and Dongdong (2012) have reported that the EFG method is more accurate compared to FEM and its workability is tested on rod and beam elements. The MeshFree methods being computationally expensive, a decomposition method has been proposed by Metsis and Papadrakakis (2012) known as the dual domain decomposition Finite Element Tearing and Interconnect (FETI) family method. The MeshFree method is subdivided into several overlapping sub-domains and the non-overlapping sub-domains by modifying the required displacement compatibility conditions. The results obtained and efficiency of the formulated method has been presented.

2.4.2 Point Interpolation and Other Methods

Point Interpolation Method (PIM) is an extension of EFG method, in which the shape functions satisfy the Kronecker delta property. In this method the shape functions are defined based on the approach followed in FEM, i.e., the assumed polynomial consists of constants equal to the number of nodes. The studies such as locally smoothing the strain field using triangular background meshes have been discussed by Xu et al. (2010). This method assures good convergence and also solutions obtained are bound from both sides. But in this method, problem of singularities has been observed and hence in order to overcome this issue radial basis functions have been adopted by Chen et al. (2010) and Cui et al. (2011). In Chen et al. (2010), different types of smoothing operations and their advantages have been discussed. In Cui et al.

(2011), edge based strain smoothing with linear interpolation technique, which provides computational efficiency has been discussed. This method has proved to be more accurate than the traditional FEM and PIM. Ferreira and Roque (2011) have presented the formulation of global unsymmetrical collocation radial basis functions based method to compute elliptic operators.

Thomas and Hermann (2004) elaborate MeshFree methods that have been based on the boundary element method, collocation method and RKPM. They have also discussed different types of integrations carried out, like direct nodal integration, background cell integration and integration over the support domain. Finite Difference Method (FDM) is one of the traditional strong-form methods; similarly collocation methods are MeshFree strong-form method. Point collocation method to model interface problems and intrinsic wedge enrichment is added to the basis function of the MLS. Numerical results have been presented to show its application to straight and curved boundaries. Use of localized radial basis approximation for the shape function construction in Chen et al. (2011b) proved to be accurate, though it is unstable. In order to obtain stability, Mohamed et al. (2012) have adopted shape function construction by using a linear interpolation function using MLS and radial basis function. This method has been proved to be efficient for the boundary value problem.

Integration is dependent on the overlapping domains and partition of unity has been used to solve the problem. Gu (2005) has discussed the development of MeshFree methods with respect to construction of shape functions and the quality of the interpolation. Further Marjan and Roman (2008) used the MLPG method to arrive at the constant number of nodes in the domain for shape function construction to a particular domain size. The line element method has been developed by Paola et al. (2008) and has adopted harmonic polynomials (Laurent Series) which satisfy the field variables in the entire domain. System equations have been solved using weak-form criteria that the square net fluxes are minimum across the border.

2.4.3 Coupling MeshFree Methods

Combinations of some of the MeshFree methods have been considered in order to increase the efficiency by decreasing the computational time. Hence methods like EFG, SPH, RKPM, MLPG, PIM and NE are coupled with each other to address some of the special issues. One such combination has been adopted by Chinesta et al. (2007), where enrichment to RKPM has been provided, but the method did not result in efficient results. Later MLS has been adopted to obtain the shape functions for NE method and this has been fused with the RKPM enrichment. This method has been adopted for several numerical examples and they have proved to be efficient. The section has also discussed on the advancements of the old techniques which aids in improving the accuracy and computational efficiency of the method.

A new weight function has been proposed by Thomas and Christian (2005), using which the boundary conditions have been imposed directly on to the nodes. It has also been found that with this method more stable results for varying size of the influence radius have been obtained. Zan et al. (2009) has derived the EFG method using weighted orthogonal basis function and has termed it as Improved EFG (IEFG) method. With this orthogonality property, the coefficients in improved MLS will be lesser than the MLS approximations and therefore will be more computationally efficient. Further new integration approach using the support domain unlike in traditional method where integration cells have been used is presented by Yan and Belytschko (2010).

In recent years, development of different materials has led to the demand for developing efficient numerical technique for their analysis. Composites and functionally graded materials are efficiently modelled using MeshFree methods which otherwise are difficult using FEM. Liew et al. (2011) have reviewed on different types of analysis used for such materials and the authors have mentioned the scope for development of these methods in 3D problems.

The other advancement in MeshFree methods with different shape for influence domain has been presented. Usually influence domains are circular or rectangle; they have suggested arbitrary convex polygon shape. This approach helps in reducing the bandwidth of stiffness matrix and also boundary condition implementation has been

made easy. Change in shape of influence domain has shown accurate results with lesser computational time. Use of elliptical shape functions instead of linear, quadratic functions and MLS method with penalty function by Hae et al. (2012) has been proved to be efficient. Higher order polynomials are used and this function has been efficient when applied to different shapes of plate under different loading and boundary conditions. Xiaoying et al. (2012) discussed on the discretization error control in EFG method, as in MeshFree methods the errors cannot be categorized as errors due to insufficient nodes or insufficient basis function. Further, it has also been highlighted that arbitrarily setting the size of nodal supports can severely affect the error control and solution accuracy.

2.5 HYBRID NUMERICAL METHODS

Hence, from the previous section, it has been clear that, the capabilities of FEM or MeshFree method can greatly be improved by combining two techniques or adopting extended features such as discontinuous functions and asymptotic crack tip function. The hybrid of XFEM and FEM gives much more accurate results without much re-meshing. But it is difficult to adopt in case of complex geometries. Similarly, hybrid of FEM and MeshFree methods are also discussed which proves to be efficient in some cases.

2.5.1 Hybrid of FEM and XFEM

Modelling cracks in finite element framework by enriching displacement function by discontinuous field and near tip asymptotic field has been presented by John and Belytschko (1999b). The same idea was extended by Sukumar et al. (2003) to solve 3D crack propagation problems, coupled with fast marching method. Quasi-static analysis of 3D crack propagation studies has been carried out by Pedro and Belytschko (2005). The authors have combined XFEM with FEM and have used linear tetrahedral elements for modelling. The method allows closed-form integration and the damage has been introduced when a consecutive model loses its stability.

Further, studies have been carried out on the different shapes of cracks such as elliptical and circular. SIF has been computed numerically and these results have

shown good agreement with the theoretical solutions. With smoothed enrichment, the accuracy increased with the rate of convergence. Mapping is another disadvantage while modelling in FEM. Using XFEM mapping of solution between the mesh is avoided so it is advantageous to use it in a nonlinear and time dependent problems. Armando et al. (2007) have studied on 3D problems without mapping and have given good correlation with the experimental results. Orthotropic crack propagation has been studied by Asadpoure and Mohammadi (2007).

2.5.2 Hybrid of FEM and MeshFree Method

MeshFree methods have proved their ability in giving accurate results, but lacks computational efficiency. Therefore, researchers have put their effort to adopt FEM and combine it with the MeshFree method in order to get the full advantage of these methods of minimizing their disadvantages. FEM has been used in the entire structure and in the sub-domain where meshes play a major role can be replaced with MeshFree methods.

FEM and EFG method have been combined together to obtain continuity and consistency between interface elements. Belytschko et al. (1995b) have implemented this on 1D cantilever beam and wave propagation problem for elasto-static and elasto-dynamic problems. Though the accuracy has improved, it lacks faster convergence due to the errors. But in case of fracture problems it proved to be efficient with reduced computational cost. Application of Dirichlet boundary condition has been carried out by Yury (1996). He has adopted a method where the whole problem space has been modelled using weighted Meshless methods and on the boundary FEM has been implemented. Rao and Rahman (2001) adopted FEM to model the region away from cracks whereas near the cracks EFG method has been used. This showed accurate results when compared with the fully MeshFree method. In the interface nodes, shape functions from both the methods have been used, the crack region or the domain of interest is modelled only by nodal points. This method has given accurate result with significant reduction in computational time. Huerta et al. (2004) improved the same idea by adopting different interpolation methods in various regions and further in place of transition, linear interpolation has been carried out. Bridging scale

and continuous blending techniques have been discussed in this paper, which addressed various approaches for nodal interpolation and convergence. Further Rabczuk and Eibl (2004) modelled pre-stressed concrete beam, where concrete is modelled as particles and steel as beam elements. The bond forces between concrete and steel are applied in tangential and normal to both particles and beam elements. It is difficult to model large changes in thickness for failure model assuming plane stress condition in this method. Rabczuk et al. (2006) coupled FEM with RKPM using different coupling techniques and suggested that each technique holds good for some kind of problems.

Linearly conforming PIM and FEM to obtain the upper bound solution have been adopted by Liu and Zhang (2008). Shape functions have been constructed using PIM either using polynomial functions or radial basis functions. Triangular elements have been used as background mesh; linear interpolation is same as in case of FEM. Quadratic interpolation discretizes the cells as interior and exterior cells. Interior cells will not have any edges of the problem space unlike exterior cells. The limit analysis of structures puts emphasis on the numerical discretization strategy adopted and on the computational limit analysis procedure. Xiao (2012) has demonstrated the procedures with one based on FEM and the other based on EFG method. The resulting discretized formulation is then solved using Second-Order Cone Programming (SOCP).

Hellinger–Reissner variational principle which is similar to that of Galerkin weak-form has been derived to solve the system equations by Liu et al. (2009). The method aids in the convergence from both bounds. Thomas and Belytschko (2010) presented crack tip modelled by MeshFree method and crack path by XFEM. The Edge-based Smoothed Finite Element Method (ES-FEM), where triangular elements have been used to generate the mesh quite easily for any complicated domains has been presented by Chen et al. (2011c). The features of ES-FEM are utilized to generate the energy error estimate. The assigned scaling factors to nodes that define the local nodal density are then refined to control the nodal density. The refinement approach is demonstrated on an automobile part that has shown the effectiveness and efficiency of the proposed method.

Material Point Method (MPM) is one of the MeshFree methods which have been used for modelling the extreme deformation without element mapping. While modelling problem of small deformation, FEM is more efficient than MPM. Lian et al. (2012) have combined FEM and MPM for problems with large deformation. Eulerian particle has been used for background meshing and Lagrangian is used to represent state variables of particles in the material domain. Further, the authors have verified this method using numerical problems and have obtained results which are agreeable with the experimental data. Another MeshFree technique RKPM has been coupled with FEM by Wu et al. (2013) in order to avoid the transition at the interface. Unique domain and nodal integrations have been performed for both the methods and state variables are stored directly at the nodal points. This method has been tested for different loading conditions such as quasi-static, impact and blast loading, and realistic results have been obtained. A coupled FEM and MeshFree method is used for numerical analysis by Ullah et al. (2013). The problem domain is first modelled using FEM and the corresponding region, which requires adaptive refinement have been modelled by MeshFree method. In these MeshFree regions local maximum entropy shape functions and FEM for straightforward implementation of essential boundary conditions have been used.

2.6 ADAPTIVE REFINEMENT

Gradient based methods are most commonly adopted for the error estimate as it does not need any special formulations. Haussler and Korn (1998) eliminated interpolation error by refining the nodes in the region of high strain gradients. Nodes have been placed at the centre of each triangular cell, which have been used for the distribution of nodes. Taylor's series has been adopted by Gavete et al. (2002) for the construction of shape function using the MLS technique. Further strain energy gradient has been used for the refinement of background cells to reduce integration error. The relative strain energy gradient has been adopted as criteria for refinement by Luo and Combe (2003) and nodes have been increased to reduce the relative error.

The refinements of nodes based on the difference between the projected and actual stress values have been discussed by Gye-Hee et al., (2003) and the nodes have been

increased in the region of computed higher difference of stresses. Error estimate based on Zienkiewicz-Zhu developed by Lee and Zhou (2004a) and Rodrigo and Marcelo (2005), in which exact stresses have been replaced by the recovery stress field. Lee and Zhou (2004a) used Moving Least Square Stationary Least Square (MLS-SLS) for the construction of shape function. MLS-SLS are compared with Belytschko's recovery scheme which adopted field variables obtained from the MLS (Liu and Bernard, 2005). MLS-SLS are largely affected by the smoothing and these problems are much more accurate than the non-smoothed method. As discussed earlier, boundary condition application is quite difficult in MeshFree method. Hence Lee and Zhou (2004b) extended the previous work by coupling it with FEM, where boundary condition has been applied through FEM. Further stress recovery in tandem with stabilized nodal integration has been carried out (Yvonnet et al., 2006).

Voronoi cell is an alternative method used for triangular cells for the distribution of nodes; it has an advantage of forming the cell for a given set of nodes. Liu and Kee (2005) considered MLS shape function and strong-form radial collocation method for solving system equations. Nodes have been introduced into Voronoi cells to reduce interpolation error. Rabczuk and Belytschko (2007) formulated the shape function using mixed Lagrangian-Euler Kernel method which can be extended to 3D structure as well. Additional particles have been introduced into the constructed Voronoi cells in the region of large strain gradients. Chen et al. (2011a) have adopted the Edge-based Smoothed Point Interpolation Method (ES-PIM). The error in the strain energy has been computed for the triangular background cells using the smoothed strains of the edges of the triangular cell. Each node in the domain has been assigned a scaling factor that controls the local nodal density.

Error estimate based on the residuals for KRPM has been carried out by Belytschko et al. (1998). In this method wavelet is used to divide the high and low scale components and these high scale components have been used as an error indicator for refinement. Rabczuk and Belytschko (2005) calculated error based on the displacement field. The error of each node has been calculated and the node which crosses certain criteria, refinement has been carried out around that node. The nodes are present in the corner of the pixels and these pixels are made sure to coincide with the background

integration cells. For refinement the node of large error is further divided into 4 pixels. The method has been much suited for solid models and not for shell models.

Collocated Discrete Least Squares (CDLS) method has been adopted by Afshar and Lashckarbolk (2008) to estimate errors directly from the least squares. Nodes have been placed in the domain such that the error is distributed in the domain evenly. All the nodes have been connected by a spring and these nodes are moved till all nodes are in equilibrium. Mesh movement in case of FEM leads to the distortion of the elements, whereas in MeshFree methods it will not. Afshar et al. (2011) has extended the same work for MLS technique and have proved to be efficient for both the methods of shape function construction.

Least square function has been used by Perazzo et al. (2008) for construction of shape function as well as error estimation. Delaunay technique has been commonly adopted for the nodal distribution, i.e. nodes are placed at the centre and the vertices of the triangular cell used for nodal distribution. Rabczuk and Samaniego (2008) modelled shear bands as a jump in displacements at discrete positions and loss of stability has been considered as a criterion for refinement.

Error estimation has been carried out using Taylor's expansion technique in the computed displacement fields by Canh et al. (2010). Using smoothed values of displacement derivatives error density has been estimated. Further Afshar et al. (2012) used Discrete Least Square (DLS) MeshFree method to evaluate the functional values at nodal points. Both the methods have used Voronoi cells for the nodal refinement. If the error exceeds the tolerance limit, nodes have been introduced on the vertices or at the centre of the Voronoi cells. The Galerkin boundary node method in which vibrational boundary integral has been combined with the MLS approximation to get trial and the test functions have been discussed by Xiaolin (2011). The error is estimated using two successive nodal arrangements and refinement has been carried out to achieve faster convergence.

Node-based Smoothed Point Interpolation Method (NS-PIM) to solve an adaptive refinement problem has been proposed by Tanga et al. (2011). The NS-PIM has been formulated using a simple four-node tetrahedral mesh. The displacement-based FEM will provide the lower bound solutions and then the upper bound solutions are

obtained using the NS-PIM, and thus the energy error estimate has been computed. The tetrahedral cells with higher energy error estimates have then been refined that can effectively capture the high stress concentrations. Ullah and Augarde (2013) suggested adaptive refinement technique for modelling elasto-plastic deformation and used stress recovery based method for error estimation.

Mixed Discrete Least Squares (MDLS) meshless method has been able to compute displacements and stresses simultaneously without using the second order differential (Amani et al.,2014). An error has been estimated based on the least square residual and both node movement and node enrichment methods have been adopted. Voronoi cells are used to identify the neighbouring nodes. MDLS is better and has faster convergence than DLS which has been discussed earlier. A node-based energy error estimate has been presented by Yiqian et al. (2014). The smooth shape functions in MeshFree methods may lead to spurious oscillation away from the region containing the error, which may result in unnecessary nodes. Therefore, to address this shortcoming a double refined technique has been presented. An adaptive numerical integration in EFG method has been carried out by Grand et al. (2015). In the existing integration methods, the integration locations are fixed and are based on the number of integration points used. In the present paper, an adaptive procedure to distribute the integration points within the problem domain has been reported. The method allows control over the accuracy of the integration and also reduces the number of integration points required.

Based on the thorough literature survey, the need for development of effective adaptive refinement scheme in MeshFree platform has been necessitated. The same have been addressed in the present work.

CHAPTER 3

FORMULATION OF EFG METHOD

3.1 CHAPTER PROLOGUE

Utility of MeshFree methods in structural mechanics with emphasis to crack studies has been elaborated in the preceding chapters. EFG method based on MLS technique for shape functions construction using nodal weighting functions for modelling of 1D and 2D problems has been presented with Lagrange multipliers for addressing boundary conditions as a precursor to extension of the method for crack analysis.

3.2 SHAPE FUNCTION BY MOVING LEAST SQUARE METHOD

Shape function or interpolation of field variables decide the accuracy of the results obtained in any numerical methods. $u(\xi, \eta)$ is the functions of field variable defined in the 2D domain and the approximation of $u(\xi, \eta)$ at a point can be given as discussed by Lancaster and Salkauskas (1981),

$$u(\xi, \eta) = \sum_{I=1}^n N_I u_I = \sum_{I=1}^n p^T \bar{A}^{-1} \bar{B}_I u_I \quad \dots 3.1$$

where,

$$\bar{A}(\xi, \eta) = \sum_{I=1}^n W(\xi - \xi_I, \eta - \eta_I) p^T(\xi_I, \eta_I) p(\xi_I, \eta_I)$$

$$\bar{B}_I = W(\xi - \xi_I, \eta - \eta_I) p(\xi_I, \eta_I),$$

$p^T(\xi, \eta) = \{1, \xi, \eta, \xi\eta, \xi^2, \eta^2, \xi^2\eta, \xi\eta^2, \xi^2\eta^2, \dots, n\}$, u_i is the field variable and n is the number of nodes chosen for the construction of shape function at the point-of-interest, W is the weighting function and has been discussed in Section 3.3

Similarly, Equation 3.1 may be reduced to 1D case,

$$u(\xi) = \sum_{I=1}^n N_I u_I = \sum_{I=1}^n p^T \bar{A}^{-1} \bar{B}_I u_I \quad \dots 3.2$$

where,

$$\bar{A}(\xi) = \sum_{l=1}^n W(\xi - \xi_l) p^T(\xi_l) p(\xi_l), \quad \bar{B}_l = W(\xi - \xi_l) p(\xi_l),$$

$$p^T(\xi) = \{1, \xi, \xi^2, \xi^3, \dots, \xi^{n-1}\}$$

The shape function and its derivatives at a point-of-interest in a plate with circular cut-out using an exponential weighting function are as shown in Figures 3.1-3.3.

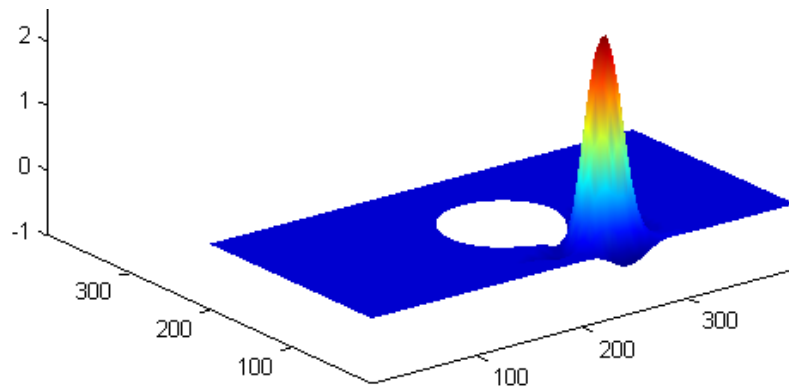


Figure 3.1 – Shape function at point-of-interest in a plate with circular cut-out

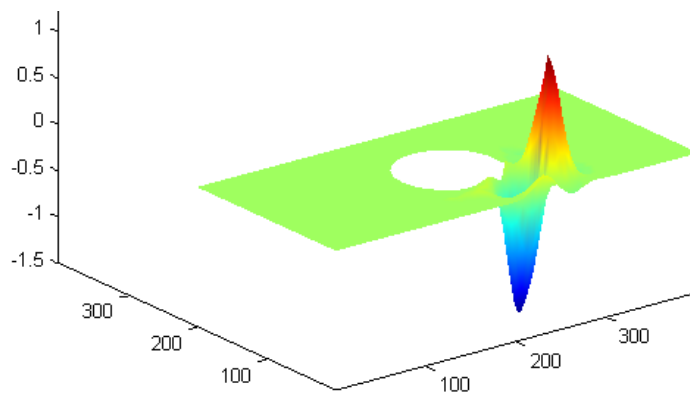


Figure 3.2 – First-order differential of the shape function w.r.t ξ on the plate

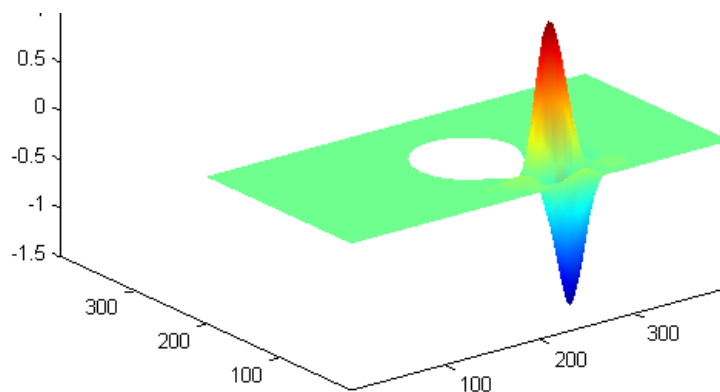


Figure 3.3 – First-order differential of the shape function w.r.t η on the plate

3.3 WEIGHTING FUNCTIONS

Galerkin's method is a method of weighted residuals, where the sum of the weighted errors gets minimized. Many suggestions for weighting function have been made in literature and a few popular are presented here. Choosing an appropriate weighting function is the most crucial step in MeshFree method. The most commonly used weighting functions are of exponential, cubic spline, quartic spline and quartic forms. These functions in a 1D space defined by the variable ξ are shown in Equations 3.3-3.6 (Liu, 2009), respectively.

$$W(\xi - \xi_I) = \begin{cases} e^{-\left(\frac{d}{\alpha}\right)^2} & \text{for } d \leq 1 \\ 0 & \text{for } d > 1 \end{cases} \quad \dots 3.3$$

$$W(\xi - \xi_I) = \begin{cases} \frac{2}{3} - 4d^2 + 4d^3 & \text{for } d \leq \frac{1}{2} \\ \frac{4}{3} - 4d + 4d^2 - \frac{4}{3}d^3 & \text{for } \frac{1}{2} < d \leq 1 \\ 0 & \text{for } d > 1 \end{cases} \quad \dots 3.4$$

$$W(\xi - \xi_I) = \begin{cases} 1 - 6d^2 + 8d^3 - 3d^4 & \text{for } d \leq 1 \\ 0 & \text{for } d > 1 \end{cases} \quad \dots 3.5$$

$$W(\xi - \xi_I) = \begin{cases} \frac{2}{3} - \frac{9}{2}d^2 + \frac{19}{3}d^3 - \frac{5}{2}d^4 & \text{for } d \leq 1 \\ 0 & \text{for } d > 1 \end{cases} \quad \dots 3.6$$

where, α is a constant taken as 0.3, $d = |\xi - \xi_I| / d_w$; ξ is any point in the 1D space, ξ_I is the point/node whose weight is computed and d_w is the smoothing length of the domain.

The compromise between the accuracy and smoothness of stress distribution lies in choosing the d_w value, as lower value of d_w leads to higher accuracy of stresses with coarser distribution and higher values will have opposite effect.

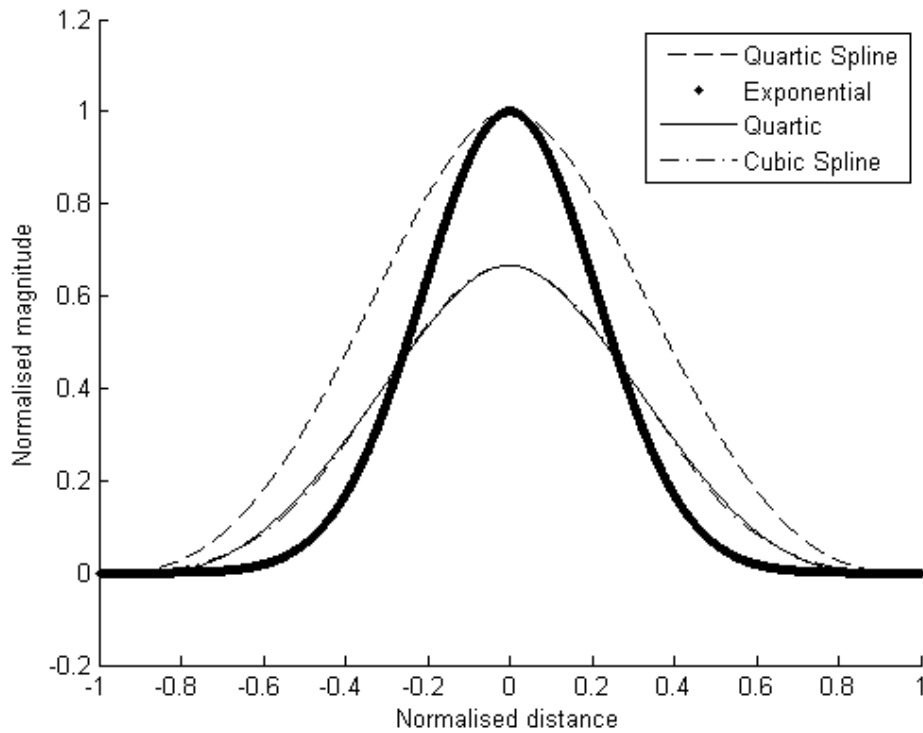


Figure 3.4 – Distribution of weights in the weight function for $\xi = -1$ to 1

The weighting functions (Eqs. 3.4-3.6) and its derivatives are drawn in Figures 3.4-3.6, where the domain size is varied from -1 to 1. It can be clearly seen in the Figures 3.4-3.6 that the exponential weight function gives higher importance to neighbouring nodes, which will be important in locating the high stress point in the problems such as crack initiation and propagation. Also, the first and second-order differential of the exponential weight function follows continuity in the domain which aids in smoother interpolation of stresses. Hence the thesis work carried out adopts the exponential weighting function for the construction of MLS shape function and has discussed in detail by taking a case of 2D weighting function.

From Equation 3.3, the exponential weight function for a 2D space defined by ξ , η coordinates and can be written in the form,

$$W(\xi - \xi_I, \eta - \eta_I) = W_1(\xi - \xi_I)W_2(\eta - \eta_I) = e^{-\left(\frac{d_\xi}{\alpha}\right)^2} e^{-\left(\frac{d_\eta}{\alpha}\right)^2} \quad \dots 3.7$$

where d_ξ and d_η can be written as $d_\xi = \frac{|\xi - \xi_l|}{d_{w\xi}}$ and $d_\eta = \frac{|\eta - \eta_l|}{d_{w\eta}}$ respectively. (ξ, η) is any point in the domain, (ξ_l, η_l) is the point/node whose weight is computed, $d_{w\xi}$ and $d_{w\eta}$ are the smoothing lengths of the domain in the directions ξ, η .

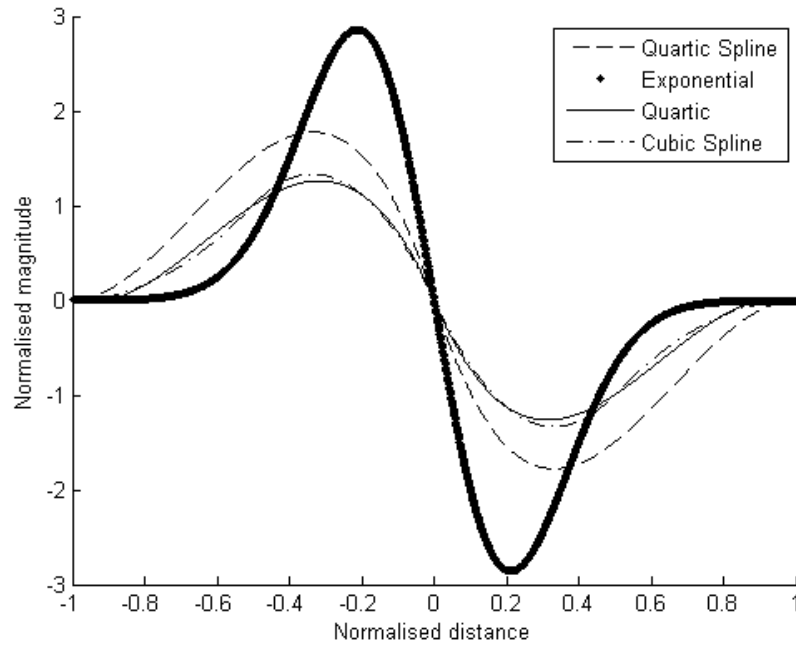


Figure 3.5 – First-order differential of the weighting functions for $\xi = -1$ to 1

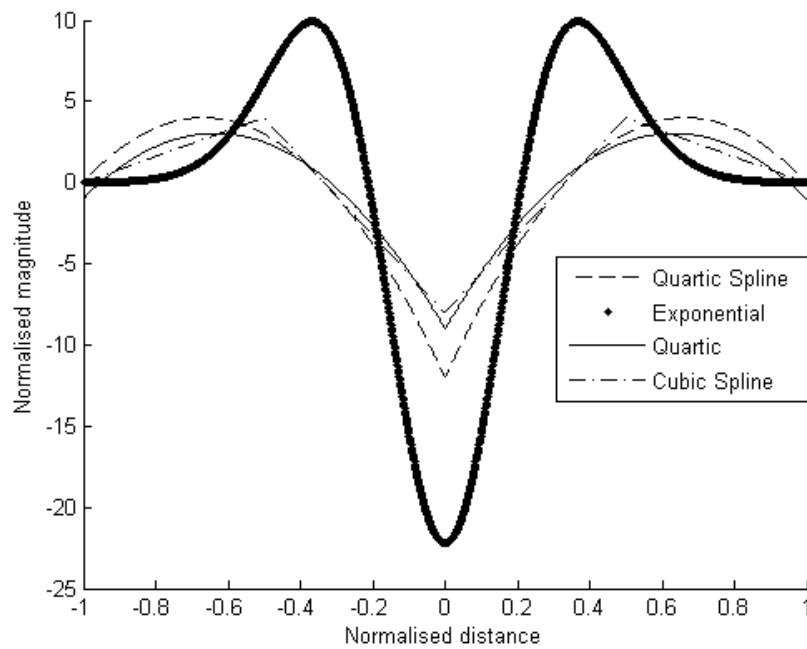


Figure 3.6 – Second-order differential of the weighting functions for $\xi = -1$ to 1

The first differential of d_ξ and d_η are,

$$\frac{\partial d_\xi}{d\xi} = \begin{cases} \frac{1}{R_\xi} & \text{if } \xi > \xi_I \\ -\frac{1}{R_\xi} & \text{if } \xi < \xi_I \end{cases} \quad \dots 3.8$$

$$\frac{\partial d_\eta}{d\eta} = \begin{cases} \frac{1}{R_\eta} & \text{if } \eta > \eta_I \\ -\frac{1}{R_\eta} & \text{if } \eta < \eta_I \end{cases} \quad \dots 3.9$$

Now differentiating the weighting function w.r.t. ξ and η we get,

$$\frac{\partial W(\xi-\xi_I, \eta-\eta_I)}{\partial \xi} = \frac{\partial W_1}{\partial \xi} W_2 = -2W_1 W_2 \left(\frac{d_\xi}{\alpha^2} \right) \left(\frac{\partial d_\xi}{\partial \xi} \right) \quad \dots 3.10$$

$$\frac{\partial W(\xi-\xi_I, \eta-\eta_I)}{\partial \eta} = W_1 \frac{\partial W_2}{\partial \eta} = -2W_1 W_2 \left(\frac{d_\eta}{\alpha^2} \right) \left(\frac{\partial d_\eta}{\partial \eta} \right) \quad \dots 3.11$$

The weight distribution of the Equation 3.7 is shown in Figure 3.7 and the distribution of first-order differential of Equation 3.7 in $\xi\eta$ coordinates are shown in Figures 3.8 and 3.9, respectively.

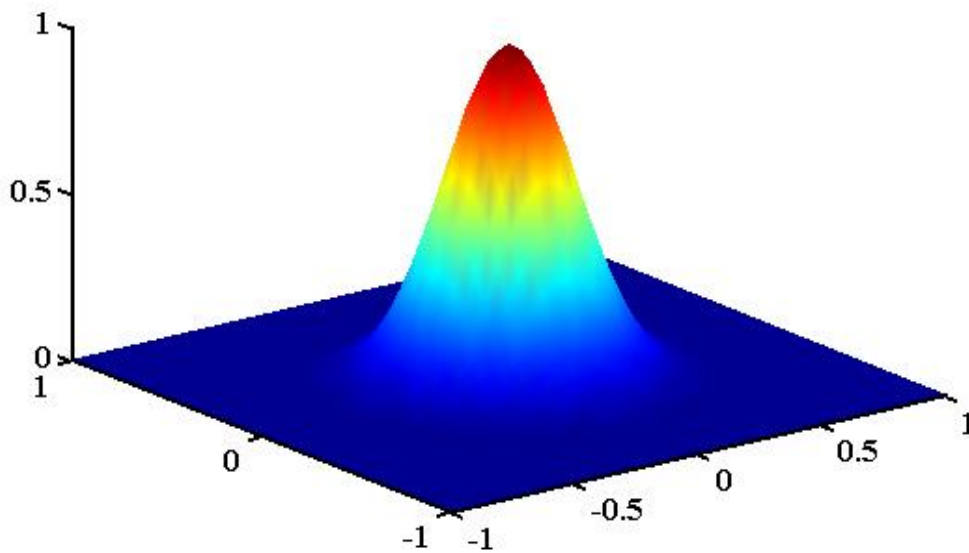


Figure 3.7 - Exponential weight function in 2D space for $\xi, \eta = -1$ to 1

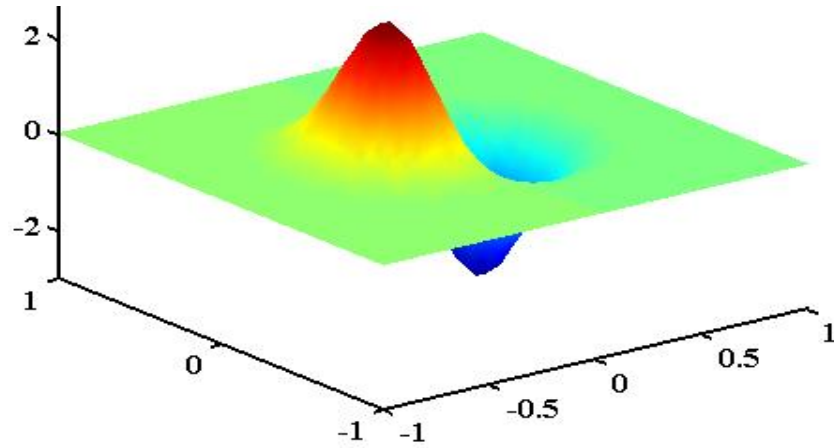


Figure 3.8 – First-order differential of the 2D exponential weight function w.r.t. ξ

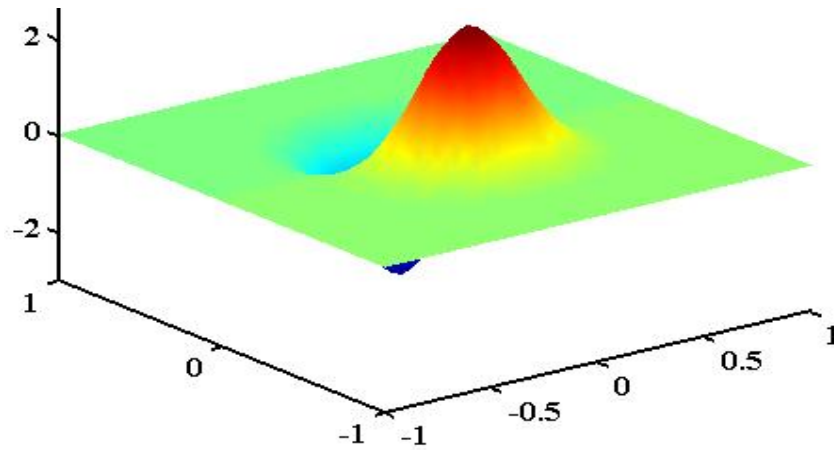


Figure 3.9 – First-order differential of the 2D exponential weight function w.r.t. η

For a 1D space defined by ξ , the first-order differential of the weighting function from Equation 3.8, can be written as,

$$\frac{\partial W(\xi-\xi_I)}{\partial \xi} = \frac{\partial W_I}{\partial \xi} = -2W_I \left(\frac{d_\xi}{\alpha^2} \right) \left(\frac{\partial d_\xi}{\partial \xi} \right) \quad \dots 3.12$$

3.4 2D PLATE FORMULATION

The plate formulation involves the derivation of stress-strain relation, kinematic relation, strain-displacement matrix and finally the stiffness matrix. To start with, an unit cell is shown to define the coordinate system, and the stresses in Figure 3.10.

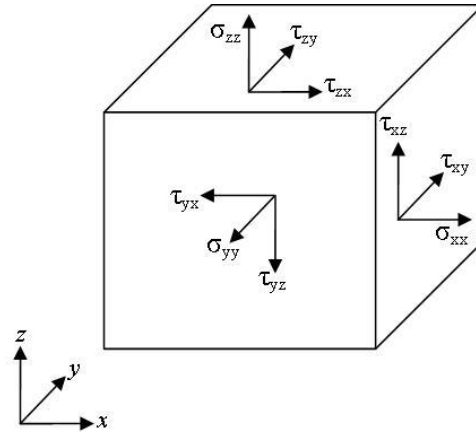


Figure 3.10 – Stress orientation in a unit cell

Based on this unit cell which is defined in an x, y rectangular coordinate system, the constitutive relation (Timoshenko and Goodier, 1970) for an isotropic material is defined,

$$\begin{Bmatrix} \sigma_{xx} \\ \sigma_{yy} \\ \sigma_{zz} \\ \tau_{yz} \\ \tau_{xz} \\ \tau_{xy} \end{Bmatrix} = \begin{bmatrix} C_{11} & C_{12} & C_{12} & 0 & 0 & 0 \\ C_{12} & C_{11} & C_{12} & 0 & 0 & 0 \\ C_{12} & C_{12} & C_{11} & 0 & 0 & 0 \\ 0 & 0 & 0 & \frac{C_{11}-C_{12}}{2} & 0 & 0 \\ 0 & 0 & 0 & 0 & \frac{C_{11}-C_{12}}{2} & 0 \\ 0 & 0 & 0 & 0 & 0 & \frac{C_{11}-C_{12}}{2} \end{bmatrix} \begin{Bmatrix} \varepsilon_{xx} \\ \varepsilon_{yy} \\ \varepsilon_{zz} \\ \gamma_{yz} \\ \gamma_{xz} \\ \gamma_{xy} \end{Bmatrix} \quad \dots 3.13$$

where, σ_{xx} , σ_{yy} and σ_{zz} are the normal stresses; τ_{yz} , τ_{xz} and τ_{xy} are the shear stresses; ε_{xx} , ε_{yy} and ε_{zz} are the normal strains; γ_{yz} , γ_{xz} and γ_{xy} are the shear strains; C_{11} and C_{12} are the material constants.

For a plane stress problem, by applying plane stress condition, Equation 3.13 may be written in the form,

$$\begin{Bmatrix} \sigma_{xx} \\ \sigma_{yy} \\ \tau_{yz} \\ \tau_{xz} \\ \tau_{xy} \end{Bmatrix} = \begin{bmatrix} \bar{C}_{11} & \bar{C}_{12} & 0 & 0 & 0 \\ \bar{C}_{12} & \bar{C}_{11} & 0 & 0 & 0 \\ 0 & 0 & \bar{C}_{44} & 0 & 0 \\ 0 & 0 & 0 & \bar{C}_{55} & 0 \\ 0 & 0 & 0 & 0 & \bar{C}_{66} \end{bmatrix} \begin{Bmatrix} \varepsilon_{xx} \\ \varepsilon_{yy} \\ \gamma_{yz} \\ \gamma_{xz} \\ \gamma_{xy} \end{Bmatrix} \quad \dots 3.14$$

where, $\bar{C}_{11} = C_{11} - C_{12}C_{11}^{-1}C_{12}$ and $\bar{C}_{12} = C_{12} - C_{12}C_{11}^{-1}C_{12}$

The kinematic relation for the 2D plate is written as,

$$\left. \begin{aligned} u &= u_0 + z\theta_y \\ v &= v_0 - z\theta_x \\ w &= w_0 \end{aligned} \right\} \quad \dots 3.15$$

where, u_0, v_0 and w_0 are mid-plane displacements of the plate along x, y and z axis, respectively. θ_x and θ_y are the mid-plane rotations along x, y axis, respectively. These detailed representations in the graphical form is shown in Figure 3.11

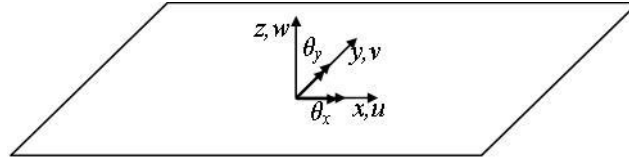


Figure 3.11 – Displacements and rotations about the mid-surface in plate formulation

By differentiating the kinematics relations shown in Equation 3.15, we get the strain relation.

$$\left. \begin{aligned} \varepsilon_{xx} &= \frac{\partial u}{\partial x} = \varepsilon_{xx}^0 + z\kappa_x \\ \varepsilon_{yy} &= \frac{\partial v}{\partial y} = \varepsilon_{yy}^0 + z\kappa_y \\ \gamma_{xy} &= \frac{\partial u}{\partial y} + \frac{\partial v}{\partial x} = \gamma_{xy}^0 + z\kappa_{xy} \\ \gamma_{xz} &= \frac{\partial u}{\partial z} + \frac{\partial w}{\partial x} = \frac{\partial w_0}{\partial x} + \theta_y \\ \gamma_{yz} &= \frac{\partial v}{\partial z} + \frac{\partial w}{\partial y} = \frac{\partial w_0}{\partial y} - \theta_x \end{aligned} \right\} \quad \dots 3.16$$

where, $\varepsilon_{xx}^0 = \frac{\partial u_0}{\partial x}$ and $\varepsilon_{yy}^0 = \frac{\partial v_0}{\partial y}$ are the in-plane normal strains; $\gamma_{xy}^0 = \frac{\partial u_0}{\partial y} + \frac{\partial v_0}{\partial x}$ is the in-plane shear strain; $\kappa_x = \frac{\partial \theta_y}{\partial x}$, $\kappa_y = -\frac{\partial \theta_x}{\partial y}$ and $\kappa_{xy} = \frac{\partial \theta_y}{\partial y} - \frac{\partial \theta_x}{\partial x}$ are the curvature strains.

From Equations 3.1 and 3.16, the strain-displacement relation may be written as,

$$\left\{ \begin{array}{c} \varepsilon_{xx}^0 \\ \varepsilon_{yy}^0 \\ \gamma_{xy}^0 \\ \kappa_x \\ \kappa_y \\ \kappa_{xy} \\ \gamma_{yz} \\ \gamma_{xz} \end{array} \right\} = \sum_{I=1}^n [B_I] \left\{ \begin{array}{c} u_{0I} \\ v_{0I} \\ w_{0I} \\ \theta_{xI} \\ \theta_{yI} \end{array} \right\} = \sum_{I=1}^n \begin{bmatrix} \frac{\partial N_I}{\partial x} & 0 & 0 & 0 & 0 \\ 0 & \frac{\partial N_I}{\partial y} & 0 & 0 & 0 \\ \frac{\partial N_I}{\partial y} & \frac{\partial N_I}{\partial x} & 0 & 0 & 0 \\ 0 & 0 & 0 & 0 & \frac{\partial N_I}{\partial x} \\ 0 & 0 & 0 & -\frac{\partial N_I}{\partial y} & 0 \\ 0 & 0 & 0 & -\frac{\partial N_I}{\partial x} & \frac{\partial N_I}{\partial y} \\ 0 & 0 & \frac{\partial N_I}{\partial y} & 0 & -N_I \\ 0 & 0 & \frac{\partial N_I}{\partial x} & N_I & 0 \end{bmatrix} \left\{ \begin{array}{c} u_{0I} \\ v_{0I} \\ w_{0I} \\ \theta_{xI} \\ \theta_{yI} \end{array} \right\} \quad \dots 3.17$$

The relation between the forces and moments with stresses can be expressed as,

$$\left. \begin{array}{l} (\bar{N}_x, \bar{N}_y, \bar{N}_{xy}) = b \int_{-h/2}^{h/2} (\sigma_{xx}, \sigma_{yy}, \tau_{xy}) dz \\ (\bar{M}_x, \bar{M}_y, \bar{M}_{xy}) = b \int_{-h/2}^{h/2} (\sigma_{xx}, \sigma_{yy}, \tau_{xy}) z dz \\ (\bar{Q}_x, \bar{Q}_y) = b \int_{-h/2}^{h/2} (\tau_{yz}, \tau_{xz}) dz \end{array} \right\} \quad \dots 3.18$$

where, \bar{N}_x , \bar{N}_y and \bar{N}_{xy} are the forces, \bar{M}_x , \bar{M}_y and \bar{M}_{xy} are the moments, \bar{Q}_x and \bar{Q}_y are the shear forces and b , h are the cross-sectional dimensions of the plate.

Substituting Equations 3.14, 3.16 in 3.18 and integrating, we get

$$\left\{ \begin{array}{c} \bar{N} \\ \bar{M} \\ \bar{Q} \end{array} \right\} = [Mat] \left\{ \begin{array}{c} \varepsilon^0 \\ \kappa \\ \gamma \end{array} \right\} = \begin{bmatrix} A & 0 & 0 \\ 0 & D & 0 \\ 0 & 0 & Y \end{bmatrix} \left\{ \begin{array}{c} \varepsilon^0 \\ \kappa \\ \gamma \end{array} \right\} \quad \dots 3.19$$

where, $\{\bar{N}\} = \{\bar{N}_x \quad \bar{N}_y \quad \bar{N}_{xy}\}^T$, $\{\bar{M}\} = \{\bar{M}_x \quad \bar{M}_y \quad \bar{M}_{xy}\}^T$, $\{\bar{Q}\} = \{\bar{Q}_x \quad \bar{Q}_y\}^T$,

$\{\varepsilon^0\} = \{\varepsilon_{xx}^0 \quad \varepsilon_{yy}^0 \quad \gamma_{xy}^0\}^T$, $\{\kappa\} = \{\kappa_x \quad \kappa_y \quad \kappa_{xy}\}^T$, $\{\gamma\} = \{\gamma_{yz} \quad \gamma_{xz}\}^T$,

$$[Y] = h \begin{bmatrix} \bar{C}_{44} & 0 \\ 0 & \bar{C}_{55} \end{bmatrix}, [A] = h \begin{bmatrix} \bar{C}_{11} & \bar{C}_{12} & 0 \\ \bar{C}_{12} & \bar{C}_{11} & 0 \\ 0 & 0 & \bar{C}_{66} \end{bmatrix}, [D] = \frac{h^3}{12} \begin{bmatrix} \bar{C}_{11} & \bar{C}_{12} & 0 \\ \bar{C}_{12} & \bar{C}_{11} & 0 \\ 0 & 0 & \bar{C}_{66} \end{bmatrix}$$

Then from Equations 3.17 and 3.19, the stiffness matrix of the domain is,

$$K = \int_{-1}^1 \int_{-1}^1 B^T [Mat] B |J| d\xi d\eta \quad \dots 3.20$$

where, $J = \begin{bmatrix} \sum_{l=1}^n \frac{\partial N_l}{\partial \xi} x_l & \sum_{l=1}^n \frac{\partial N_l}{\partial \xi} y_l \\ \sum_{l=1}^n \frac{\partial N_l}{\partial \eta} x_l & \sum_{l=1}^n \frac{\partial N_l}{\partial \eta} y_l \end{bmatrix}$ and x_l and y_l are the coordinates of the nodes in the

domain for construction of shape function. The problem space is integrated using the integration cells, which is defined using the natural coordinates $\xi\eta$.

Equation 3.20 is numerically integrated by applying Gaussian quadrature, which is represented in terms of Gauss points and Gauss weights as,

$$K = \sum_{i=1}^{m_g} \sum_{j=1}^{n_g} w_i w_j B^T(\xi_i, \eta_j) [Mat] B(\xi_i, \eta_j) |J(\xi_i, \eta_j)| \quad \dots 3.21$$

where, m_g and n_g are the number of Gauss points along x and y coordinates.

3.5 1D BEAM FORMULATION

The stress-strain relation for an isotropic material in 1D (Figure 3.12) can be obtained from Equation 3.13,

$$\begin{Bmatrix} \sigma_{xx} \\ \tau_{xy} \end{Bmatrix} = \begin{bmatrix} C_{11} & 0 \\ 0 & \frac{C_{11}-C_{12}}{2} \end{bmatrix} \begin{Bmatrix} \epsilon_{xx} \\ \gamma_{xy} \end{Bmatrix} = \begin{bmatrix} E & 0 \\ 0 & G \end{bmatrix} \begin{Bmatrix} \epsilon_{xx} \\ \gamma_{xy} \end{Bmatrix} \quad \dots 3.22$$

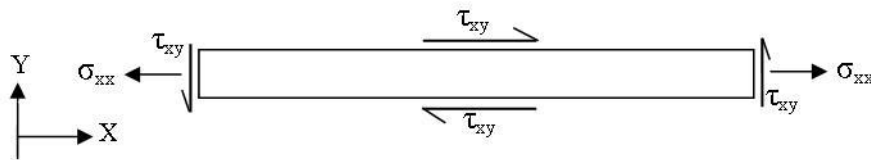


Figure 3.12 - Stress resultants on 1D beam

Similarly, the kinematic relations are,

$$\left. \begin{aligned} u &= u_0 - y\theta_z \\ v &= v_0 \end{aligned} \right\} \quad \dots 3.23$$

where, u_0 and v_0 are mid-plane displacements along x and y directions respectively, and θ_z is the mid-plane rotation as shown in Figure 3.13

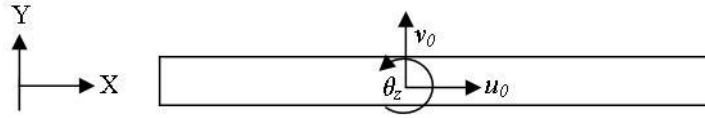


Figure 3.13 – Displacements and rotation on 1D beam

For an 1D beam, the strains obtained from the kinematic relation (Equation 3.23) in the form,

$$\left. \begin{aligned} \varepsilon_{xx} &= \frac{\partial u}{\partial x} = \varepsilon_{xx}^0 + y\kappa_x \\ \gamma_{xy} &= \frac{\partial u}{\partial y} + \frac{\partial v}{\partial x} = \frac{\partial v_0}{\partial x} - \theta_z \end{aligned} \right\} \dots 3.24$$

where, $\varepsilon_{xx}^0 = \frac{\partial u_0}{\partial x}$ is the in-plane strain; $\kappa_x = -\frac{\partial \theta_z}{\partial x}$ is the curvature strain

The strain-displacement matrix is obtained by substituting the shape functions derived from Equation 3.2,

$$\left\{ \begin{array}{c} \varepsilon_{xx_0} \\ k_x \\ v_{xy_0} \end{array} \right\} = \sum_{i=1}^n B_i \left\{ \begin{array}{c} u_i \\ v_i \\ \theta_{zi} \end{array} \right\} = \sum_{i=1}^n \left[\begin{array}{ccc} \frac{\partial N_i}{\partial x} & 0 & 0 \\ 0 & 0 & \frac{\partial N_i}{\partial x} \\ 0 & \frac{\partial N_i}{\partial x} & N_i \end{array} \right] \left\{ \begin{array}{c} u_i \\ v_i \\ \theta_{zi} \end{array} \right\} \dots 3.25$$

The relation of forces and moment with stresses is,

$$\left. \begin{aligned} \bar{N}_x &= \int_{-h/2}^{h/2} \sigma_{xx} b dy \\ \bar{M}_x &= \int_{-h/2}^{h/2} \sigma_{xx} y b dy \\ \bar{Q}_x &= \int_{-h/2}^{h/2} \tau_{xy} b dy \end{aligned} \right\} \dots 3.26$$

where, \bar{N}_x , \bar{M}_x and \bar{Q}_x are force, moment and shear force respectively, and b , h are the cross-sectional dimensions of the plate.

Substituting Equation 3.22 and 3.24 in Equation 3.26, we get

$$\begin{Bmatrix} \bar{N}_x \\ \bar{M}_x \\ \bar{Q}_x \end{Bmatrix} = [MAT] \begin{Bmatrix} \varepsilon_{xx}^0 \\ \kappa_x \\ \gamma_{xy} \end{Bmatrix} = \begin{bmatrix} EA & 0 & 0 \\ 0 & EI & 0 \\ 0 & 0 & GA \end{bmatrix} \begin{Bmatrix} \varepsilon_{xx}^0 \\ \kappa_x \\ \gamma_{xy} \end{Bmatrix} \quad \dots 3.27$$

where, E is the Young's modulus, I is area moment of inertia and A_C is the cross-sectional area.

Then the stiffness matrix can be derived,

$$K = \int_{-1}^1 B^T [Mat] B |J| d\xi \quad \dots 3.28$$

where, $J = \sum_{l=1}^n \frac{\partial N_l}{\partial x} x_l$ and x_l is the co-ordinate of the nodes in the domain

Equation 3.28 is numerically integrated by applying Gaussian quadrature, which is represented in terms of Gauss points and weights as,

$$K = \sum_{i=1}^{n_g} W_i B^T(\xi_i) [Mat] B(\xi_i) J(\xi_i) \quad \dots 3.29$$

where, n_g is the total number of Gauss points in the problem space.

3.6 APPLICATION OF BOUNDARY CONDITION AND TRACTION FORCE

As the MLS shape functions does not satisfy Kronecker delta property, boundary condition cannot be applied directly using Gauss elimination. Hence Lagrange multipliers are used for boundary condition application and the same is detailed in Section 3.6.1. Further the uniformly distributed load along the plate edges are discussed in Section 3.6.2.

3.6.1 Application of Boundary Condition by Lagrange Multipliers

The boundary condition application using Lagrange multipliers can be written as,

$$\begin{bmatrix} K & \bar{G}^T \\ \bar{G} & 0 \end{bmatrix} \begin{Bmatrix} u \\ \lambda \end{Bmatrix} = \begin{Bmatrix} F \\ 0 \end{Bmatrix} \quad \dots 3.30$$

where \bar{G} is the Lagrange multiplier matrix, λ is the Lagrange multiplier, and F is applied force.

The \bar{G} matrix consists of multi-point constraint that applies the required boundary constraints in the problem space. If Γ_λ is the one-dimensional domain along which the boundary constraints to be imposed, then the matrix \bar{G} may be written as,

$$\bar{G} = -\int_{\Gamma_\lambda} N_\lambda^T N d\Gamma_\lambda = -\sum_{i=1}^{n_\lambda} w_i N_\lambda^T(\xi_i) N(\xi_i) \frac{L_\lambda}{2} \quad \dots 3.31$$

where, N_λ is the shape function that interpolates λ along the domain Γ_λ , L_λ is the length of the domain and n_λ is the number of Gauss points along the domain Γ_λ required for numerical integration and ξ is the natural coordinate in 1D that defines the boundary domain.

For a 1D beam formulation, the boundary condition is applied at a point and therefore simply reduces to the form,

$$\bar{G} = -N(\xi_i) \quad \dots 3.32$$

3.6.2 Application of Traction Force along a Line in Problem Space

If Γ_p is the one-dimensional domain along which the uniform pressure load is to be applied and it can be represented as shown,

$$f = P \int_{\Gamma_p} N d\Gamma_p = P \sum_{i=1}^{n_p} w_i N(\xi_i) \frac{L_p}{2} \quad \dots 3.33$$

where P is the applied pressure along the domain Γ_p , L_p is the length domain Γ_p and n_p is the number of Gauss points along the domain Γ_p .

For a 1D beam formulation, Equation 3.33 simply reduces to the form,

$$f = P^l N(\xi_i) \quad \dots 3.34$$

where P^l simply becomes a point load.

3.7 DISPLACEMENTS, STRAINS AND STRESSES

The displacement of the field variables and the constraint forces are computed as,

$$\begin{Bmatrix} u \\ \lambda \end{Bmatrix} = \begin{bmatrix} K & G^T \\ G & 0 \end{bmatrix}^{-1} \begin{Bmatrix} F \\ 0 \end{Bmatrix} \quad \dots 3.35$$

Then the displacement at any point-of-interest is obtained from the above equation using shape function as,

$$\bar{u}(x, y) = N(x, y)u \quad \dots 3.36$$

The normal, curvature and out-of-plane strain at a given point-of-interest are computed using the strain-displacement equation as,

$$\varepsilon(x, y) = B(x, y)u \quad \dots 3.37$$

where, $\varepsilon = \left\{ \varepsilon_{xx}^0 \quad \varepsilon_{yy}^0 \quad \gamma_{xy}^0 \quad \kappa_x \quad \kappa_y \quad \kappa_{xy} \quad \gamma_{yz} \quad \gamma_{xz} \right\}^T$

Subsequently, the stresses are computed,

$$\begin{Bmatrix} \sigma_{xx} \\ \sigma_{yy} \\ \tau_{xy} \\ \tau_{yz} \\ \tau_{xz} \end{Bmatrix} = \begin{bmatrix} \bar{C}_{11} & \bar{C}_{12} & 0 & 0 & 0 \\ \bar{C}_{12} & \bar{C}_{11} & 0 & 0 & 0 \\ 0 & 0 & \bar{C}_{44} & 0 & 0 \\ 0 & 0 & 0 & \bar{C}_{55} & 0 \\ 0 & 0 & 0 & 0 & \bar{C}_{66} \end{bmatrix} \begin{bmatrix} 1 & 0 & 0 & z & 0 & 0 & 0 & 0 \\ 0 & 1 & 0 & 0 & z & 0 & 0 & 0 \\ 0 & 0 & 1 & 0 & 0 & z & 0 & 0 \\ 0 & 0 & 0 & 0 & 0 & 0 & 1 & 0 \\ 0 & 0 & 0 & 0 & 0 & 0 & 0 & 1 \end{bmatrix} \begin{Bmatrix} \varepsilon_{xx}^0 \\ \varepsilon_{yy}^0 \\ \gamma_{xy}^0 \\ \kappa_x \\ \kappa_y \\ \kappa_{xy} \\ \gamma_{yz} \\ \gamma_{xz} \end{Bmatrix}$$

... 3.38

where, z is the coordinate in thickness and varies bottom to top surface of the plate from $-h/2$ to $h/2$.

From the above equation, the principal (Equation 3.39) and von Mises (Equation 3.40) stresses are computed and the same has been followed in 1D beam formulation as well.

$$\sigma_{1,2} = \frac{\sigma_{xx} + \sigma_{yy}}{2} \pm \sqrt{\left(\frac{\sigma_{xx} - \sigma_{yy}}{2}\right)^2 + \tau_{xy}^2} \quad \dots 3.39$$

$$\sigma_v = \sqrt{\sigma_1^2 - \sigma_1\sigma_2 + \sigma_2^2} \quad \dots 3.40$$

CHAPTER 4

EFG CODE FOR BEAMS AND PLATES - TESTING AND VERIFICATION

4.1 CHAPTER PROLOGUE

The EFG code for 1D beam bending and 2D plate analysis has been verified using standard benchmark problems available in beam bending and axially loaded plate structures with high stress concentrations. Convergence studies have also been presented to show the efficacy of the developed procedure by comparison with FEM and closed-form solutions. Capability of MeshFree method in high stress gradient computation has also been tested and superiority of EFG over FEM has been highlighted.

4.2 VERIFICATION USING 1D BEAM STRUCTURES

In this study, two simple beam structures are considered. The first beam is a cantilever with vertical point load at the free end and the second beam is simply supported at ends and centrally loaded. The representations of these two cases are shown in Figures 4.1 and 4.2, respectively. In Table 4.1, the material properties used in the structural models throughout the thesis is shown. Section properties (breadth and depth) for 1D beam are taken as 100mm.

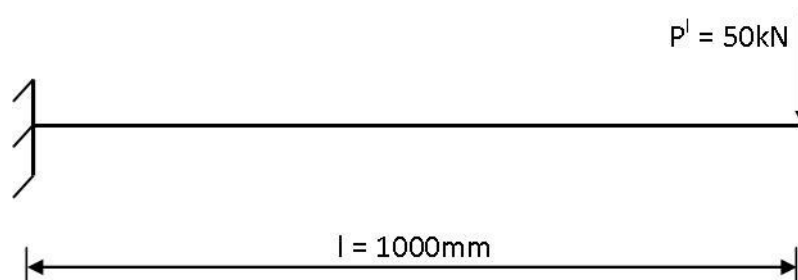


Figure 4.1 – Cantilever beam with vertical tip load

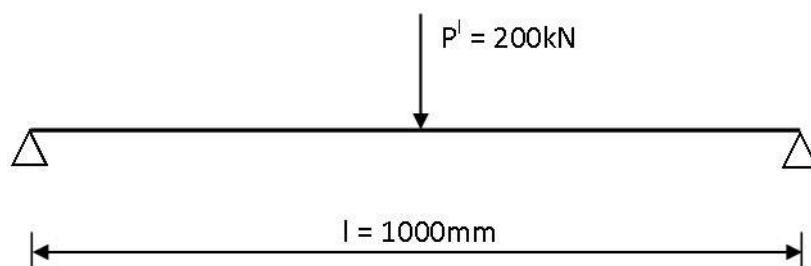


Figure 4.2 – Simply-supported beam with vertical centre load

Table 4.1 – Material properties of mild steel used in the thesis

| Properties | Value |
|-----------------------|--------|
| Modulus of Elasticity | 210GPa |
| Poisson's Ratio | 0.33 |

The displacements and stresses are computed using MeshFree method, and comparisons are made with beam theories and FEM solution (Table 4.2). MeshFree solutions match with the closed-form solutions. Figures 4.3 and 4.4 show the convergence of displacement for cantilever and simply-supported beams respectively. In both the cases, it can be seen that convergence of EFG is better with lesser number of nodes than FEM. Also as seen in Figures 4.5 and 4.6, displacements along the length are given. Finally, the stress values presented in Figures 4.7 and 4.8 indicate stresses obtained by EFG compare more smoothly than FEM.

Table 4.2 – Displacement and stress in the considered 1D beams

| Beam Type | Maximum Displacement (mm) | | | | Bending Stress (MPa) | | |
|------------------|---------------------------|------------|------|-------|----------------------|-----|-------|
| | Euler Bernoulli | Timoshenko | FEM | MFree | Exact solution | FEM | MFree |
| Cantilever | 9.52 | 9.61 | 9.61 | 9.61 | 300 | 298 | 300 |
| Simply-supported | 2.38 | 2.47 | 2.47 | 2.47 | 300 | 297 | 300 |

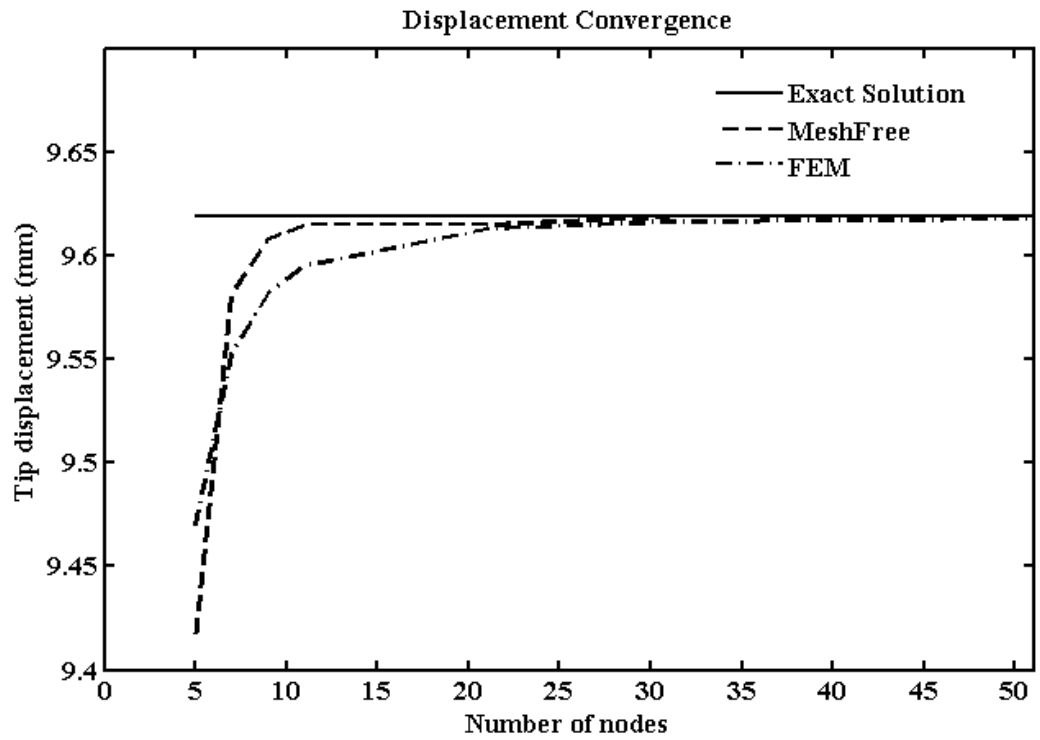


Figure 4.3 – Displacement convergence in cantilever beam

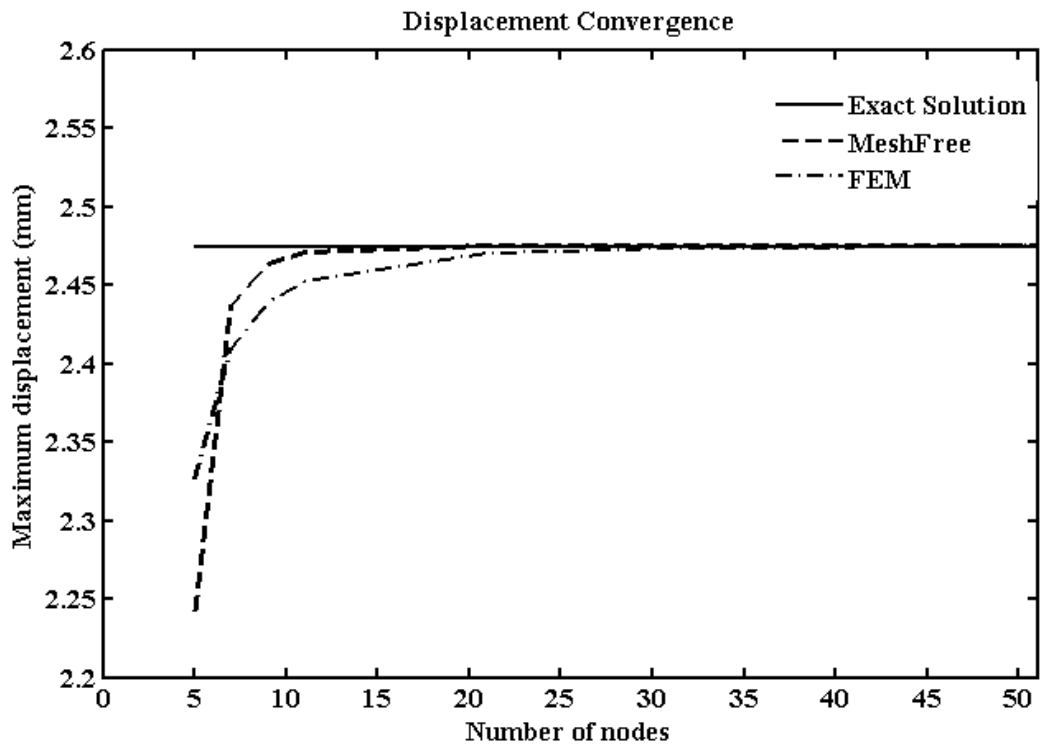


Figure 4.4 – Displacement convergence in simply-supported beam

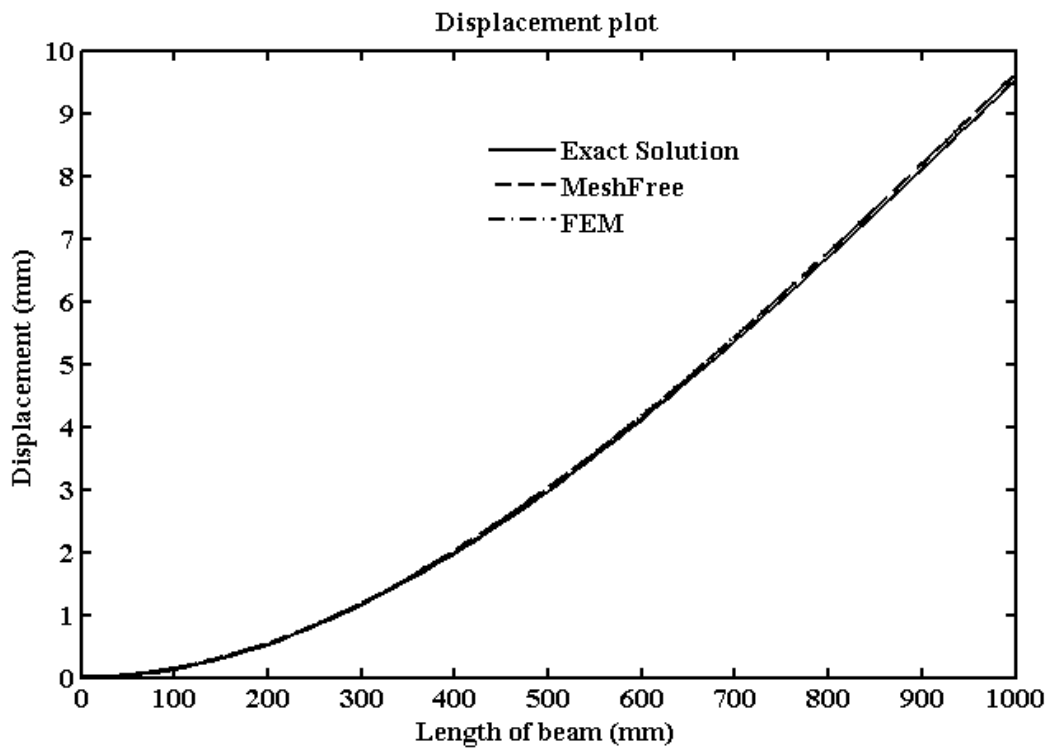


Figure 4.5 – Displacement distribution along the length of cantilever beam

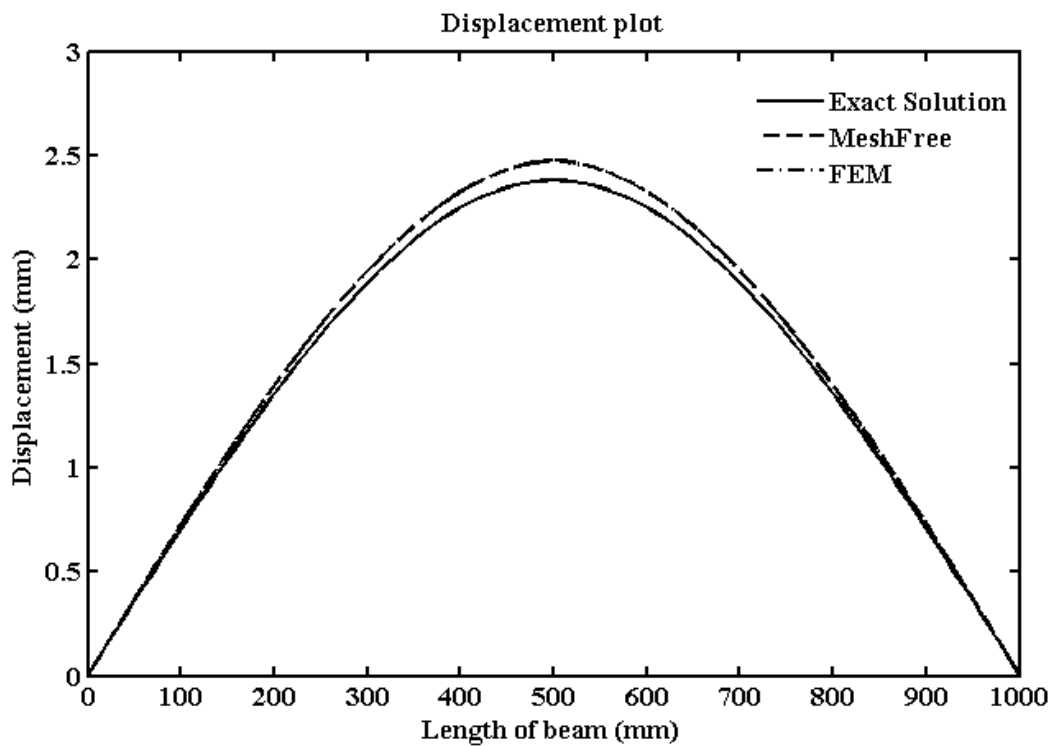


Figure 4.6 – Displacement distribution along the length of simply-supported beam

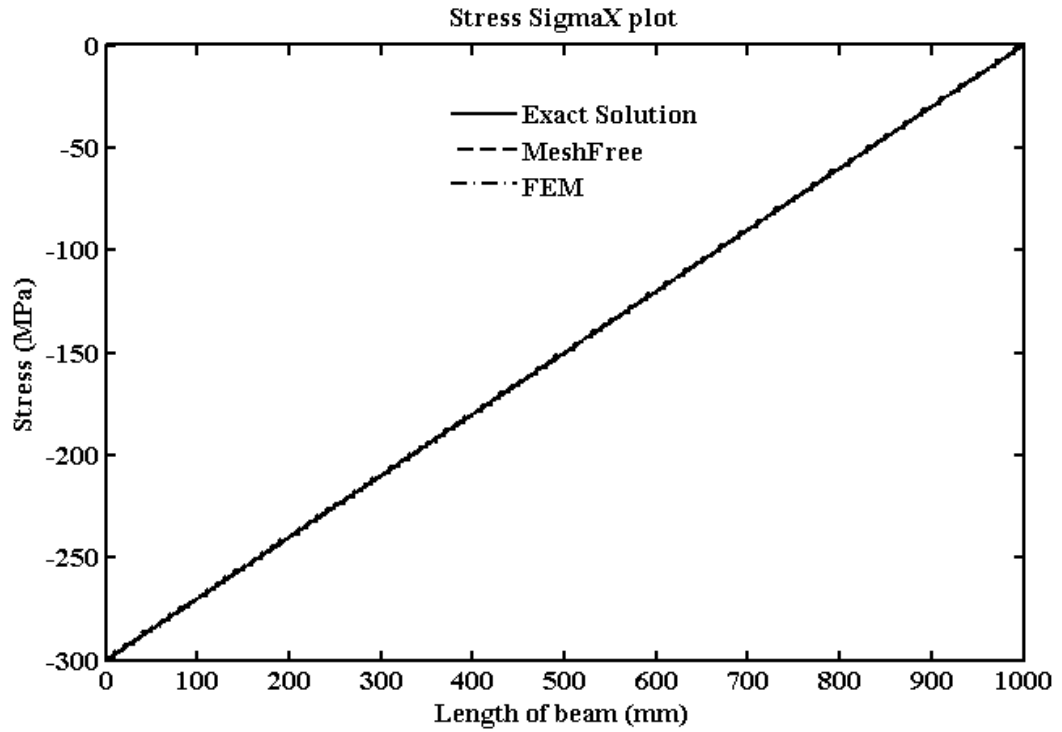


Figure 4.7 – Stress distribution along the length of cantilever beam

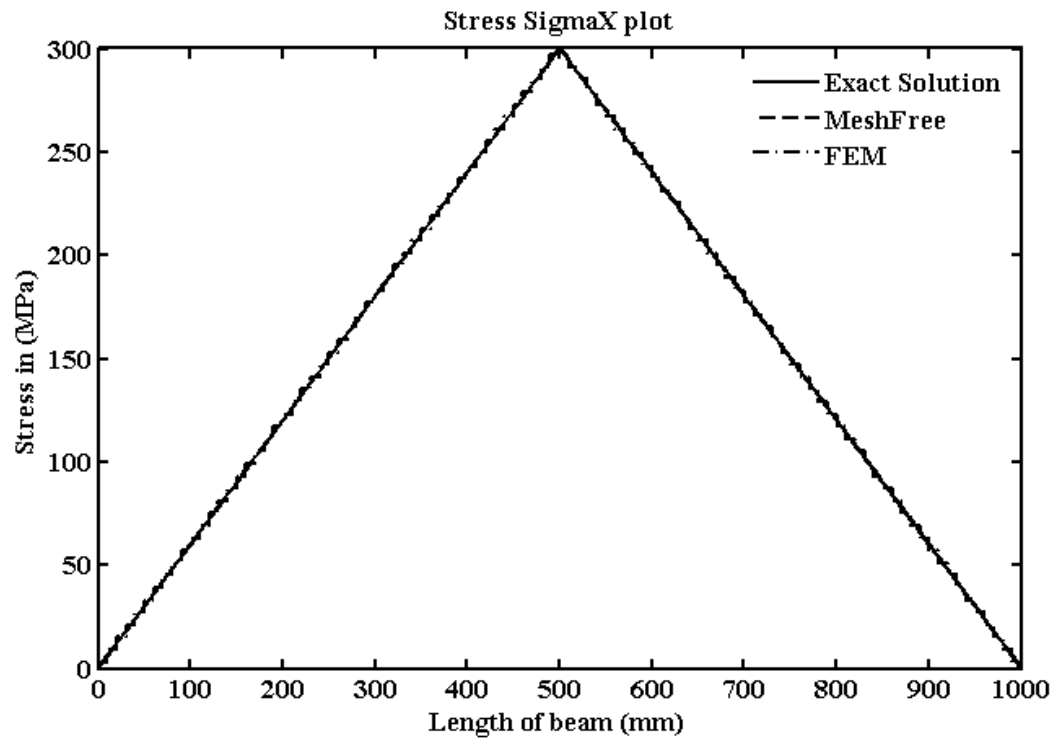


Figure 4.8 – Stress distribution along the length of simply-supported beam

4.3 VERIFICATION USING 2D STRUCTURES

In this section, analysis carried out on a simple beam structure for displacement convergence studies and computations of SCF for punctured rectangular plates have been presented.

4.3.1 A Simple 2D Beam

The one end of the 2D beam (2mm thick) is constrained to have zero displacements and the other end is axially loaded with uniformly distributed loads as shown in Figure 4.9. Axially loaded beams arrive at the exact solution with much lesser nodes compared to that of transverse loading, as seen in Figure 4.10, for EFG and FEM convergence.

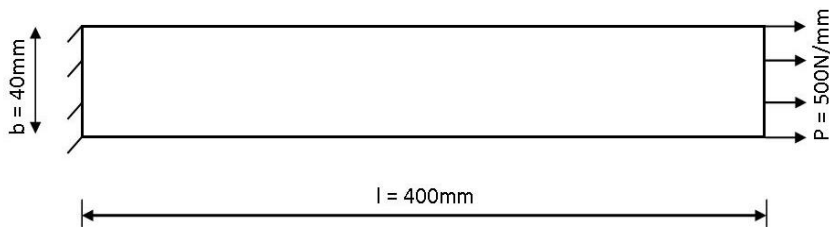


Figure 4.9 – A simple 2D beam structure

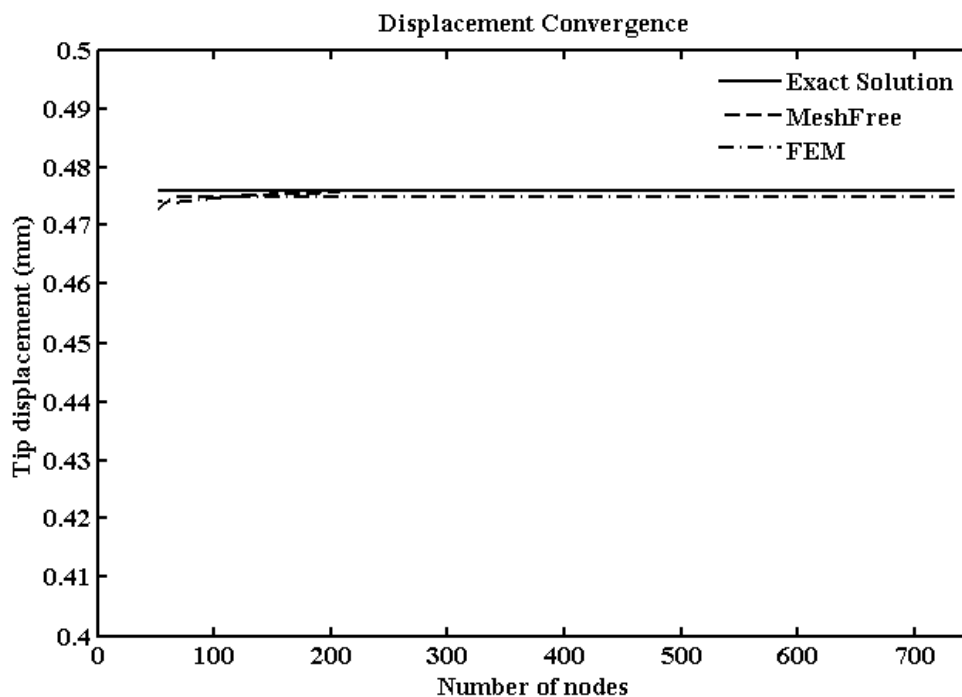


Figure 4.10 – Displacement convergence in 2D beam structure

Displacement and stress distribution for coarse and fine nodal density have been presented in Figures 4.11 and 4.12 respectively. Coarse and fine nodal densities adopted are around 100 and 700 in both FEM and MeshFree methods. Smoother stress distribution of EFG results is clearly observed.

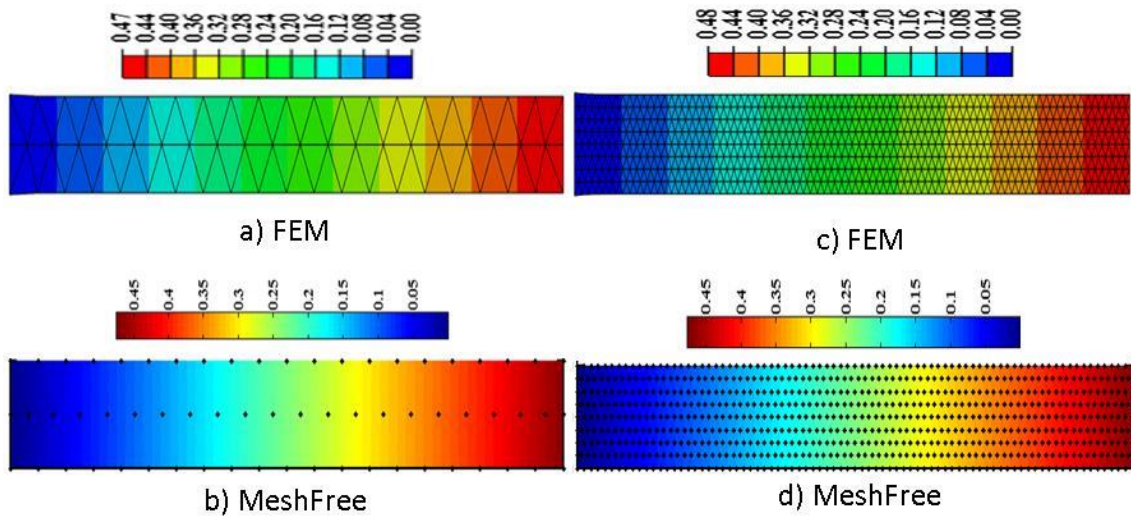


Figure 4.11 – Displacement plot for coarse and fine nodal density in 2D beam

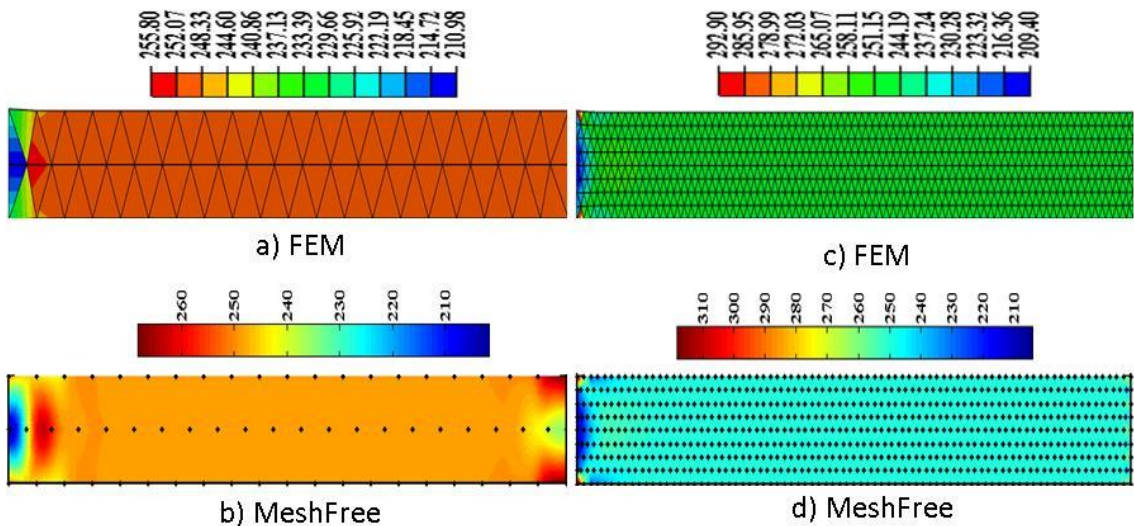


Figure 4.12 – Von Mises stress plot for coarse and fine nodal density in 2D beam

4.3.2 Rectangular Plates with Geometrically Induced Stress Concentrations

Applicability of EFG method in computation of SCF have been presented and explained. Three rectangular plates one with centre circular cut-out and the other two with semi-circular and V-notches at opposite edges as detailed in Figures 4.13-4.15

have been investigated. These plates are constrained with zero displacement at the shorter left edge and on the right edge uniformly distributed axial load is applied. Table 4.3 gives the comparison of results of investigation with closed-form solutions. Plate thickness of 2mm is considered throughout.

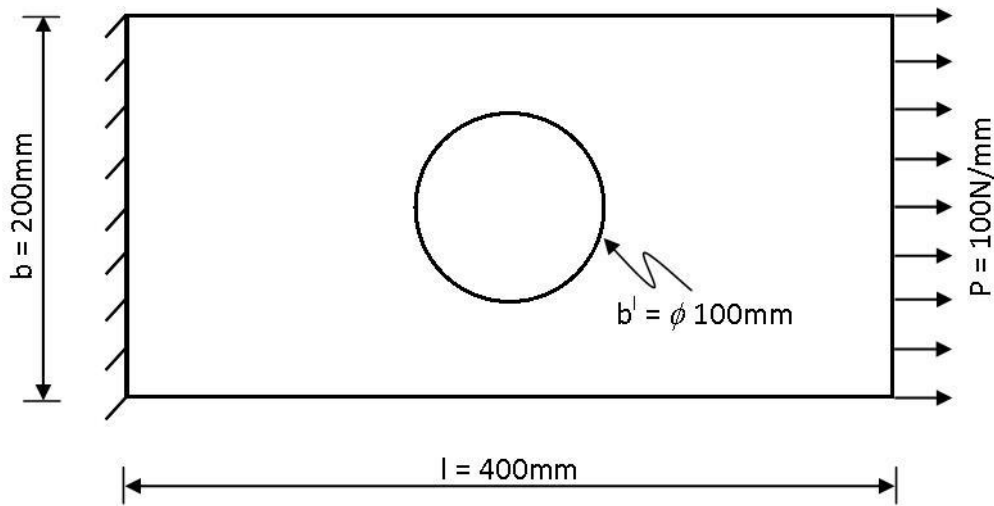


Figure 4.13 – Geometry of plate with centre circular cut-out (Plate 1)

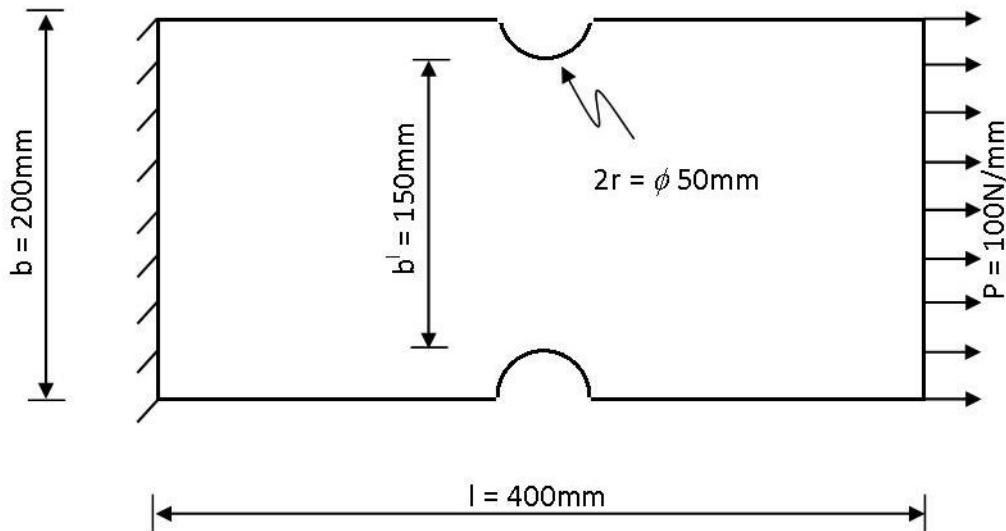


Figure 4.14 – Geometry of plate with two semi-circular notches (Plate 2)

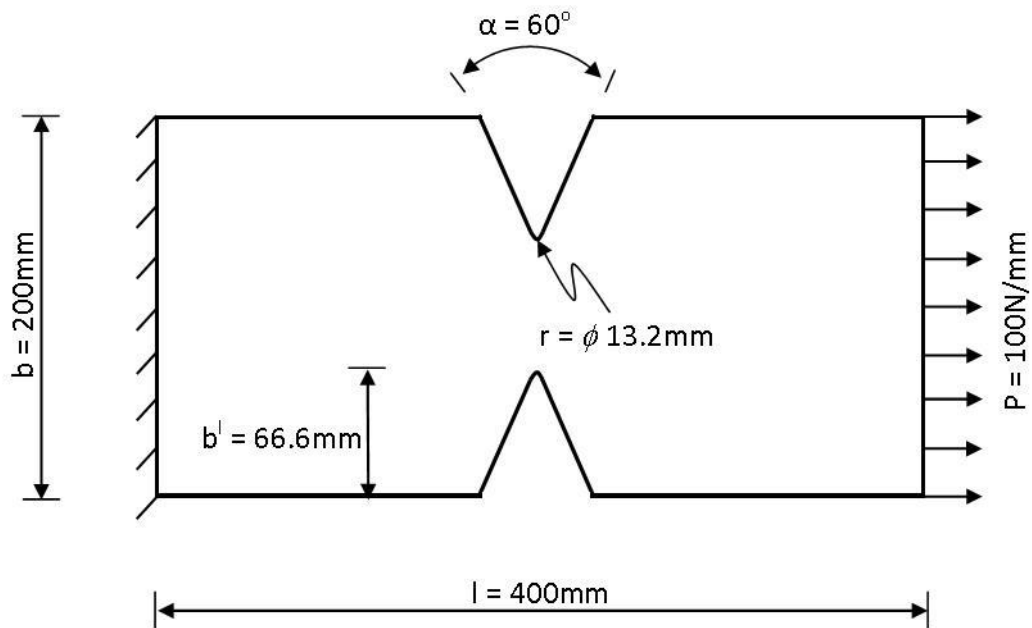


Figure 4.15 – Geometry of plate with two V-notches (Plate 3)

Table 4.3 – SCF values from different methods

| Plate Type | Min. Area for load transfer mm ² | Nominal Stress MPa | Stress Concentration Factor (SCF) | | |
|------------|---|--------------------|-----------------------------------|------|-------|
| | | | Exact | FEM | MFree |
| Plate 1 | 200 | 100 | 2.15 | 1.96 | 2.37 |
| Plate 2 | 300 | 66.66 | 2.26 | 2.01 | 2.22 |
| Plate 3 | 133.32 | 133.32 | 2.73 | 1.95 | 2.58 |

In both the methods, the SCF is calculated for fine nodal density. Tabulated results shows the better approximation of the SCF values by EFG method compared to that of FEM. For plate with centre circular cut-out, though the difference is well within 10% in both the cases, MeshFree has given values higher than the closed-form solutions. This is attributed to over smoothing of nodes and enhanced proximity to closed-form solutions is possible with increase in number of Gauss points. In case of plates with two semi-circular notches and two V-notches at opposite edges, respectively EFG method has shown difference of 2% and 6% on the lower side compared to 11% and 29% obtained from FEM. The miss match in SCF is more in

FEM than EFG method for V-notched plate owing to the failure of FEM to address high stress gradients associated with sudden change in the geometry. Hence it is evident that EFG is superior to FEM in addressing situations where high stress gradients have to be handled.

Displacement distributions are shown in Figures 4.16-4.18, for the three plate structures. These figures include the coarse and fine distribution of nodes in FEM and MeshFree methods. In coarse nodal density, 250 nodes are present whereas in fine nodal density there are 3500 nodes. Von Mises stress distribution for all three cases are shown in Figures 4.19-4.21. Smoother stress distribution can be observed in EFG method for both coarse and fine nodal densities. Further Table 4.4 gives the maximum displacements and stresses (σ_{xx}), which aids in calculation of SCF values for both the method. (Formulae for the closed-form SCF calculation are detailed in Appendix I)

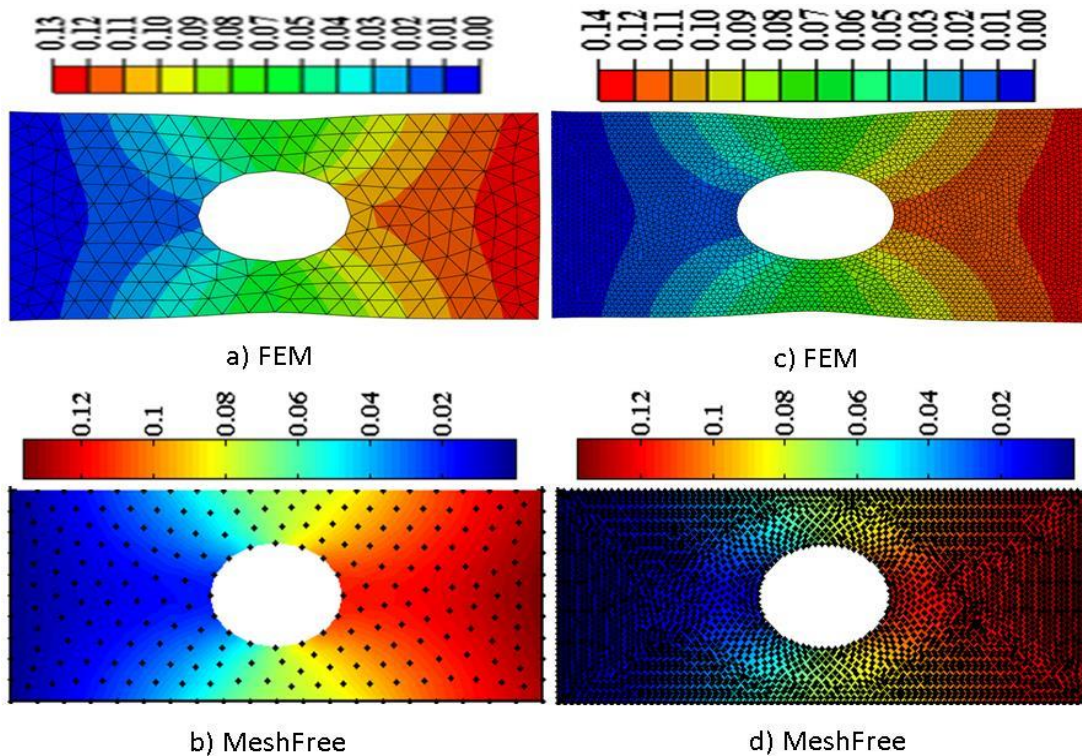


Figure 4.16 – Displacement plot for fine and coarse nodal density in Plate 1

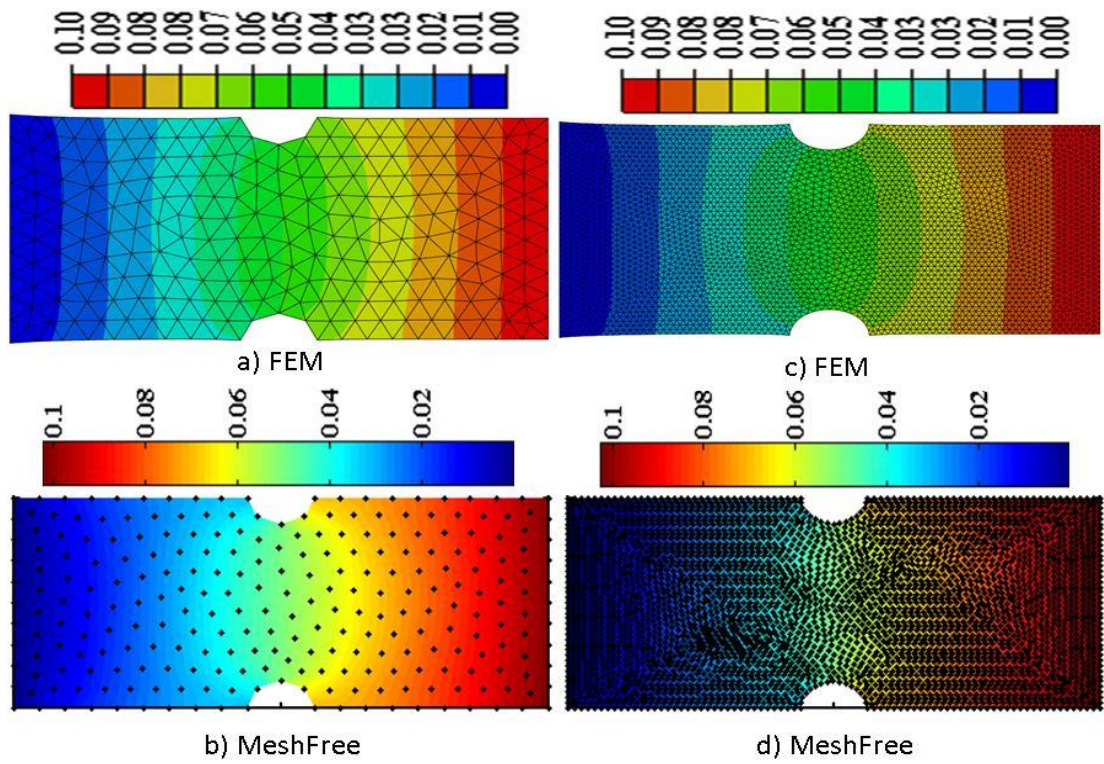


Figure 4.17 – Displacement plot for fine and coarse nodal density in Plate 2

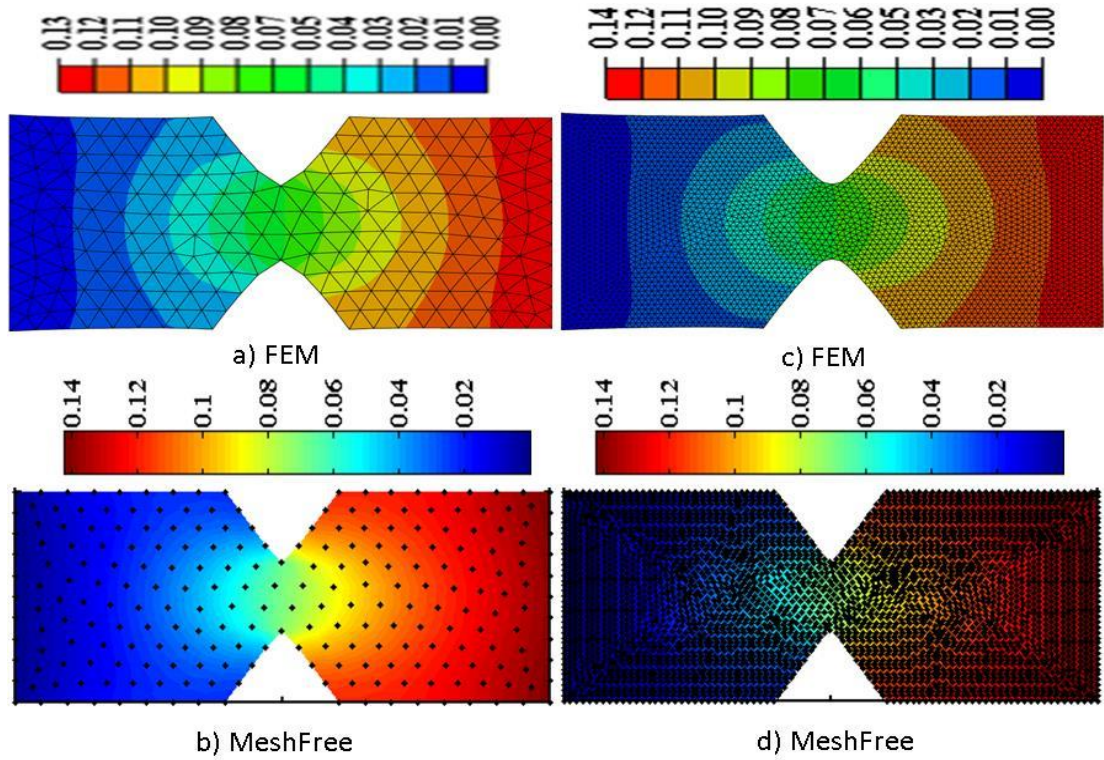


Figure 4.18 – Displacement plot for coarse and fine nodal density in Plate 3

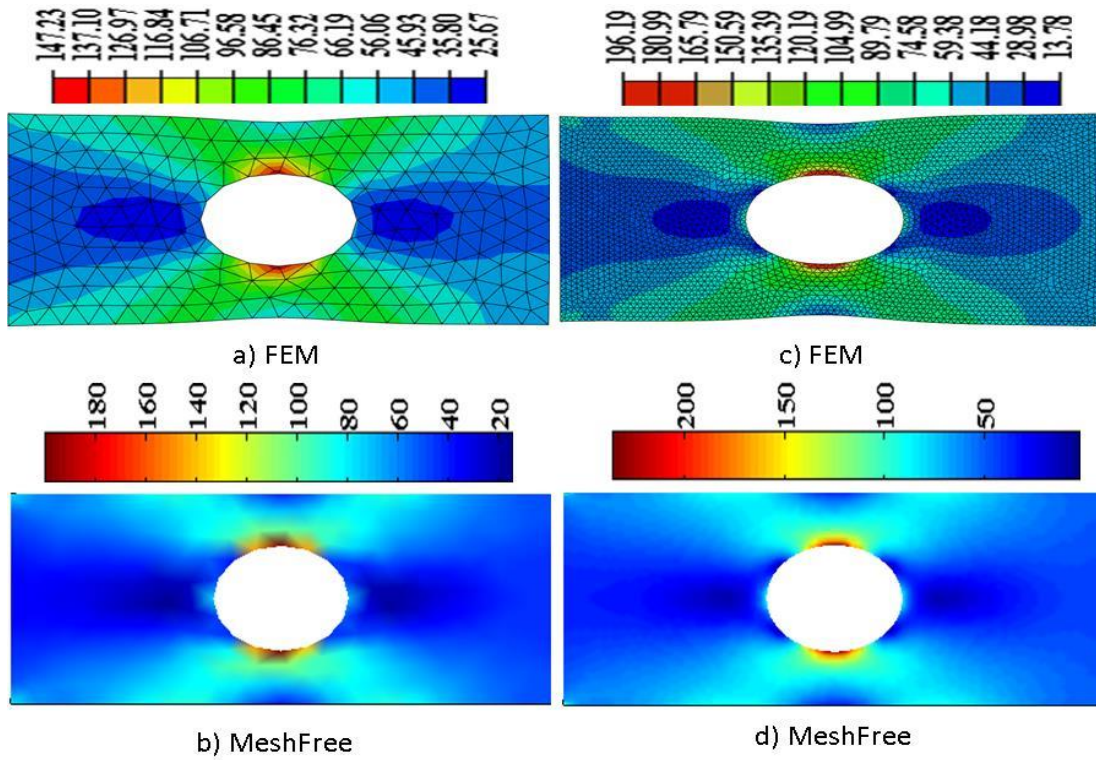


Figure 4.19 – Von Mises stress plot for coarse and fine nodal density in Plate 1

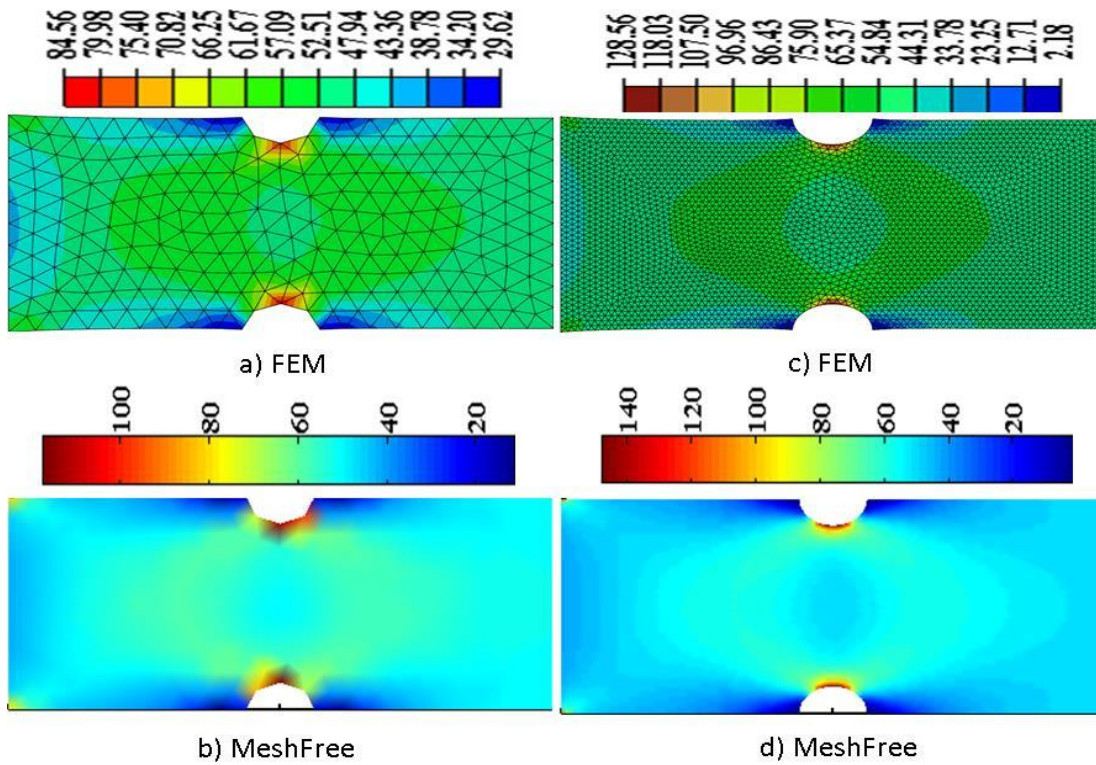


Figure 4.20 – Von Mises stress plot for coarse and fine nodal density in Plate 2

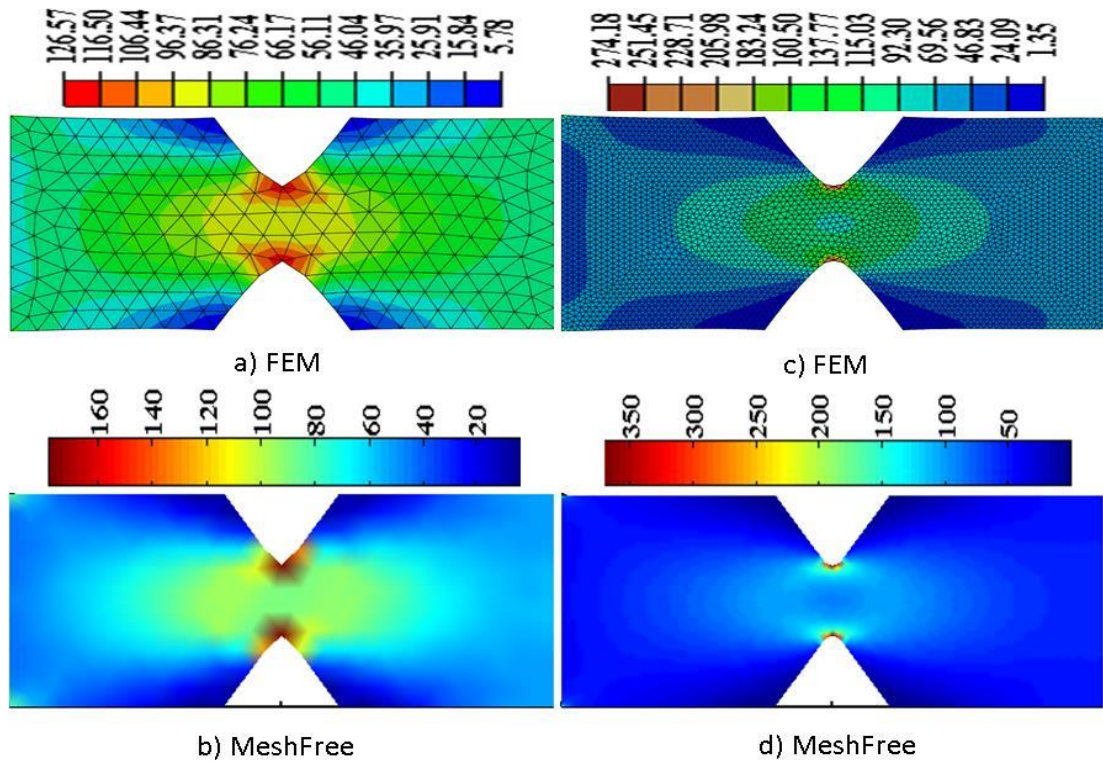


Figure 4.21 – Von Mises stress plot for coarse and fine nodal density in Plate 3

Table 4.4 – Computed displacements and stresses

| Beam Type | Nodal density | Maximum Displacement (mm) | | Maximum Stress (MPa) | |
|-----------|---------------|---------------------------|-------|----------------------|--------|
| | | FEM | MFree | FEM | MFree |
| Plate 1 | Coarse | 0.130 | 0.136 | 152.5 | 207.36 |
| | Fine | 0.135 | 0.137 | 200 | 237.45 |
| Plate 2 | Coarse | 0.100 | 0.102 | 89.18 | 124.65 |
| | Fine | 0.101 | 0.102 | 134.3 | 148.01 |
| Plate 3 | Coarse | 0.134 | 0.142 | 132.1 | 202.02 |
| | Fine | 0.142 | 0.147 | 293.8 | 387.87 |

CHAPTER 5

EFG IN CRACK PROPAGATION ANALYSIS

5.1 CHAPTER PROLOGUE

Usage potential of EFG in addressing high stress gradients and its superiority over FEM has been demonstrated in the preceding chapter. Its utility in crack propagation analysis has been presented in the sections that follow. Computation of SIF employing strain energy release rate has been explained and is adopted for crack propagation identification. Results of the investigation have been compared, verified and validated with the study reported by Patricio and Mattheij, (2007). Enhancement to computational capabilities by way of strain energy based refinement of integration and triangular cells have been proposed with illustration to demonstrate efficacy of the technique.

5.2 FORMULATION FOR MODELLING CRACK PROPAGATION

The propagation path of the crack is directed by the intensity of stress defined by SIF (K_I , K_{II} and K_{III}) at the crack tip. When material crosses a critical value of SIF, the cracks starts and continues to propagate to failure or to a point where SIF drops below critical SIF value.

5.2.1 SIF from Strain Energy Release Rate

The SIF can be computed by measuring the strain energy release rate around the crack tip using J-integral. The crack considered is as shown in Figure 5.1, where Δa is the assumed incremental length of the crack, ahead of the crack tip, r is the length that varies from 0 to Δa , δ_1 and δ_2 is the amount by which the crack opens on application of load and is measured behind the crack tip at r along the local axis 1 and 2, respectively, and σ_{22} , τ_{12} are the normal and shear stresses measured ahead of the crack tip at r in the local axis (123). Then the strain energy release rate for mode I and mode II crack opening is represented using the integral (Chow and Atluri, 1995),

$$G_I = \frac{1}{2\Delta a} \int_0^{\Delta a} \sigma_{22}(r) \delta_2(\Delta a - r) dr \quad \dots 5.1$$

$$G_{II} = \frac{1}{2\Delta a} \int_0^{\Delta a} \sigma_{12}(r) \delta_1(\Delta a - r) dr \quad \dots 5.2$$

In terms of normal coordinates, in order to evaluate the integral in Equations 5.1 and 5.2, the strain energy release rate is represented in the numerical integration form,

$$G_I = \frac{1}{2\Delta a} \int_{-1}^1 \sigma_{22}(\xi) \delta_2(1-\xi) \frac{\Delta a}{2} d\xi = \frac{1}{4} \sum_{i=1}^{n_c} w_i \sigma_{22}(\xi) \delta_2(1-\xi) \quad \dots 5.3$$

$$G_{II} = \frac{1}{2\Delta a} \int_{-1}^1 \tau_{12}(\xi) \delta_1(1-\xi) \frac{\Delta a}{2} d\xi = \frac{1}{4} \sum_{i=1}^{n_c} w_i \tau_{12}(\xi) \delta_1(1-\xi) \quad \dots 5.4$$

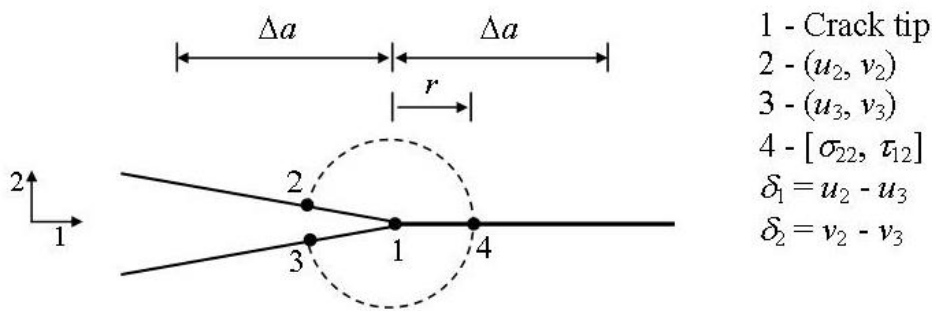


Figure 5.1 – Crack Tip

From the energy release rate, the SIF for mode I and mode II crack opening is written as,

$$K_I = \sqrt{G_I E} \quad \dots 5.5$$

$$K_{II} = \sqrt{G_{II} E} \quad \dots 5.6$$

5.2.2 Stresses and Displacements in Arbitrarily Orientated Crack

If the crack is arbitrarily oriented at angle θ , then the global stresses and displacements in xyz coordinate is transformed to the local 123 coordinates by using the following stress and displacement transformation equations,

$$\sigma_{22} = \frac{\sigma_{xx} + \sigma_{yy}}{2} - \frac{\sigma_{xx} - \sigma_{yy}}{2} \cos(2\theta) - \tau_{xy} \sin(2\theta) \quad \dots 5.7$$

$$\tau_{12} = \frac{\sigma_{xx} - \sigma_{yy}}{2} \sin(2\theta) + \tau_{xy} \cos(2\theta) \quad \dots 5.8$$

$$\delta_1 = \delta_x \cos(\theta) + \delta_y \sin(\theta) \quad \dots 5.9$$

$$\delta_2 = \delta_x \sin(\theta) + \delta_y \cos(\theta) \quad \dots 5.10$$

5.2.3 SIF Condition for Crack Growth

The crack grows when the SIF crosses the critical SIF. This condition for crack to grow, when subjected to pure mode I loading is,

$$K_I \geq K_{Ic} \quad \dots 5.11$$

For a mixed mode, i.e. when the crack is subjected to mode I and mode II loading, for the crack to grow the following condition needs to be satisfied given by (Patricio and Mattheij, 2007),

$$\frac{4\sqrt{2}K_{II}^3 \left(K_I + 3\sqrt{K_I^2 + 8K_{II}^2} \right)}{\left(K_I^2 + 12K_{II}^2 - K_I\sqrt{K_I^2 + 8K_{II}^2} \right)^{3/2}} \geq K_{Ic} \quad \dots 5.12$$

For a mild steel material, the critical SIF (K_{Ic}) is $4427 \text{ N/mm}^{1.5}$.

5.2.4 Crack Propagation Angle under Combined Mode I, Mode II Loading

If the crack propagates, then its propagation angle is measured from the SIF using the following equation (Patricio and Mattheij, 2007),

$$\theta_c = 2 \tan^{-1} \left(\frac{1}{4} \left(\frac{K_I}{K_{II}} \pm \sqrt{\left(\frac{K_I}{K_{II}} \right)^2 + 8} \right) \right) \quad \dots 5.13$$

where θ_c is the crack propagation angle, which is measured w.r.t. to the local axis 1 and is anti-clockwise in the plane 12.

The iterative process involved in the propagation of crack is as shown in Figure 5.2.

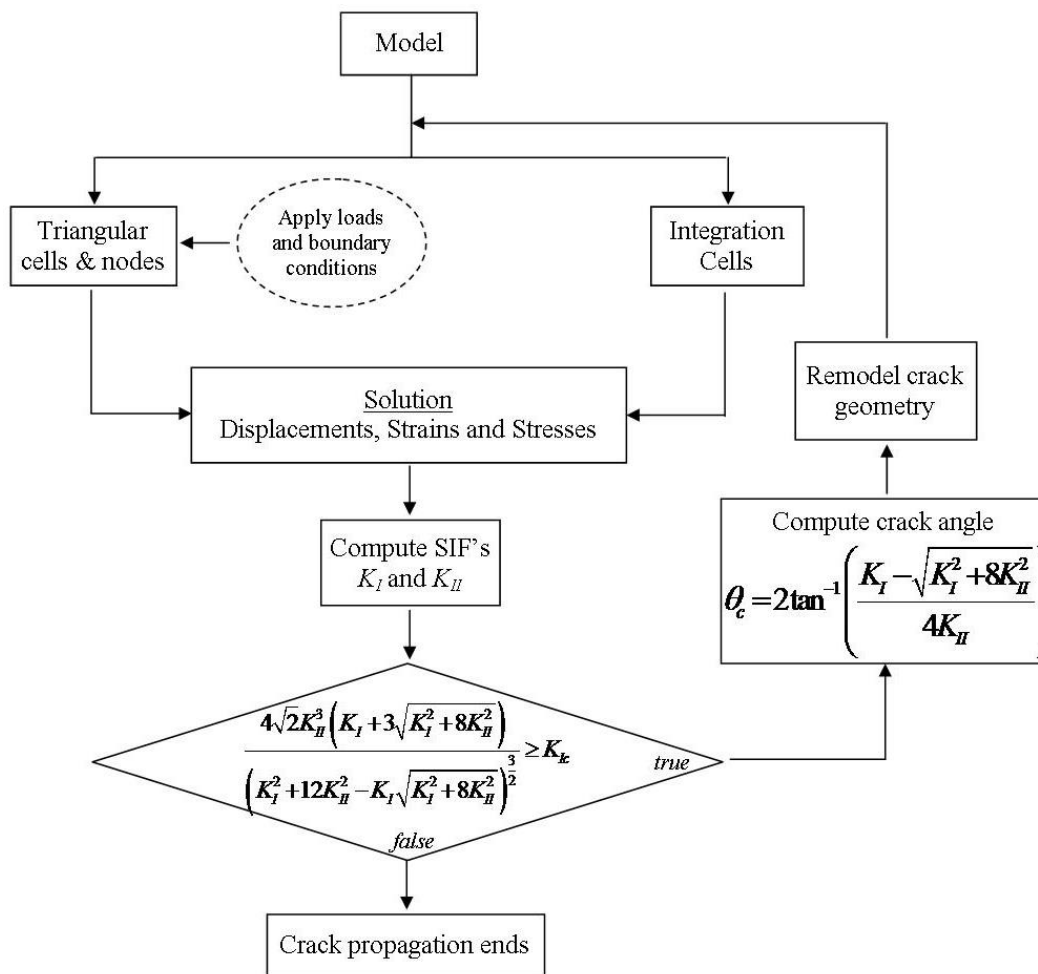


Figure 5.2 – Iterative process involved in crack propagation

5.3 NUMERICAL DEMONSTRATION OF CRACK PROPAGATION ANALYSIS

5.3.1 Verification of SIF Computation

To verify the SIF computation, a plate fixed on one of its shorter edges and uniformly loaded on the other is considered for the analysis. A pre-initiated vertical crack at the centre of the plate with length 100mm has been created in the geometric model and determination of SIF has been attempted to arrive at nodal density and distribution for convergence and accuracy. Assumed step length (Δa) dictates prediction of crack path and as reported in literature should be small enough to yield better approximation. The plate analysed is shown in Figure 5.3 with a step length (Δa) of 2.5mm has been considered and Figures 5.4 and 5.5 gives analysis results for displacements and von

Mises stresses. The smooth distribution of result is clearly evident and SIF value is in good agreement with closed-form. In order to verify SIF obtained by EFG method, closed-form solution (Equation is in Appendix I) available for the stated problem is used. The material properties (Refer to Chapter 4 Table 4.1) and plate thickness is taken as 2mm.

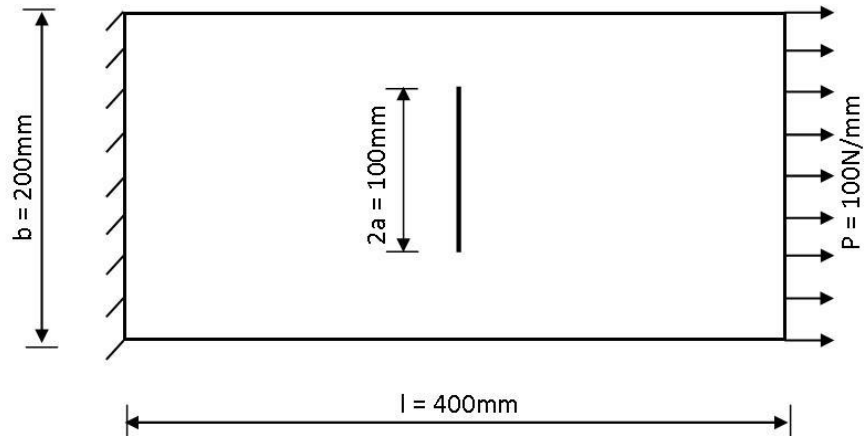


Figure 5.3 – Geometry of the plate with centre vertical crack

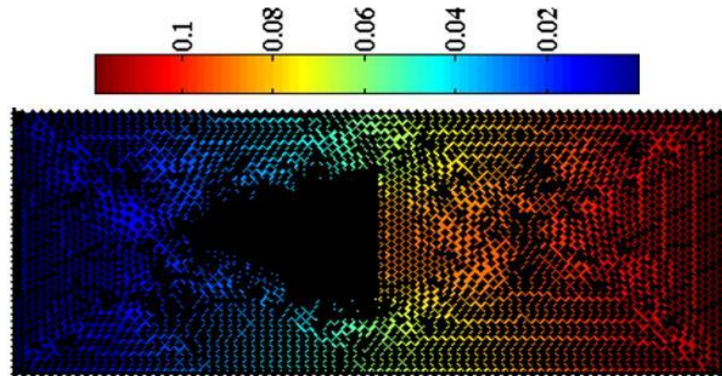


Figure 5.4 – Node and displacement distribution in plate with centre vertical crack

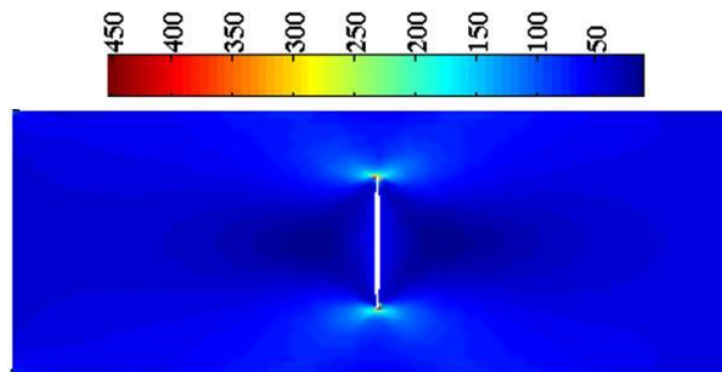


Figure 5.5 – Von Mises stress distribution in plate with centre vertical crack

Table 5.1 – Computed results for plate with centre crack

| Displacement (mm) | Stress (MPa) | SIF (N/mm ^{1.5}) | |
|----------------------|--------------|----------------------------|-------|
| | | Closed-form | MFree |
| 0.119 | 516.31 | 680 | 673 |

5.3.2 Crack Propagation in a Plate With Inclined Edge Crack

Crack propagation path identification attempted by Patricio and Mattheij (2007) using XFEM has been considered for investigation by proposed technique. The geometry of the plate is shown in Figure 5.6, where the crack is inclined at an angle of 67.5deg to the edge of the plate. One of the shorter edges of the plate is constrained and on the other end uniformly distributed loaded is applied. Under this configuration of plate and loading, the crack tip will be subjected to both mode I and mode II loading.

The crack propagation has been simulated and SIF for crack growth (Equation 5.12) has been computed and shown in Table 5.2. Crack growth is indicated by SIF being higher than critical SIF (K_{Ic}). The displacement and von Mises stress distribution in the plate at different iteration step of the crack growth are presented in Figures 5.7 and 5.8. Crack propagation obtained has been compared with the results reported by Patricio and Mattheij (2007) and is presented in Figure 5.9.

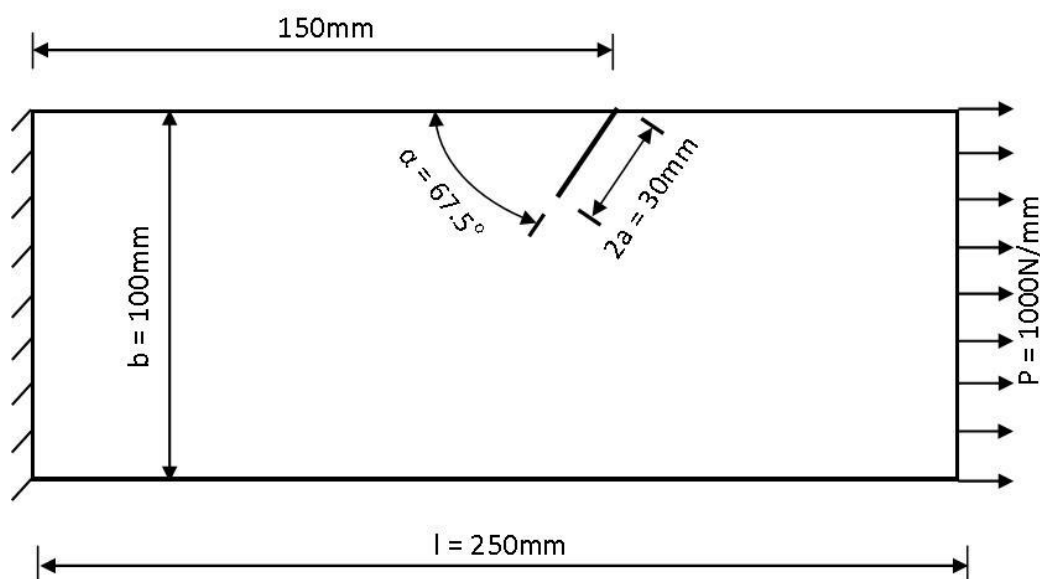


Figure 5.6 – Geometry of the plate with inclined edge crack

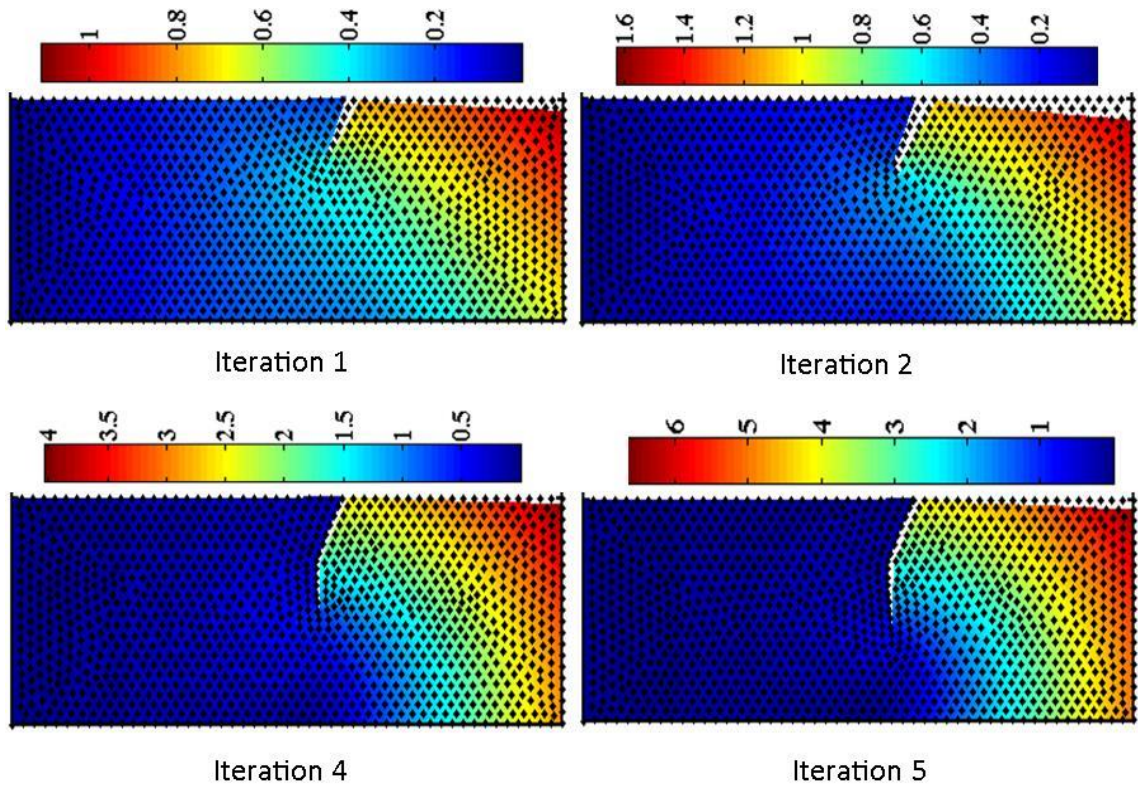


Figure 5.7 – Displacement and node distribution for plate with inclined edge crack

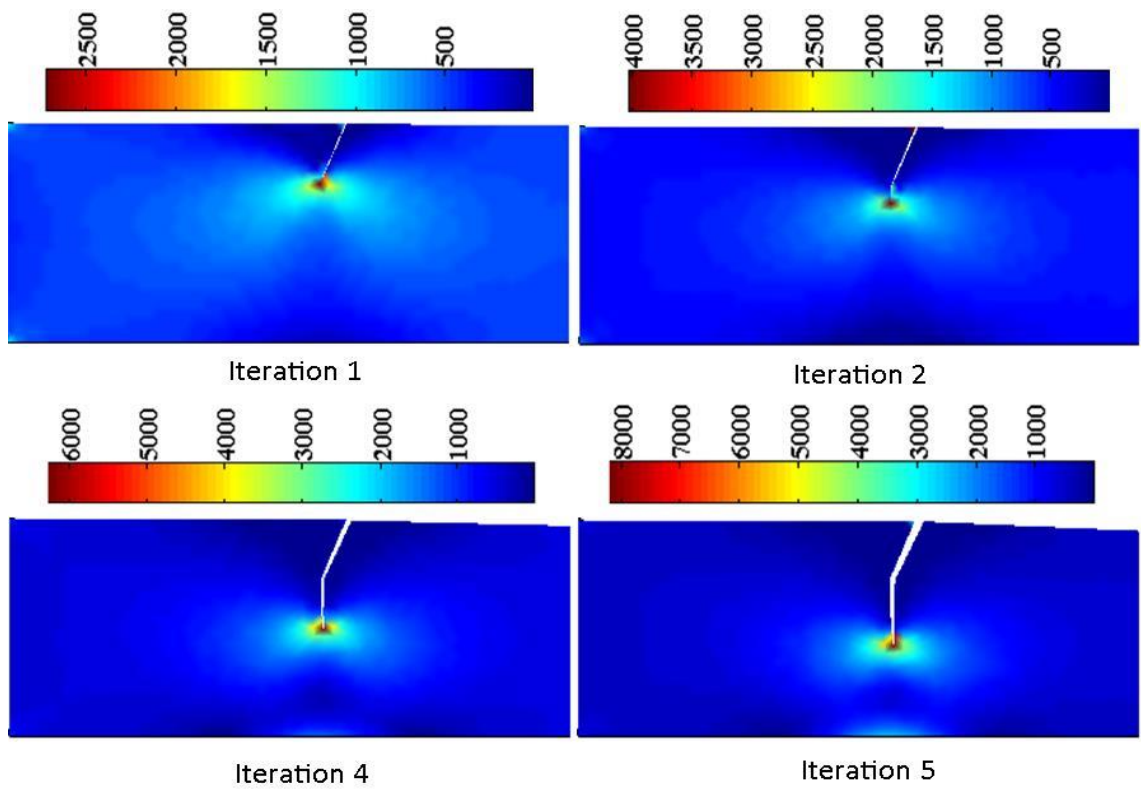


Figure 5.8 – Von Mises stress distribution for plate with inclined edge crack

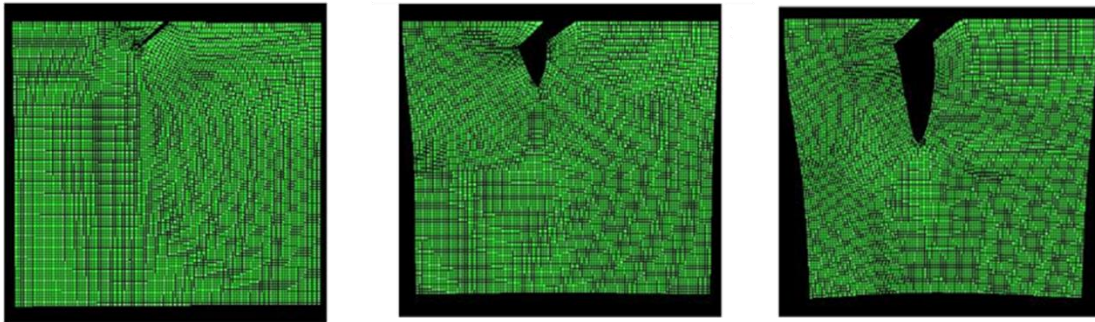


Figure 5.9– Crack path as shown in literature for plate with inclined crack

Table 5.2 – Displacement, stress and SIF for plate with inclined edge crack

| Iteration No. | Displacement (mm) | Stress (MPa) | SIF* (N/mm ^{1.5}) | Indication | Inclination |
|---------------|-------------------|--------------|-----------------------------|-------------------------|-------------|
| 1 | 0.938 | 2972.6 | 5373 | propagates | 21.56° |
| 2 | 1.241 | 3820.5 | 7379 | propagates | 0° |
| 3 | 1.795 | 5817.1 | 10727 | propagates | 0° |
| 4 | 2.795 | 7753.7 | 14527 | propagates | 0° |
| 5 | 4.341 | 10094 | 19714 | continues till breakage | 0° |

*For steel critical SIF =4427 N/mm^{1.5} and if it exceeds critical crack propagates.

5.3.3 Crack Propagation in a Punctured Plate With Edge Crack

The geometry of the plate (steel) is shown in Figure 5.10, with one of the shorter edge fixed and the other subjected to uniformly distributed load. The computed SIF for crack growth at various steps are tabulated in Table 5.3. SIF value increases or decreases based on the crack path taken and if it falls below critical SIF (K_{IC}), ceases to propagate. The displacement and von Mises stress plot at different iteration step can be seen in Figure 5.11 and 5.12, respectively.

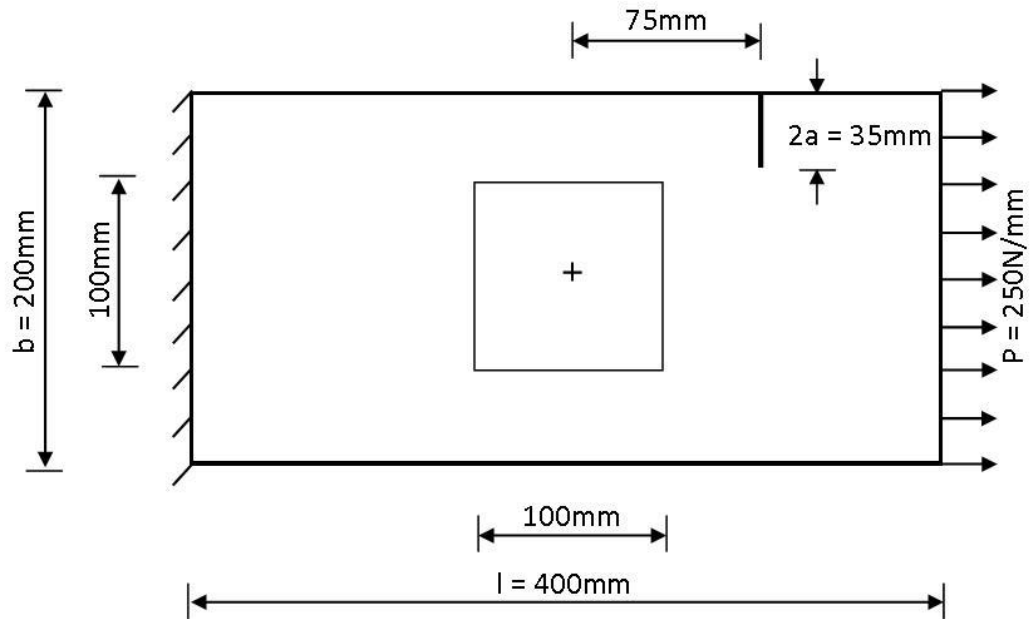


Figure 5.10 – Geometry of the punctured plate with edge crack

Table 5.3 – Displacement, stress and SIF for punctured plate with edge crack

| Iteration No. | Displacement (mm) | Stress (MPa) | SIF ($\text{N}/\text{mm}^{1.5}$) | Indication | Inclination |
|---------------|-------------------|--------------|------------------------------------|------------------------------|---------------|
| 1 | 1.086 | 2077 | 4662.9 | propagates | 4.76° |
| 2 | 1.288 | 3701.2 | 7186.1 | propagates | 1.94° |
| 3 | 1.532 | 4500.3 | 8939.7 | propagates | 11.64° |
| 4 | 1.815 | 5154.9 | 9368.4 | propagates | 16.53° |
| 5 | 1.873 | 5573.6 | 4798.6 | propagates | 28.78° |
| 6 | 2.451 | 6360.3 | 5079.1 | propagates | 19.49° |
| 7 | 2.808 | 6244 | 9461.6 | propagates | 55.61° |
| 8 | 3.012 | 7001 | 0 | negative energy release rate | - |

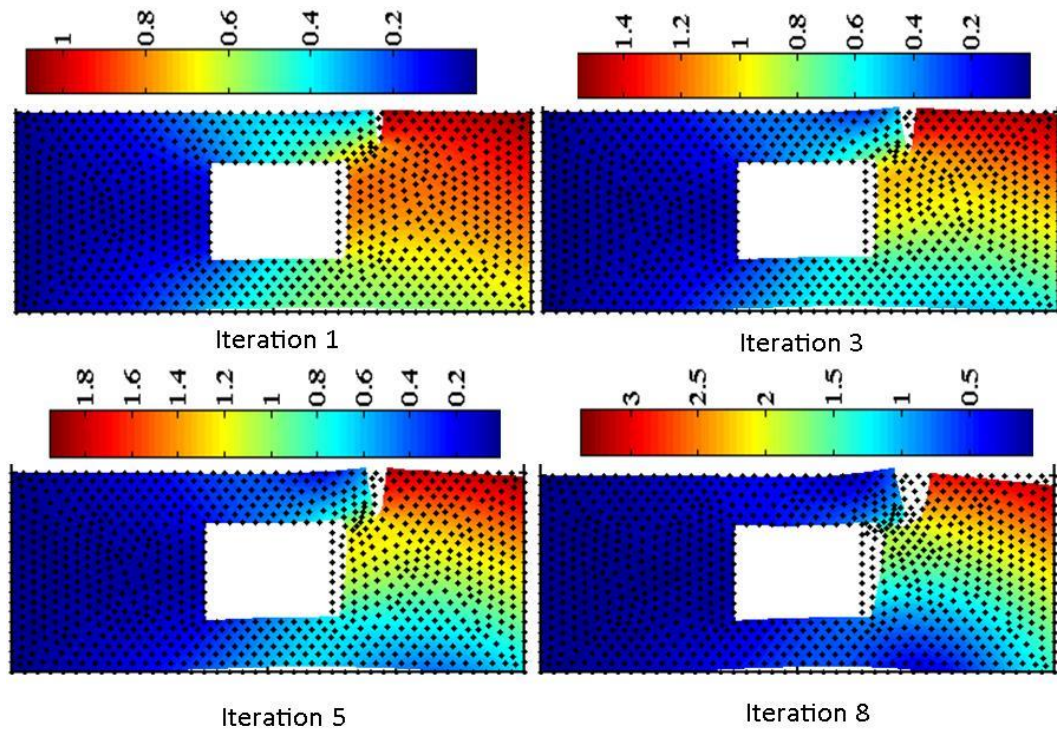


Figure 5.11 – Displacement and node distribution in punctured plate with edge crack

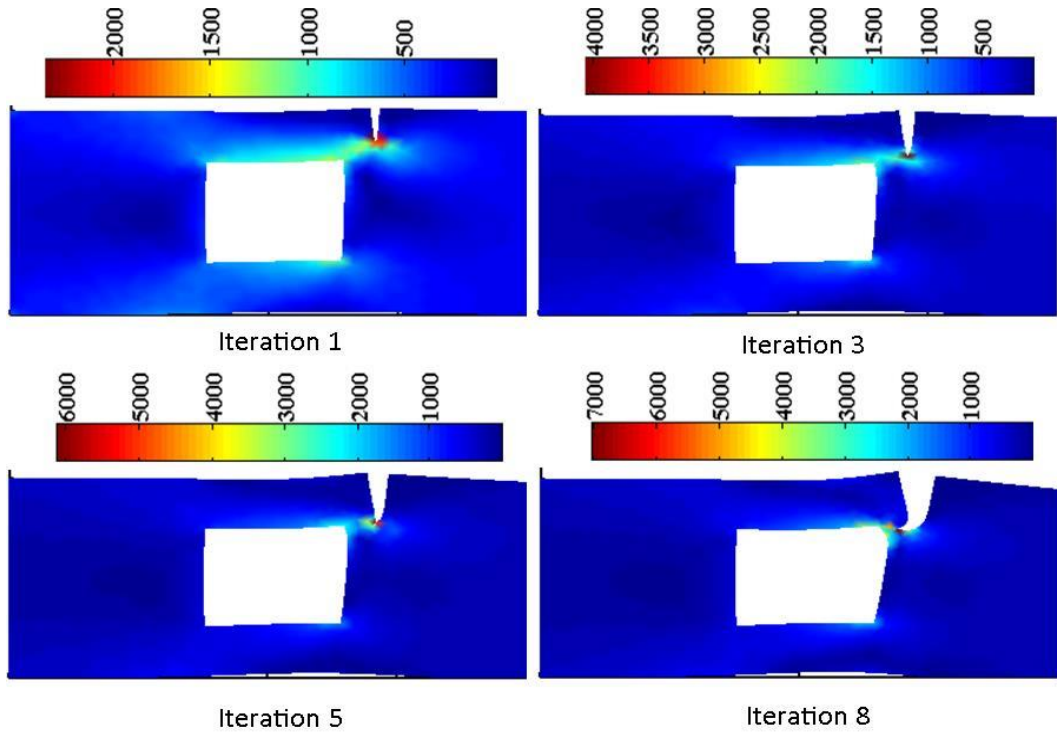


Figure 5.12 – Von Mises stress distribution for punctured plate with edge crack

5.4 DEVELOPED METHODOLOGY FOR ADAPTIVE REFINEMENT

Strain energy density computations is necessary and forms the basis for reassessment and reallocation of nodes. Computation details are as under.

5.4.1 Strain Energy Density in Integration Cell

The strain energy density in integration cell is computed for the i^{th} cell,

$$S_{IC}^{(i)} = \frac{\frac{1}{2} \int_{V_c^{(i)}} \sigma^T \varepsilon dV_c^{(i)}}{\int_{V_c^{(i)}} dV_c^{(i)}} = \frac{t \sum_{j=1}^n w_j \sigma_j^T \varepsilon_j |J^{(i)}|}{t \sum_{j=1}^n w_j |J^{(i)}|} \quad \dots 5.14$$

where V_c is the volume of the i^{th} cell; σ and ε are the stresses and strains; n is the number of Gauss points in the integration cell, w_j is Gauss weight in the numerical integration of the cell energy.

5.4.2 Cell Refinement Based on Strain Energy

Strain energy density computed as in the preceding section is employed in cell refinement, wherein cell with high strain energy density above the set threshold value is chosen and refined by dividing one cell into four cells (Figure 5.13). The process is continued till the energy density in all the cells is below the set threshold value.

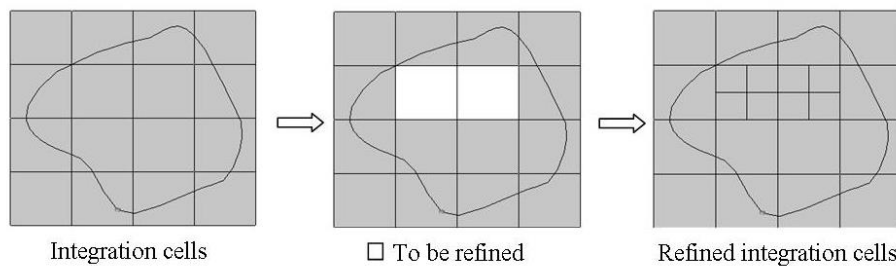


Figure 5.13 – Refinement of integration cells by sub-dividing each cell into four cells

5.4.3 Strain Energy Density in Triangular Cell

The strain energy density in the triangular cell is computed from the strain energy of integration cells based on the area contributed by them to each of the triangular cell. This is mathematically represented for the i^{th} triangular cell,

$$S_{TC}^{(i)} = \frac{\sum_{j=1}^n S_{IC}^{(j)} \bar{A}_{TC}^{(j)}}{A_{TC}} \quad \dots 5.15$$

where n is the number of integration cells that overlaps a given i^{th} triangular cell; \bar{A}_{TC} is the area common to the j^{th} integration cell and the i^{th} triangular cell.

5.4.4 Node Refinement Based on Strain Energy

The nodal refinement is achieved using the following three steps:

1. The triangular cells with high strain energy densities above the set threshold are identified (Equation 5.15) for refinement
2. Each of these identified triangular cells are subdivided into four triangular cells thus adding additional nodes on the vertices of the triangle in the region of refinement.
3. Further, the triangular cells are redefined such that no free edges exist in the refined region.

The detailed steps of nodal refinement are shown in Figure 5.14. The threshold is taken in this work as the convergence of the stress value, i.e. if the stresses from the previous iteration do not deviate by more than 10% difference then the further refinement is terminated. Higher levels of accuracy are possible at the expense of computation time and efforts. The procedure is detailed in Figure 5.15.

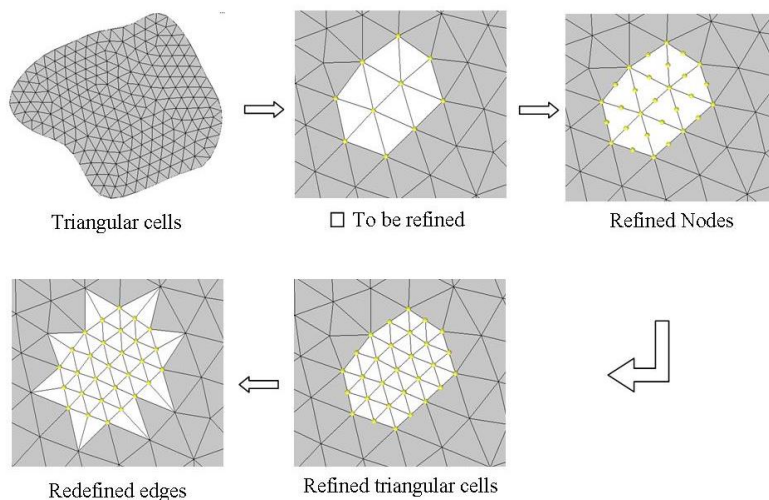


Figure 5.14 – Refinement of nodes by sub-dividing each triangular cell into four cells

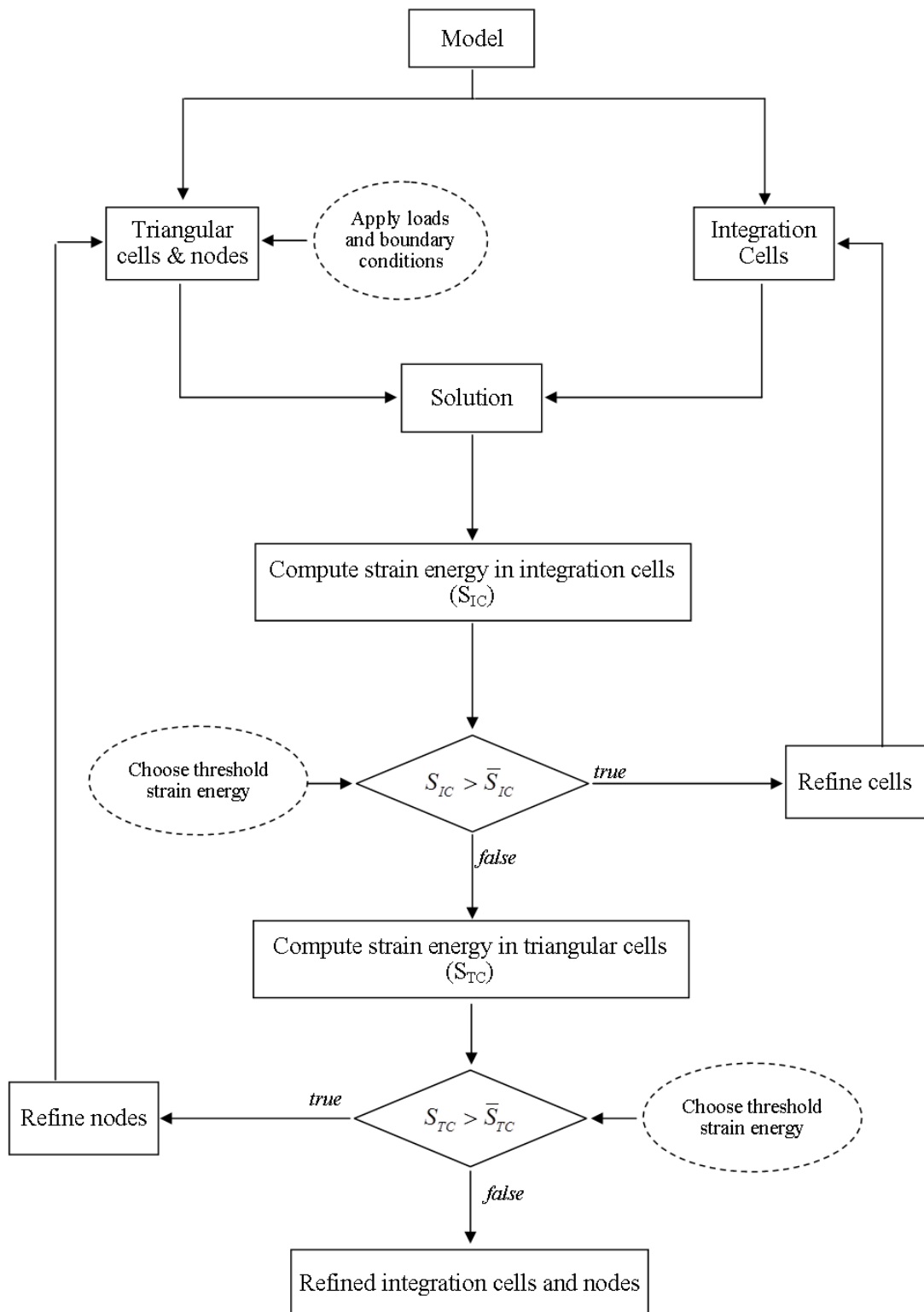


Figure 5.15 – Adaptive refinement of integration cells and nodal density

5.5 ILLUSTRATION OF ADAPTIVE REFINEMENT

5.5.1 Adaptive Refinement on Rectangular Plate with Semi-Circular Notches

The strategy for adaptive refinement is detailed in this section. In the first iteration, the displacements and stresses are computed with very coarse nodal and integration cell density (Table 5.4). In each iteration, the cells that lie in the top 20% of the strain energy levels are subjected to refinement. Table 5.4 shows the refinement iterations followed and the number of nodes and cells obtained in each step.

In Figures 5.16 and 5.17, the strain energy distribution of integration and triangular cells are shown, respectively, where refinement is seen to occur around the high stress regions. As the iterations increase, the computed stress values saturate and the refinement is stopped when the computed stress difference is less than 10%. A drastic reduction of about 86% of nodes with acceptable accuracy has been observed. Displacement distribution along with the refined nodes and von Mises stress distributions are shown in Figures 5.18 and 5.19 respectively.

Table 5.4 – Adaptive refinement iterations in plate with semi-circular notches

| Refinement of | No. of Cells | No. of Nodes | Displacement (mm) | Stress (MPa) |
|---|--------------|--------------|-------------------|--------------|
| None | 50 | 261 | 0.101 | 116.86 |
| Cell | 74 | 261 | 0.101 | 120.14 |
| Node | 74 | 367 | 0.102 | 151.1 |
| Cell | 146 | 367 | 0.102 | 157.51 |
| Node | 146 | 485 | 0.102 | 164.8 |
| fine nodal density (Uniform Distribution) | 200 | 3580 | 0.102 | 148.01 |

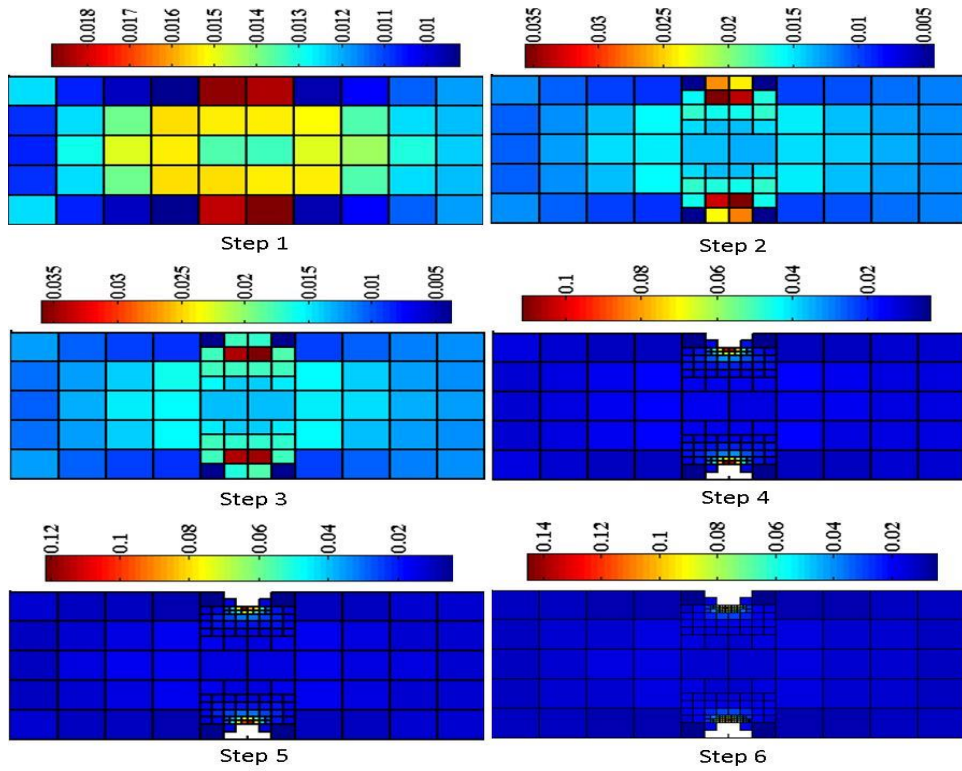


Figure 5.16 – Strain energy in integration cells of plate with semi-circular notches

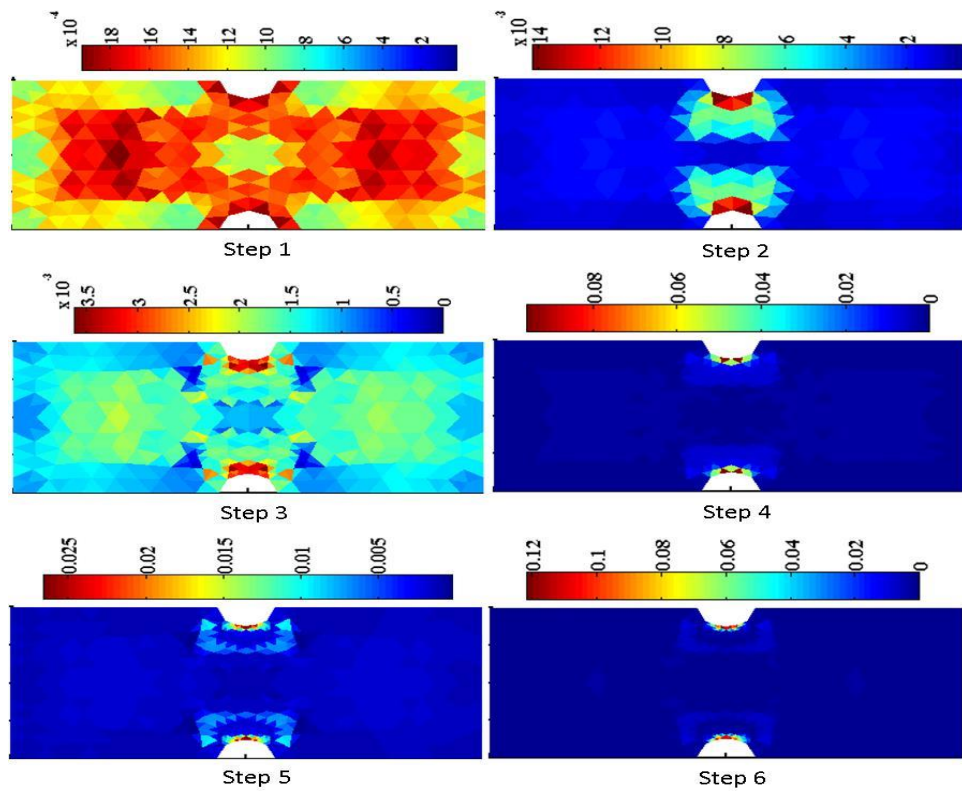


Figure 5.17 – Strain energy in triangular cells of plate with semi-circular notches

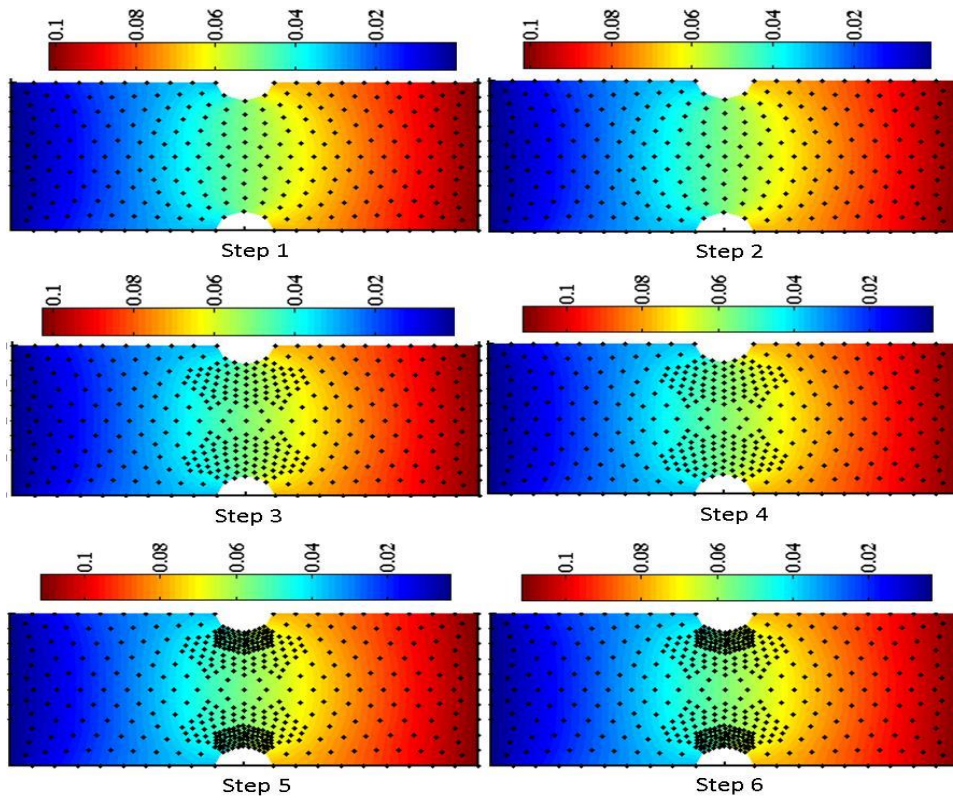


Figure 5.18 – Displacement plot of adaptively refined plate with semi-circular notches

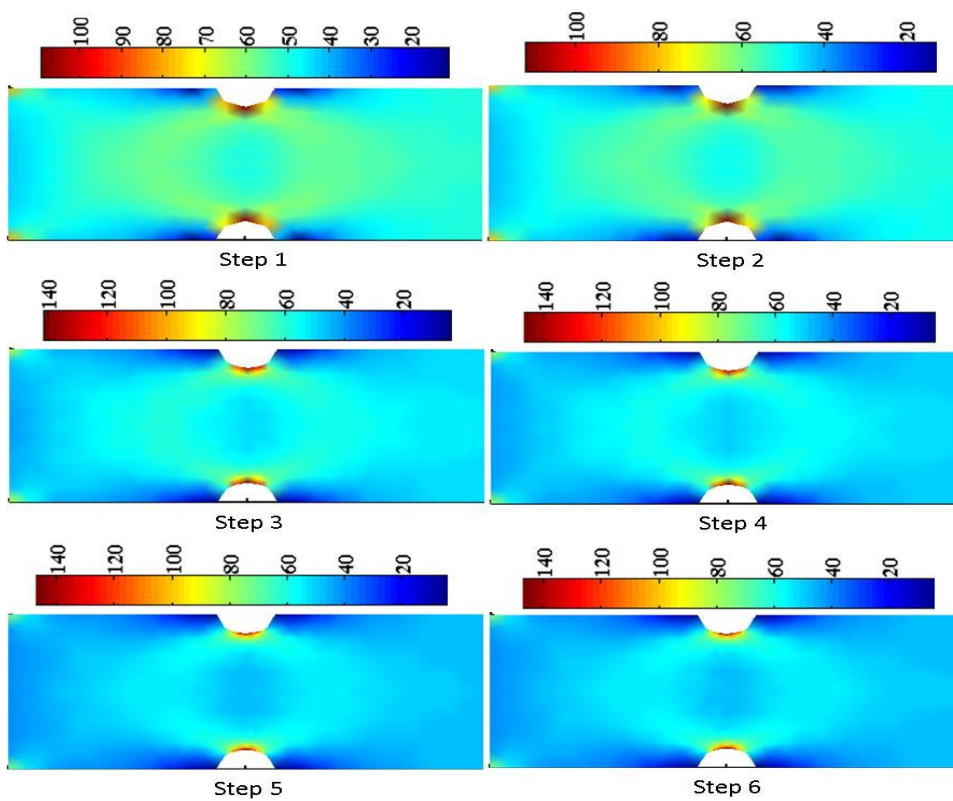


Figure 5.19 – Von Mises stress of adaptively refined plate with semi-circular notches

5.5.2 Adaptive Refinement on Rectangular Plate with Angled Edge Crack

The displacements and stresses computed for very coarse density of nodes and integration cells in the initial iteration are as shown in Table 5.5. This has been followed by the refinement of top 20% of the strain energy levels. Number of iterations and the number of nodes and cells obtained as results for each step are presented in Table 5.5.

The refinement of integration and triangular cells around the crack tip occurs after every iteration and the strain energy distribution for the same can be observed in Figures 5.20 and 5.21 respectively. About 75% reduction of nodes can be observed with acceptable accuracy. Further Displacement distributions along with the refined nodes (Figure 5.22) and von Mises stress distributions (Figure 5.23) are presented.

Table 5.5 – Adaptive refinement iterations in plate with inclined edge crack

| Refinement of | No. of Cells | No. of Nodes | Displacement (mm) | Stress (MPa) |
|--|--------------|--------------|-------------------|--------------|
| None | 40 | 96 | 0.852 | 1036.8 |
| Cell | 67 | 96 | 0.853 | 1036.5 |
| Node | 67 | 183 | 0.994 | 2874.5 |
| Cell | 91 | 183 | 0.995 | 2886.8 |
| Node | 91 | 291 | 1.03 | 2978.8 |
| With fine nodal density (uniform distribution) | 208 | 1211 | 0.938 | 2972.6 |

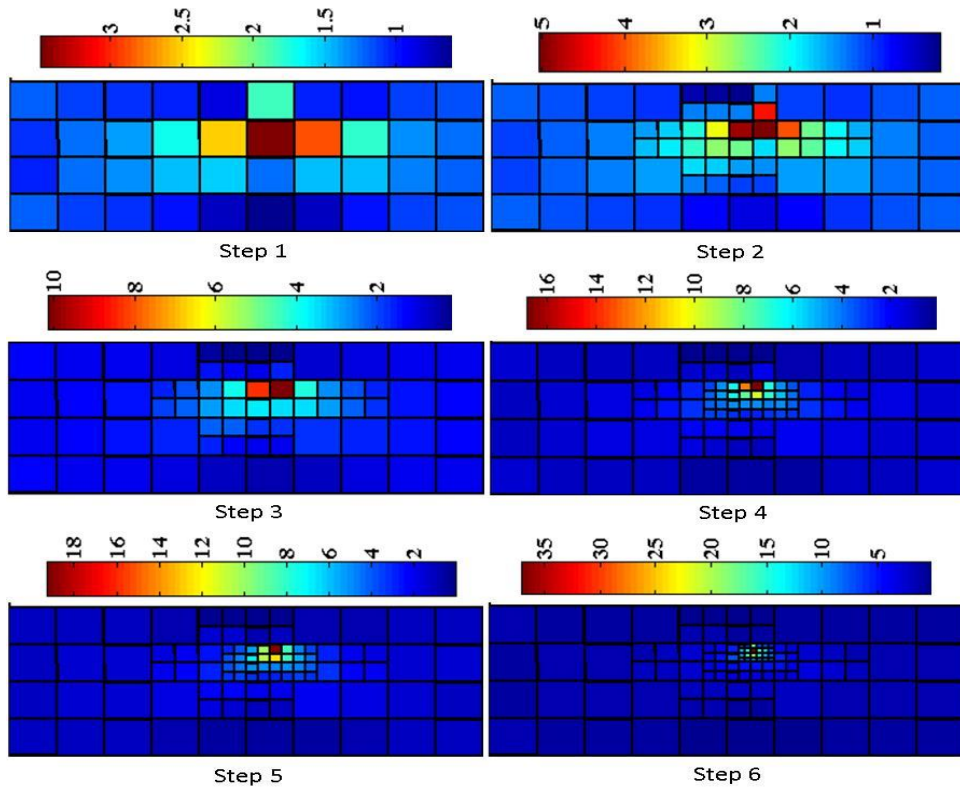


Figure 5.20 – Strain energy in integration cells for plate with inclined edge crack

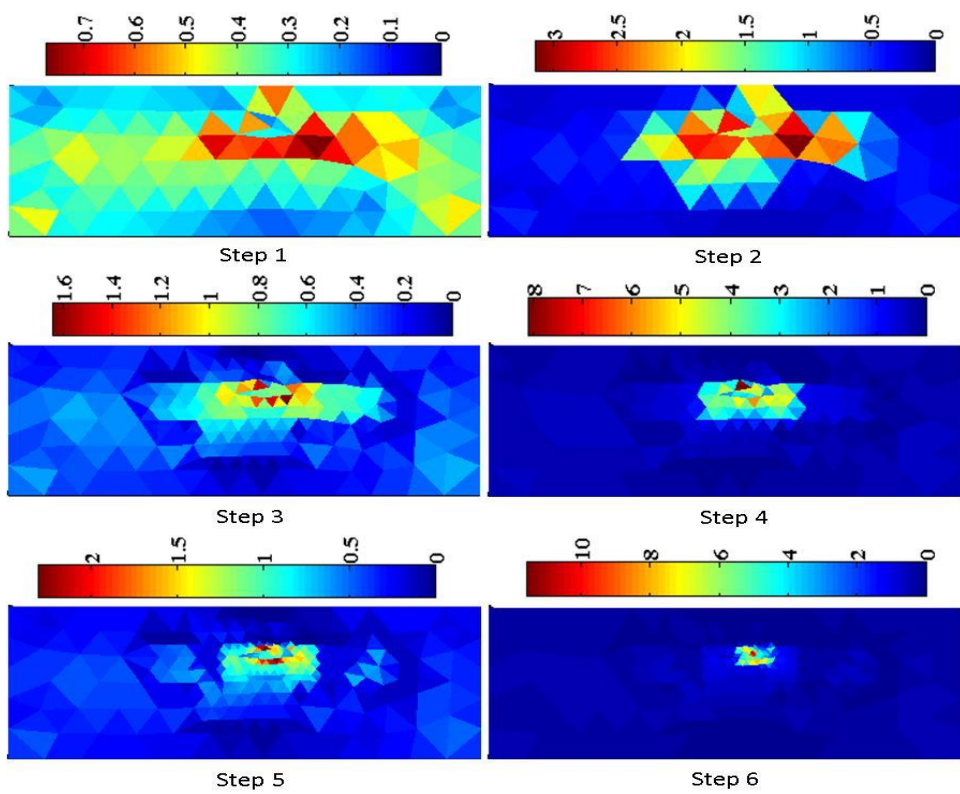


Figure 5.21 – Strain energy in triangular cells for plate with inclined edge crack

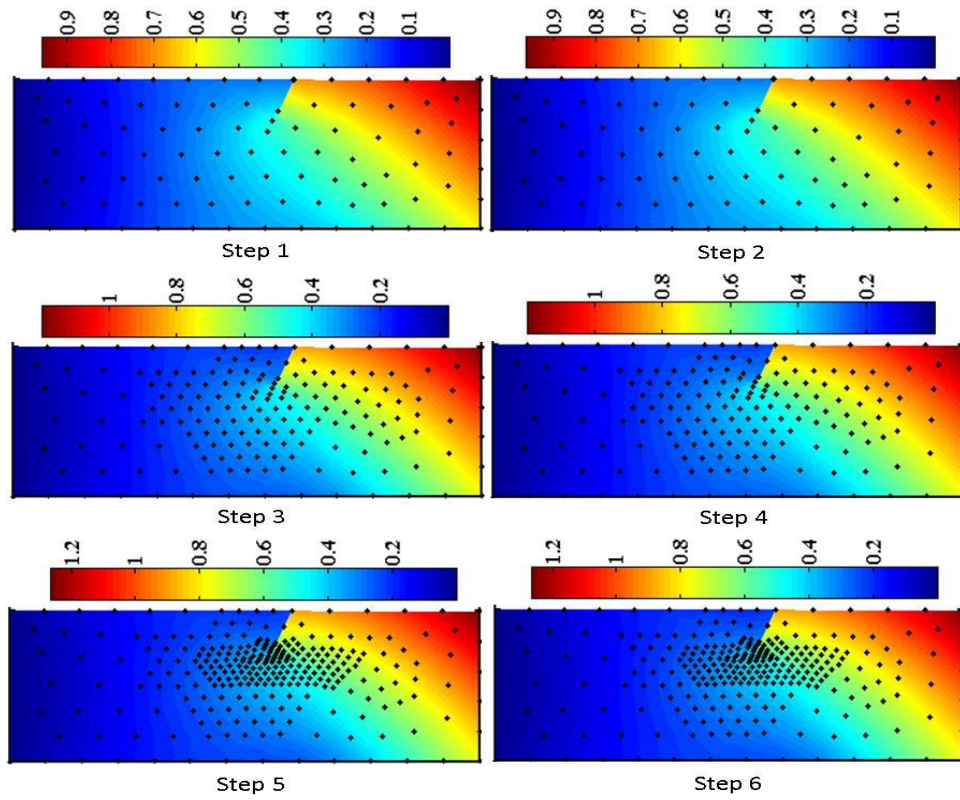


Figure 5.22 – Displacement plot of adaptively refined plate with inclined edge crack

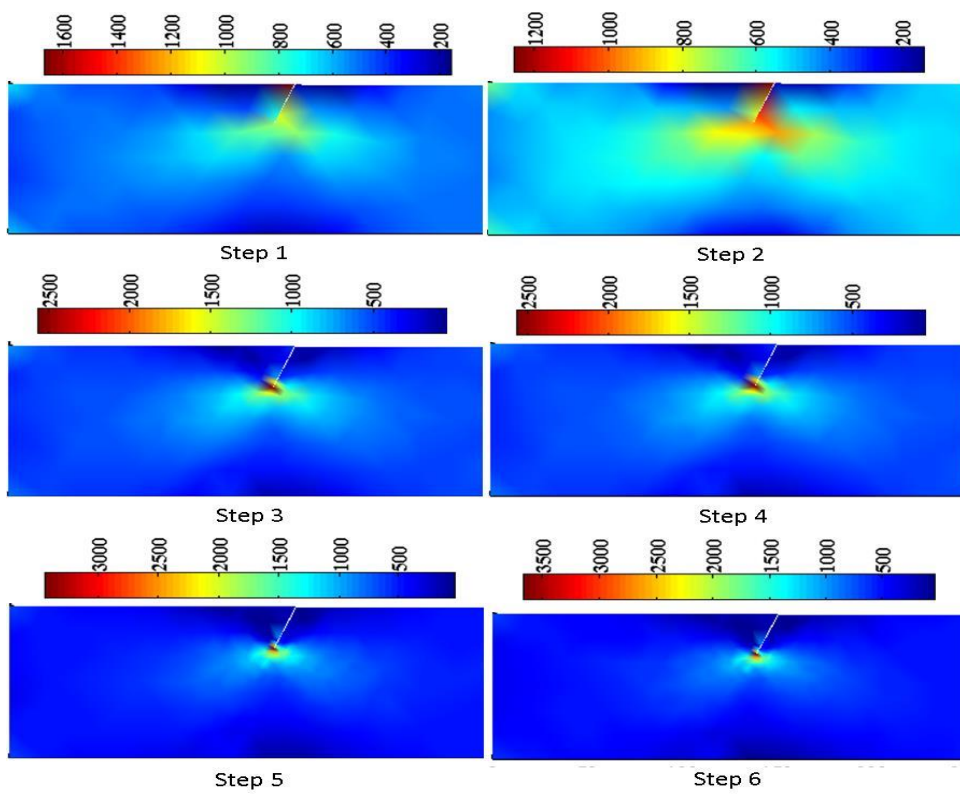


Figure 5.23 – Von Mises stress of adaptively refined plate with inclined edge crack

CHAPTER 6

CONCLUSIONS

6.1 BRIEF SUMMARY OF THE WORK

Detailed literature survey carried out helped in recognising the fact that MeshFree methods have tremendous application in addressing unresolved issues in high stress gradient problems. EFG was identified as the most suitable technique and analysis code was developed with adaptive refinement strategy. Several sequential and logical steps in the development of *Adaptive refinement scheme for EFG based MeshFree method for modelling and simulating high stress gradients in plate structures* which finds application in crack formation-propagation analysis have been summarized.

- ✓ The EFG based MeshFree method for analysis of 1D beam and 2D plate structures has been formulated. MLS technique has been employed for deriving shape function and issue of violation of Kronecker delta property has been addressed by adopting Lagrange multipliers.
- ✓ MATLAB[®] code developed has been tested for stability, convergence and accuracy. 1D and 2D analysis in comparison with traditional FEM has also been made.
- ✓ Adaptive refinement scheme for EFG based MeshFree method for modelling and simulating high stress gradients in plate structures has been conceived, mathematically represented, calibrated, verified and validated.

6.2 CONCLUSIONS

The need for current investigation has been clearly spelt out. The mode and method for *Adaptive refinement scheme for EFG based MeshFree method for modelling and simulating high stress gradients in plate structures* which is of great utility in crack analysis has been elaborated. Encouraging results obtained from the study leads to the following conclusion

1. 1D beam analysis for convergence, displacement and stress distribution

CONCLUSIONS

- ✓ MeshFree method has shown better and faster convergence of displacement with minimum of 11 nodes whereas FEM has taken about 30 nodes
 - ✓ Both MeshFree and FEM have shown smoother distribution of displacements along the length of the beam. However MeshFree yields much smoother stress distribution.
2. 2D plate analysis, the displacement and stress analysis on plates with geometrically induced stress concentrations
- ✓ The computed SCF's for the three plates, i.e. plates with centre circular cut-out, two semi-circular notches on opposite edges and two V-notches on opposite edges, respectively have shown +10%, -2% and -6% difference in EFG method. Whereas FEM has yielded -10%, -11% and -29% errors. As indicated by the proximity of the results with closed-form solutions it is evident, from the result of V-notch case that EFG method is more capable of capturing sudden change in gradients than FEM.
3. Crack propagation analysis, the computation of SIF's and propagation paths
- ✓ SIF computed in case of plate with centre vertical crack is in very close agreement with the closed-form solution, the difference being just 2%.
 - ✓ The crack propagation analysis in plate with angled edge crack has yielded results that are in very close agreement with that reported in literature (Patricio and Mattheij, 2007).
4. The efficacy of adaptive refinement scheme
- ✓ Reduction of 86% and 76% of node numbers and 27% and 56% of integration cell numbers on the two illustrated problems has been accomplished by the scheme suggested and adopted which greatly reduce the computational efforts without compromising on stability, convergence and accuracy

Hence ***Adaptive refinement scheme for EFG based MeshFree method for modelling and simulating high stress gradients in plate structures*** can find application potential as a valid decision making tool in real time monitoring of structures and components.

6.3 SCOPE FOR FUTURE WORK

Capabilities of *Adaptive refinement scheme for EFG based MeshFree method for modelling and simulating high stress gradients in plate structures* can be enhanced by

1. Employment of order reduction techniques like static condensation or component mode synthesis for handling the models with large number of degrees of freedom.
2. Extensions to 3D problems may be attempted.

APPENDIX I

The closed-form solutions used for verification of the developed code for the problems considered are given here.

I.1 CLOSED FORM SOLUTION FOR BEAM UNDER TRANSVERSE LOADING

The displacement along the length of cantilever beam (Figure 4.1) Euler-Bernoulli (Equation I.1) and Timoshenko (Equation I.2) beam is given by following equations,

$$U = \frac{P^l x^2 (3l - x)}{6EI} \quad \dots I.1$$

$$U = \frac{P^l}{EI} \left[\frac{l^3}{3} - \frac{x l^2}{2} + \frac{x^3}{6} \right] + \frac{P^l (l - x)}{kAG} \quad \dots I.2$$

where $k = 2/3$ is the shear correction factor E modulus of elasticity, $G = \frac{1-\mu}{E}$ is the shear modulus, A is the cross-sectional area, I is the area moment of inertia, l is the length of the beam, P^l is the applied load, and the maximum displacement is obtained by substituting $x = l$ in Equations (I.1) and (I.2).

Also, for simply-supported beam (Figure 4.2), the displacement using Euler-Bernoulli (I.3) and Timoshenko (I.4) beam theories, the displacement is computed as,

$$U = \frac{P^l x^2}{48EI} (3l^2 - 4x^2) \quad \dots I.3$$

$$U = \frac{P^l l^3}{48EI} \left(1 + 3.9 \frac{h^2}{l^2} \right) \quad \dots I.4$$

where the maximum displacement is obtained by substituting $x=l/2$ in Equation (I.3).

The stresses along the length can be computed,

$$\sigma = \frac{M}{I} y \quad \dots I.5$$

where, the moment $M = P'x$ for cantilever beam and $M = \frac{P'x}{2}$ for simply-supported beam

I.2 ANALYTICALLY COMPUTED SCF FOR PLATES

For a plate with centre circular cut-out (Figure 4.13), the nominal stress (Equation I.6) and SCF (Equation I.7) is written as follows,

$$\sigma_{nom} = \frac{F}{h(b-b')} \quad \dots I.6$$

$$K_t = 3.00 - 3.140\left(\frac{b'}{b}\right) + 3.667\left(\frac{b'}{b}\right)^2 - 1.527\left(\frac{b'}{b}\right)^3 \quad \dots I.7$$

where t is the thickness of the plate.

For a plate with two semi-circular notches on opposite edges (Figure 4.14), the nominal stress (Equation I.8) and SCF (Equation I.9) is written,

$$\sigma_{nom} = \frac{F}{hb'} \quad \dots I.8$$

$$K_t = 3.065 - 3.472\left(\frac{2(b-b')}{b}\right) + 1.009\left(\frac{2(b-b')}{b}\right)^2 - 0.405\left(\frac{2(b-b')}{b}\right)^3 \quad \dots I.9$$

For a plate with two V-notches on opposite edges (Figure 4.15), the nominal stress (Equation I.8) and SCF (Equation I.9) is,

$$\sigma_{nom} = \frac{F}{hb'} \quad \dots I.10$$

$$K_t = C_1 + C_2\sqrt{K_{tu}} + C_3\sqrt{K_{tu}} \quad \dots I.11$$

where,

$$C_1 = -10.01 + 0.1534\alpha - 0.000647\alpha^2, \quad C_2 = 13.60 - 0.2140\alpha + 0.000973\alpha^2,$$

$$C_3 = -3.781 + 0.07873\alpha - 0.000392\alpha^2, \quad K_{tu} = C_{tu1} + C_{tu2}\left(\frac{2b'}{b}\right) + C_{tu3}\left(\frac{2b'}{b}\right)^2 + C_{tu4}\left(\frac{2b'}{b}\right)^3,$$

$$C_{iu1} = 1.037 + 1.991\sqrt{\frac{b'}{r}} + 0.002\left(\frac{b'}{r}\right), \quad C_{iu2} = -1.886 - 2.181\sqrt{\frac{b'}{r}} - 0.048\left(\frac{b'}{r}\right),$$

$$C_{iu3} = 0.649 + 1.086\sqrt{\frac{b'}{r}} + 0.142\left(\frac{b'}{r}\right), \quad C_{iu4} = 1.218 - 0.922\sqrt{\frac{b'}{r}} - 0.086\left(\frac{b'}{r}\right)$$

I.3 ANALYTICALLY COMPUTED SIF FOR PLATES

The SIF for plate with centre vertical crack shown in Figure 5.3 is given as,

$$K_I = \sigma\sqrt{\Pi a} \left[\begin{array}{l} 1 + 0.043\left(\frac{a}{b}\right) + 0.491\left(\frac{a}{b}\right)^2 + 7.2125\left(\frac{a}{b}\right)^3 - 28.403\left(\frac{a}{b}\right)^4 \\ + 59.583\left(\frac{a}{b}\right)^5 - 65.278\left(\frac{a}{b}\right)^6 + 29.762\left(\frac{a}{b}\right)^7 \end{array} \right] \quad \dots I.12$$

REFERENCES

- Afshar M. H. and Lashckarbolok M. (2008), "Collocated Discrete Least-squares (CDLS) Meshless Method: Error Estimate and Adaptive Refinement" *International Journal for Numerical Methods in Fluids*, 56, 1909-1928
- Afshar M.H., Naisipour M. and Amani J. (2012), "Node Moving Adaptive Refinement Strategy for Planar Elasticity Problems using Discrete Least Squares Meshless Method" *Finite Elements in Analysis and Design*, 47, 1315-1325
- Afshar M.H., Amani J. and Naisipour M. (2011), "A Node Enrichment Adaptive Refinement in Discrete Least Squares Meshless Method for Solution of Elasticity Problems" *Engineering Analysis with Boundary Elements*, 36, 385-393
- Andrzej S. (2002), "Modelling of singular stress fields using finite element method" *International Journal of Solids and Structures*, 39, 4787-4804
- Anita H. and Peter H. (2004), "A finite element method for the simulation of strong and weak discontinuities in solid mechanics" *Computer Methods in Applied Mechanics and Engineering*, 193, 3523-3540
- Antonio H. and Sonia F. M. (2001), "Locking in the Incompressible Limit for the Element-free Galerkin Method" *International Journal for Numerical Methods in Engineering*, 51, 1361-1383
- Antonio H., Belytschko T., Sonia F. M. and Rabczuk T. (2004), "MeshFree Methods" *Encyclopaedia of Computational Mechanics*, John Wiley & Sons, Ltd.,
- Amani J., Saboor B. A. and Rabczuk T. (2014), "Error Estimate and Adaptive Refinement in Mixed Discrete Least Squares Meshless Method" *Mathematical Problems in Engineering*, Article ID 721240, 16
- Armando D. C., Dae-Jin K. and Ivo B. (2007), "A Global-Local Approach for the Construction of Enrichment Functions for the Generalized FEM and Its Application to Three-Dimensional Cracks" *Advances in MeshFree techniques*, Springer, 1-26
- Arun C. O., Rao B. N. and Srinivasan S.M. (2010), "Continuum damage growth analysis using element free Galerkin method" *Indian Academy of Sciences*, 35(3), 279-301
- Asadpoure A. and Mohammadi S. (2007), "Developing new enrichment functions for crack simulation in orthotropic media by the extended finite element method" *International Journal for Numerical Methods in Engineering*, 69, 2150-2172
- Belytschko T., Lu Y.Y. and Gu L. (1994), "Element-free Galerkin method" *International Journal For Numerical Methods In Engineering*, 37, 229-256
- Belytschko T., Lu Y.Y. and Gu L. (1995a), "Crack propagation by element-free Galerkin methods" *Engineering Fracture Mechanics*, 51, 2, 295-315
- Belytschko T., Organ D. and Krongauz Y. (1995b), "A coupled Finite element-element-free Galerkin method" *Computational Mechanics*, 17, 186-195
- Belytschko T., Krongauz Y., Organ D., Fleming M., Krysl I. (1996), "MeshLess methods: An overview and recent developments" *Computer methods in applied mechanics and engineering*, 139, 3-47
- Belytschko T. and Tabbara M. (1996), "Dynamic Fracture using Element-Free Galerkin Methods" *International Journal for Numerical Methods in Engineering*, 39
- Belytschko T., Liu W.K. and Mike S. (1998), "On Adaptivity and Error Criteria for Meshfree Methods" *Advances in Adaptive Computational Methods in Mechanics*
- Belytschko T. and Black T. (1999), "Elastic Crack Growth in Finite Elements with Minimal Remeshing" *International Journal for Numerical Methods in Engineering*, 45, 601-620

REFERENCES

- Belytschko T., Organ D. and Gerlach C. (2000), "Element-free Galerkin methods for dynamic fracture in concrete" *Computer Methods in Applied Mechanics and Engineering*, 187, 385-399
- Belytschko T., Moes N., Usui S. and Parimik C. (2001), "Arbitrary discontinuities infinite elements" *International Journal for Numerical Methods in Engineering*, 50, 993-1013
- Bouchard P.O., Bay F. and Chastel Y. (2003), "Numerical modelling of crack propagation: automatic remeshing and comparison of different criteria", *Computer Methods in Applied Mechanics and Engineering*, 192, 3887-3908
- Bordas S., Rabczuk T. and Goangseup Z. (2008), "Three-dimensional crack initiation, propagation, branching and junction in non-linear materials by an extended MeshFree method without asymptotic enrichment", *Engng. Fracture Mechanics*, 75, 943-960
- Canh V. Le, Harm A. and Mathew G. (2010), "Adaptive Element-free Galerkin Method Applied to the Limit Analysis of Plates", *Computer Methods in Applied Mechanics and Engineering*, 199, 2487-2496
- Chen L., H. Nguyen-Xuan, T. Nguyen-Thoi, Zeng K. Y. and Wu S. C. (2010), "Assessment of smoothed point interpolation methods for elastic mechanics", *Int. J. Numer. Meth. Biomed. Engng.*, 26, 1635-1655
- Chen L., Zhang G. Y., Zhang J., Nguyen-Thoi T. and Tang Q. (2011^a), "An adaptive edge-based smoothed point interpolation method for mechanics problems", *International Journal of Computer Mathematics*, 88:11, 2379-2402
- Chen J., Sheng W. C. and Hsin Y. H. (2011^b), "Recent developments in stabilized Galerkin and collocation MeshFree methods", *Computer Assisted Mechanics and Engineering Sciences*, 18, 3-21
- Chen L., Zhang G. Y., Zhang J. and Jia P. G. (2011^c), "An Edge-based Smoothed Finite Element Method for Adaptive Analysis", *Structural Engineering and Mechanics*, 39: 6, 000-000
- Chinesta F., Yvonnet J., Villon P., Breitkopf P., Joyot P., Alfaro I. and Cueto E. (2007), "New Advances in MeshLess Methods: Coupling Natural Element and Moving Least Squares Techniques", *Advances in MeshFree techniques*, Springer, 97-121
- Chow W. T. and Atluri S. N. (1995), "Finite element calculation of stress intensity factors for interfacial cracks using virtual crack closure integral", *Computational Mechanics*, 16, 417-425
- Cui X. Y., Liu G. R., Li G. Y., and Zhang G. Y. (2011), "A thin plate formulation without rotation DOFs based on the radial point interpolation method and triangular cells", *Int. J. Numer. Meth. Engng.*, 85, 958-986
- Dolbow J. and Belytschko T. (1998), "An Introduction to Programming the Meshless Element Free Galerkin Method", *Archives of Computational Methods in Engineering*, 5, 3, 207-241
- Eigel M., George E. and Kirkilionis M. (2010), "A mesh-free partition of unity method for diffusion equations on complex domains", *IMA Journal of Numerical Analysis*, 30, 629-653
- Fan S. C., Liu X. and Lee C. K. (2004), "Enriched Partition of Unity Finite Element Method for Stress Intensity Factors at Crack Tips", *Computers and Structures*, 82, 445-461
- Ferreira A. J. M. and Roque C. M. C. (2011), "Analysis of thick plates by radial basis functions", *Acta Mech* 217, 177-190
- Fleming M., Chus Y. A., Morant B. and Belytschko T. (1997), "Enriched Element-Free Galerkin Methods for Crack Tip Fields", *International Journal for Numerical Methods in Engineering*, 40, 1483-1504
- Gavete L., Cuesta J. L. and Ruiz A. (2002), "A Procedure for Approximation of the Error in the EFG Method", *International Journal for Numerical Methods in Engineering*, 53, 677-690
- Giner E., Sukumar N., Tarancon J. F. and Fuenmayor F. J. (2009), "An Abaqus Implementation of the Extended Finite Element Method", *Engineering Fracture Mechanics*, 76, 347-368

- Goangseup Z. and Belytschko T. (2003), “New Crack-Tip Elements for XFEM and Applications to Cohesive Cracks”, *International Journal for Numerical Methods in Engineering*, 57, 2221–2240
- Goangseup Z., Jeong-Hoon S., Elisa B., Sang-Ho L. and Belytschko T. (2004), “A Method for Growing Multiple Cracks without Remeshing and its Application to Fatigue Crack Growth”, *Institute of Physics Publishing Modelling and Simulation in Materials Science and Engineering*, 12, 901-915
- Goangseup Z, Rabczuk T. and Wolfgang W. (2007), “Extended MeshFree methods without branch enrichment for cohesive cracks”, *Computer Mechanics*, 40, 367-382
- Grand R. J., Adam W. and Karol M. (2015), “Adaptive Numerical Integration in Element-free Galerkin Methods for Elliptic Boundary Value Problems”, *Engineering Analysis with Boundary Elements*, 51, 52-63
- Gu Y.T. (2005), “MeshFree Methods and their Comparisions”, *International Journal of Computational Methods*, 2, ISSN: 1793-6969,477
- Gye-Hee L., Heung-Jin C. and Chang-Koon C. (2003), “Adaptive Crack Propagation Analysis with the Element-Free Galerkin Method”, *International Journal for Numerical Methods in Engineering*, 56, 331–350
- Hae-Soo O., Christopher D. and Jae W. J. (2012), “MeshFree particle methods for thin plates”, *Computer Methods in Applied Mechanical Engineering*, 209–212, 156–171
- Haussler-Combe U. and Korn C. (1998), “An Adaptive Approach with the Element-Free-Galerkin Method”, *Computer Methods in Applied Mechanics and Engineering*, 162, 203-222
- John D. and Belytschko T. (1999a), “Volumetric Locking in the Element Free Galerkin Method”, *International Journal for Numerical Methods in Engineering*, 46, 925–942
- John D. and Belytschko T. (1999b), “Numerical Integration of the Galerkin Weak Form in Meshfree Methods”, *Computational Mechanics*, 23, 219-230
- John D., Nicolas M. and Belytschko T. (2000), “Discontinuous Enrichment in Finite Elements with a Partition of Unity Method”, *Finite Elements in Analysis and Design*, 36, 235-260
- Karihaloo B.L. and Xiao Q.Z. (2003), “Modelling of stationary and growing cracks in FE framework without re-meshing: a state-of-the-art review”, *Computers and Structures*, 81, 119-129
- Krysl P. and Belytschko T. (1999), “Analysis of thin plates by the element-free Galerkin method”, *Computational Mechanics*, 17, 26-35
- Lancaster P. and Salkauskas K. (1981), “Surfaces Generated by Moving Least Squares Methods”, *Mathematics of Computation*, 37, 141-158
- Lee C.K. and Zhou C.E. (2004^a), “On Error Estimation and Adaptive Refinement for Element Free Galerkin Method Part I: Stress Recovery and a Posteriori Error Estimation”, *Computer and Structures*, 82, 413-428
- Lee C.K. and Zhou C.E. (2004^b), “On Error Estimation and Adaptive Refinement for Element Free Galerkin Method Part I: Stress Recovery and a Posteriori Error Estimation”, *Computer and Structures*, 82, 429-443
- Lian Y.P., Zhang X., Liu Y. (2012), “An adaptive finite element material point method and its application in extreme deformation problems”, *Computer Methods in Applied Mechanics and Engg.*, 27, 275–285
- Liew K. M., Xin Z. and Antonio J. M .F. (2011), “A review of MeshLess methods for laminated and functionally graded plates and shells”, *Composite Structures*, 93, 2031–2041
- Liu G.R. and Tu Z.H. (2002), “An Adaptive Procedure Based on Background Cells for Meshless Methods”, *Computer Methods in Applied Mechanics and Engineering*, 191, 1923-1943
- Liu G. R. and Bernard B. T. K. (2005), “An Adaptive Meshfree Least-Squares Method”, *Centre for ACES, Department of Mechanical Engineering, National University of Singapore*

REFERENCES

- Liu G.R. and Gu Y.T. (2005), "An Introduction to Meshfree Methods and their Programming", Springer, Netherlands
- Liu G.R. and Zhang G.Y. (2008), "Upper Bound Solution to Elasticity Problems: A Unique Property of the Linearly Conforming Point Interpolation Method (LC-PIM)", *International Journal for Numerical Methods in Engineering*, 74, 1128-1161
- Liu G.R. (2009), "MeshFree Methods Moving beyond the Finite Element Method", Second edition, CRC press, Taylor and Francis group, New York
- Liu G.R., Nguyen-Xuana H., Nguyen-Thoib T. and Xub X. (2009), "A Novel Galerkin-like Weakform and a Superconvergent Alpha Finite Element Method (S α FEM) For Mechanics Problems using Triangular Meshes", *Journal of Computational Physics*, 228, 4055–4087
- Luo Y. and Combe U. H. (2003), "A Gradient-based Adaptation Procedure and its Implementation in the Element-Free Galerkin Method", *International Journal For Numerical Methods In Engineering*, 56, 1335–1354
- Marjan S. and Roman T. (2008), "Meshless Solution of a Diffusion Equation with Parameter Optimization and Error Analysis", *Engineering Analysis with Boundary Elements*, 32, 567-577
- Mark A. F. (1997), "The element free Galerkin method for fatigue and quasi-static fracture", PhD. thesis, Northwestern University, Evanston, Illinois
- Mergheim J., Kuhl E. and SteinmannP. (2005), "A finite element method for the computational modelling of cohesive cracks", *Int. J. Numer.Meth.Engng.*, 63, 276–289
- Metsis P. and Papadrakaki M. (2012), "Overlapping and Non-overlapping Domain Decomposition Methods for Large-scale Meshless EFG Simulations", *Computer Methods in Applied Mechanics and Engineering*, 229–232, 128–141
- Mohamed H. A., BakreyA.E. and AhmedS.G. (2012), "A collocation MeshFree method based on multiple basis functions", *Engineering Analysis with Boundary Elements*, 36, 446–450
- Nicolas M., John D. and Belytschko T. (1999), "A finite element method for crack growth without remeshing", *International Journal for Numerical Methods in Engineering*, 46, 131-150
- Pant M., SinghI.V. andMishraB.K. (2013) "A novel enrichment criterion for modeling kinked crack using element free Galerkin method" *Journal of Mechanical Sciences* 68, 140-149
- Paola M. D., Pirrotta A. and Santoro R. (2008), "Line element-less method (LEM) for beam torsion solution (truly no-mesh method)", *ActaMech*, 195, 349–364
- Patricio M. and Mattheij R. (2007), Crack propagation analysis, CASA report, 07-03
- Pedro M. A., Areias and Belytschko T. (2005), "Analysis of three-dimensional crack initiation and propagation using the extended finite element method", *International Journal for Numerical Methods in Engineering*, 63, 760–788
- Perazzo F., Lohner R. and Perez-Pozo L. (2008), "Adaptive Methodology for Meshless Finite Point Method", *Advances in Engineering Software*, 39, 156-166
- Petr K. and Belytschko T. (1999), "The Element Free Galerkin Method for Dynamic Propagation of Arbitrary 3-D Cracks", *International Journal for Numerical Methods in Engineering*, 44, 767–800
- PinkangX. and Dongdong W. (2012), "A Spectrum Analysis of GalerkinMeshFree Method", *International Conference on Advances in Computational Modelling and Simulation, Procedia Engineering*, 31, 996 – 1000
- Rabczuk T. and Belytschko T. (2003), "An Adaptive Continuum/Discrete Approach for MeshFree Particle Methods", *Latin American Journal of Solids and Structures*, 1, 141-166
- Rabczuk T. and Eibl J. (2004), "Numerical Analysis of Prestressed Concrete Beams Using a Coupled Element Free Galerkin/Finite Element Approach", *International Journal of Solids and Structures*, 41, 1061-1080

- Rabczuk T. and Belytschko T. (2004), “Cracking Particles: A Simplified Meshfree Method for Arbitrary Evolving Cracks”, *International Journal for Numerical Methods in Engineering*, 61, 2316-2343
- Rabczuk T. and Belytschko T. (2005), “Adaptivity for Structured Meshfree Particle Methods in 2D and 3D”, *International Journal for Numerical Methods in Engineering*, 63, 1559–1582
- Rabczuk T., Xiao S. P. and Sauer M. (2006), “Coupling of Mesh-free Methods with Finite Elements: Basic Concepts and Test Results”, *Communications in Numerical Methods in Engineering*, 22, 1031–1065
- Rabczuk T. and Belytschko T. (2007), “A three-dimensional large deformation meshfree method for arbitrary evolving cracks”, *Computer Methods in Applied Mechanics and Engineering*, 196, 2777-2799
- Rabczuk T. and Samaniego E. (2008), “Discontinuous Modelling of Shear Bands using Adaptive MeshFree Methods”, *Computer Methods in Applied Mechanics and Engineering*, 197, 641-668
- Rao B.N. and Rahman S. (2001), “A coupled MeshLess finite element method for fracture analysis of cracks”, *International Journal of Pressure Vessels and Piping*, 78, 347-357
- Rao B.N. and Rahman S. (2003), “Mesh-free analysis of cracks in isotropic functionally graded materials”, *Engineering Fracture Mechanics*, 70, 1-27
- Rethore J., Gravouil A. and Combescure A. (2004), “A stable numerical scheme for the finite element simulation of dynamic crack propagation with re-meshing”, *Computer Methods Appl. Mech. Engrg.*, 193, 4493–4510
- Robert C. D., David S. M., Michael E. P. and Robert J. W. (2001), “Concepts and Application of Finite Element Analysis”, Fourth edition, John Wiley and sons, INC.
- Stolarska M., Chopp D. L., Moes N. and Belytschko T. (2001), “Modelling Crack Growth by Level sets in the Extended Finite Element Method”, *International Journal for Numerical Methods in Engineering*, 51, 943-960
- Sukumar N., Moes N., Moran B. and Belytschko T. (2000), “Extended Finite element method for three-dimensional crack modelling”, *International Journal for Numerical Methods in Engineering*, 48, 1549-1570
- Sukumar N., Chopp D.L. and Moran B. (2003), “Extended finite element method and fast marching method for three-dimensional fatigue crack propagation”, *Engineering Fracture Mechanics*, 70, 29-48
- Tanga Q., Zhang G.Y., Liu G.R., Zhong Z.H. and He Z.C. (2011), “A Three-dimensional Adaptive Analysis Using the Meshfree Node-Based Smoothed Point Interpolation Method (NS-PIM)”, *Engineering Analysis with Boundary Elements*, 35:10, 1123–1135
- Thomas M. and Belytschko T. (2010), “Dynamic Fracture with Meshfree Enriched XFEM”, *Acta Mechanica*, 213, 53–69
- Thomas M. and Christian B. (2005), “A Moving Least Squares Weighting Function for the Element-free Galerkin Method which almost Fulfills Essential Boundary Conditions”, *Structural Engineering and Mechanics*, 21:3, 315-332
- Thomas-Peter F. and Hermann-Georg M. (2004), “Classification and Overview of MeshFree Methods”, Technical report, Institute of Scientific Computing Technical University Braunschweig, Brunswick, Germany
- Thomas-Peter F. and Belytschko T. (2010), “The extended/generalized finite element method: An overview of the method and its applications”, *International Journal for Numerical Methods in Engineering*, 84, 253–304
- Timon R. and Goangseup Z. (2007), “A MeshFree method based on the local partition of unity for cohesive cracks”, *Computer Mechanics*, 39, 743-760

REFERENCES

- Timon R., Stéphane B. and Goangseup Z. (2007), “A three-dimensional MeshFree method for continuous multiple-crack initiation, propagation and junction in statics and dynamics”, *ComputMech*, 40, 473–495
- Timoshenko S.P. and Goodier J.N. (1970) “Theory of Elasticity” 3rd edition, McGraw-Hill, New York
- Ullah Z. and Augarde C.E. (2013), “Finite Deformation Elasto-plastic Modelling using an Adaptive Meshless Method”, *Computers and Structures*, 118, 39-52
- Ullah Z., Coombs W.M. and Augarde C.E. (2013), “An Adaptive Finite Element/Meshless Coupled Method Based on Local Maximum Entropy Shape Functions for Linear and Nonlinear Problems”, *Computer Methods in Applied Mechanics and Engineering*, 267, 111–132
- Ventura G., Xu J. X. and Belytschko T. (2002), “A vector level set method and new discontinuity approximations for crack growth by EFG”, *International Journal for Numerical Methods in Engineering*, 54, 923-944
- Vinh P. N., Rabczuk T., Stéphane B. and Marc D. (2008), “Review MeshLess methods: A review and computer implementation aspects”, *Mathematics and Computers in Simulation*, 79, 763–813
- Wang H. and Wang S. (2010), “A simplified mesh-free method with embedded discontinuities”, *Int. J. Numer. Meth. Biomed. Engng.*, 26, 1404–1416
- Wu Y., Magallanes J., Choi H., and Crawford J. (2013), “Evolutionarily Coupled Finite-Element Mesh-Free Formulation for Modelling Concrete Behaviors under Blast and Impact Loadings”, *J. Eng. Mech.*, 139(4), 525–536
- Xiao H. Z., Ping Z. and Lin Z. (2012), “A simple technique to improve computational efficiency of MeshLess methods”, *International Conference on Advances in Computational Modelling and Simulation*, *Procedia Engineering*, 31, 1102 – 1107
- Xiaolin L. (2011), “Adaptive methodology for the MeshLess Galerkin boundary node method”, *Engineering Analysis with Boundary Elements*, 35, 750–760
- Xiaoying Z., Claire H. and Charles A. (2012), “On Error Control in the Element-free Galerkin Method”, *Engineering Analysis with Boundary Elements*, 36, 351-360
- Xu X., Liu G.R., Gu Y.T., Zhang G.Y., Luo J.W. and Peng J.X. (2010), “A point interpolation method with locally smoothed strain field (PIM-LS2) for mechanics problems using triangular mesh”, *Finite Elements in Analysis and Design*, 46, 862–874
- Yan L. and Belytschko T. (2010), “A New Support Integration Scheme for the Weak Form in Mesh-free Methods”, *International Journal for Numerical Methods in Engineering*, 82, 699–715
- Yazid A. and Abdelmadjid H. (2008), “A survey of the extended finite element”, *Computers and Structures*, 86, 1141–1151
- Yiqian H., Haitian Y., and Andrew J. D. (2014), “A Node-based Error Estimator for the Element-free Galerkin (EFG) Method”, *International Journal of Computational Methods*, 11:4, 24
- Yvonnet J., Coffignal G., Ryckelynck D., Lorong P. and Chinesta F. (2006), “A Simple Error Indicator for MeshFree Methods Based on Natural Neighbors”, *Computers and Structures*, 84, 1301-1312
- Yury K. (1996), “Application of MeshLess methods to solid mechanics”, PhD. thesis, Northwestern University, Illinois
- Zan Z., Peng Z. and Liew K.M. (2009), “Improved Element-free Galerkin Method for Two-dimensional Potential Problems”, *Engineering Analysis with Boundary Elements*, 33, 547-554
- Zienkiewicz O. C., Taylor R.L. and Zhu J.Z. (2005), “The Finite Element Method Its Basics and Fundamentals”, sixth edition, Elsevier, Oxford UK

PUBLICATIONS FROM THE PRESENT WORK

INTERNATIONAL JOURNALS

Bhavana Patel S S, Babu Narayan K S and Venkataramana K, (2014), “Modeling high stress gradients in plates by meshfree method”, *Journal of Civil Engineering Technology and Research*, Vol.2, No.1 (2014), pp.71-76.

Bhavana Patel S S, Venkataramana K, Babu Narayan K S, Bhagyashri Parla and Kimura Y (2014), “Structural health monitoring techniques in civil engineering : an overview”, *International Journal of Earth Sciences and Engineering*, Vol.7, No.01, February 2014, pp. 305-312.

Bhavana Patel S S, Babu Narayan K S and Venkataramana K., “Strategy for refinement of nodal densities and integration cells in EFG technique” *Structural Engineering and Mechanics An International Journal – Techno Press* (under review)

Bhavana Patel S. S., Babu Narayan K S and Venkataramana K., “Strain Energy based Refinement of Nodes and Integration Cells on Plates with Geometrically Induced Stress Concentration” *International Journal for Computational Methods in Engineering Science & Mechanics* (under review)

INTERNATIONAL CONFERENCE PROCEEDINGS

Bhavana Patel S S, Babu Narayan K S and Venkataramana K, (2016), “Adaptive Refinement Strategy for Crack Propagation Analysis using EFG method”, Sixth International Congress on Computational Mechanics and Simulation (ICCMS 2016), June 27 – July 01, 2016. (Accepted for presentation).

Bhavana Patel S S, Babu Narayan K S and Venkataramana K, (2015), “Effect of Nodal Placement for a Beam using MeshFree Method”, *Proc. of 4th International Engineering Symposium (IES 2015)*, March 4-6, 2015, Kumamoto University, Japan, Paper No. C1-6.

PUBLICATIONS FROM THE PRESENT WORK

Bhavana Patel S S, Babu Narayan K S and Venkataramana K, (2014), “Adaptive Refinement of Nodal Distribution in MeshFree Method”, *Proc. of Sixth International Conference on Theoretical, Applied, Computational and Experimental Mechanics (6th ICTACEM 2014) held at IIT Kharagpur during December 29-31, 2014, paper ID-165.*

Bhavana Patel S S, Babu Narayan K S and Venkataramana K,(2014), “Meshfree methods for plate analysis”, *Proc. Of International Conference on Emerging Trends in Engineering (ICETE-2014) held at Nitte, India during May 15-17, 2014, pp.21-26.*

Bhavana Patel S S, Venkataramana K, Babu Narayan K S, Bhagyashri Parla and Vijaya Vishnu Mayya (2013), “Structural health monitoring techniques in civil engineering: an overview”, *Proc. of 3rd International Engineering Symposium, March 4-6, 2013, Kumamoto University, Japan, Paper No. C7-1, pp.C711-C718.*

NATIONAL CONFERENCE PROCEEDINGS

Bhavana Patel S S, Babu Narayan K S and Venkataramana K. (2014), “Domain Selection in Meshfree Method”, *Proc. of First Annual Conference on Innovations and Developments in Civil Engineering (ACIDIC-2014), held at NITK, Surathkal, India, during May 19-20, 2014, pp.600-607.*

Bhavana patel S S, Babu Narayan K S and Venkataramana, K. (2014), “EFG vs. FEM for Beam Analysis”, *Proc. of National Conference on Advancements in Materials, Construction and Sustainable Environment (AMCSE 2014) held at Kalasalingam University, Tamil Nadu on March 29, 2014.*

Bhavana S. S. Patel, Babu K. S. Narayan, and Katta Venkataramana (2013), “EFG-MLS MeshFree Method to Resolve Beam Bending Problem Issues in FEM” *Research Scholars Day 2013, Indian Institute of Space Science and Technology (IIST), Thiruvananthapuram, India, December 16-17, 2013.*

CURRICULUM VITAE

PERSONAL DETAILS

Name : Bhavana Patel S.S.
Area of Interest : Finite Element Analysis, Structural Dynamics, MeshFree Method
Contact Details : E-mail: bhavana8patel@gmail.com
Mobile : 9686444880

EDUCATIONAL QUALIFICATION

| | | |
|-------------------------------------|---|---------|
| Ph.D. (Structural Engineering) | National Institute of Technology Karnataka | Ongoing |
| M.Tech. (Structural Engineering) | Manipal University | 2012 |
| B.E. (Civil Engineering) | Karunya University | 2010 |

RESEARCH PUBLICATIONS

| | National | International |
|------------|----------|---------------|
| Journal | - | 2 |
| Conference | 5 | 7 |

